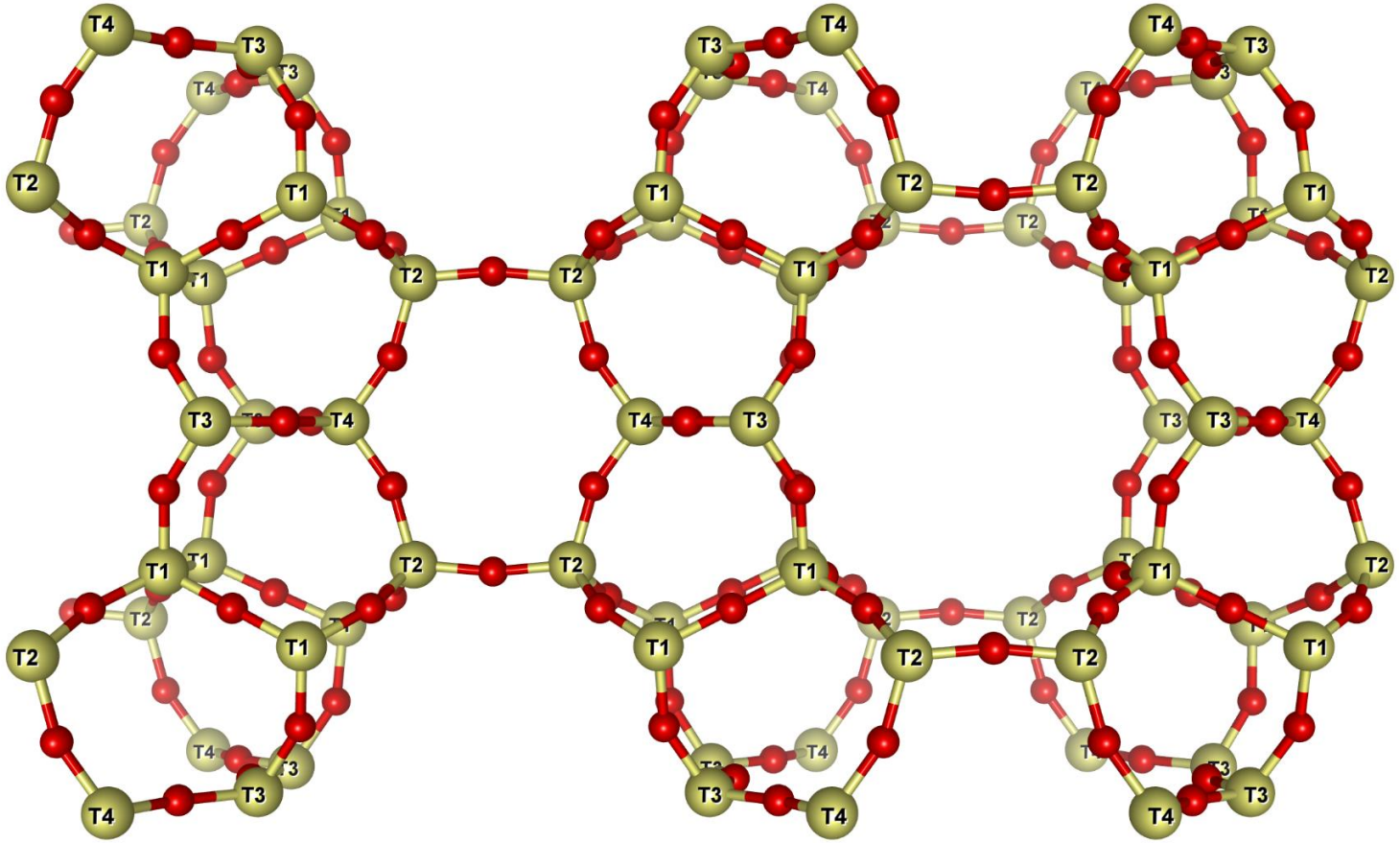

Fundamentals and applications of X-ray diffraction. Applications in catalysts characterization.

Przemyslaw Rzepka

Institute for Chemical and Bioengineering, ETH Zurich, Zurich, Switzerland
Laboratory for Catalysis and Sustainable Chemistry, Paul Scherrer Institute, Villigen, Switzerland

Outline

1. Crystal lattice. Symmetry
2. X-ray diffraction
3. Braggs' peaks positions. Indexing
4. Relative intensities of Braggs' Peaks. Structure factor. Structure refinement
5. Sample preparation
6. Examples

What is crystal?

A material has a crystal structure if its constituents (such as atoms, molecules, or ions) are arranged in a 3D translationally periodic order forming a crystal lattice.

Crystal = Lattice * Motif

What is crystal?

~~A material has a crystal structure if its constituents (such as atoms, molecules, or ions) are arranged in a 3D translationally periodic order forming a crystal lattice~~

Crystal = Lattice * Motif

A material is a crystal if displays a sharp diffraction pattern with most of intensity concentrated in relatively sharp Bragg peaks**.**

Institute for Chemical and Bioengineering, ETH Zurich, Zurich, Switzerland
Laboratory for Catalysis and Sustainable Chemistry, Paul Scherrer Institute, Villigen, Switzerland

Symmetry

Fundamental property of the orderly arrangements of atoms found in crystalline solids

Unit cell. Translational symmetry

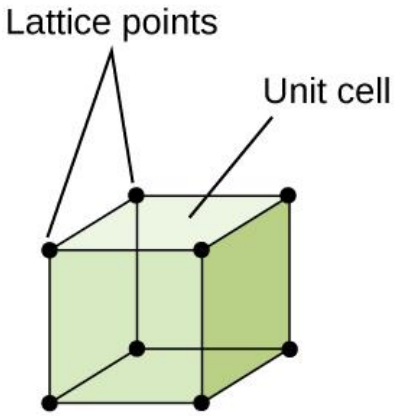

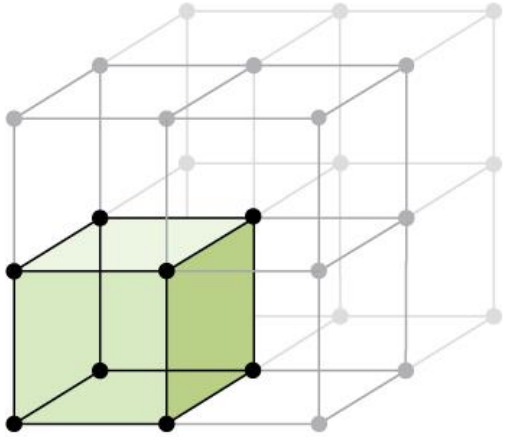

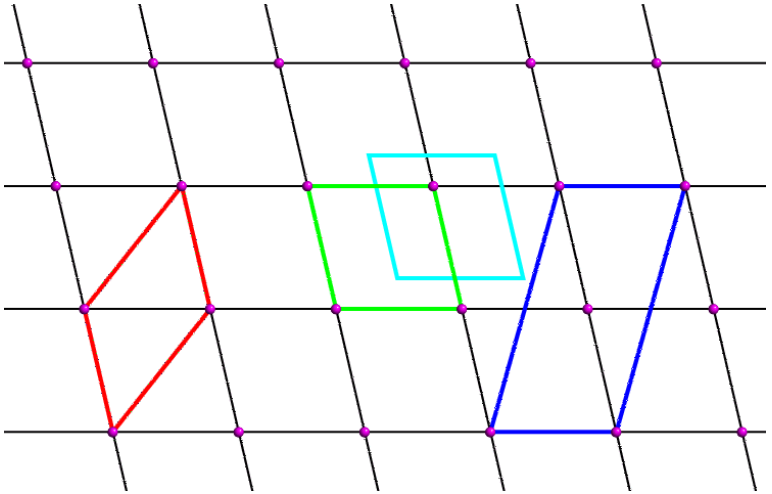

Unit cell: smallest unit that repeats in the lattice (translation)

- minimum number of lattice points
- origin on one lattice point
- angles as close to 90° as possible

Institute for Chemical and Bioengineering, ETH Zurich, Zurich, Switzerland
Laboratory for Catalysis and Sustainable Chemistry, Paul Scherrer Institute, Villigen, Switzerland
Przemyslaw Rzepka

Unit cell centering

Unit cell: smallest unit that repeats in the lattice (translation)

- Primitive unit cell: lattice point only at corners
- Non-primitive unit cell: lattice points also at other positions

Centering Type	Symbol
Primitive - no centering	P
A-face centered	A
B-face centered	B
C-face centered	C
All-face centered	F
Body centered	I
Rhombohedrally centered	R

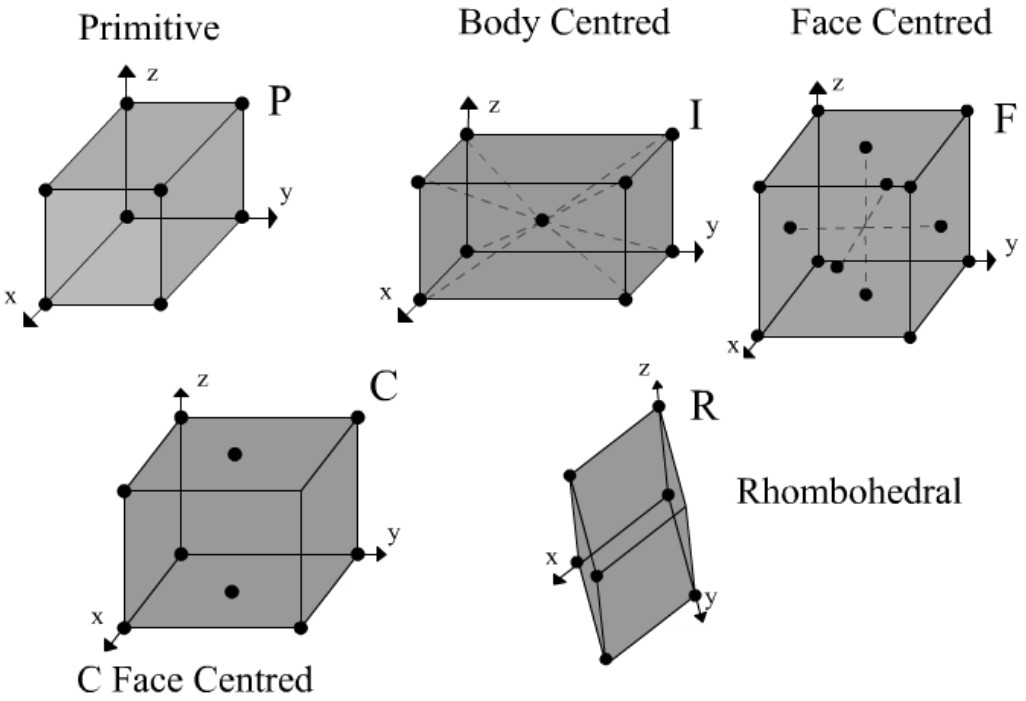

Institute for Chemical and Bioengineering, ETH Zurich, Zurich, Switzerland
Laboratory for Catalysis and Sustainable Chemistry, Paul Scherrer Institute, Villigen, Switzerland

Crystal systems

Combining a lattice with the different orders of rotation symmetry leads to the seven possible crystal systems

Crystal System	Characteristic Symmetry	Unit-Cell Parameters
Triclinic	1× 1-fold	$a \neq b \neq c$; $\alpha \neq \beta \neq \gamma$
Monoclinic	1× 2-fold	$a \neq b \neq c$; $\alpha = \gamma = 90°$; $\beta \neq 90°$
Orthorhombic	3× 2-fold	$a \neq b \neq c$; $\alpha = \beta = \gamma = 90°$
Tetragonal	1× 4-fold	$a = b \neq c$; $\alpha = \beta = \gamma = 90°$
Trigonal	1× 3-fold	$a = b \neq c$; $\alpha = \beta = 90°$; $\gamma = 120°$
Hexagonal	1× 6-fold	$a = b \neq c$; $\alpha = \beta = 90°$; $\gamma = 120°$
Cubic	4× 3-fold	$a = b = c$; $\alpha = \beta = \gamma = 90°$

Bravais lattices

Combining crystal systems with unit cell centerings leads to the fourteen possible Bravais lattices

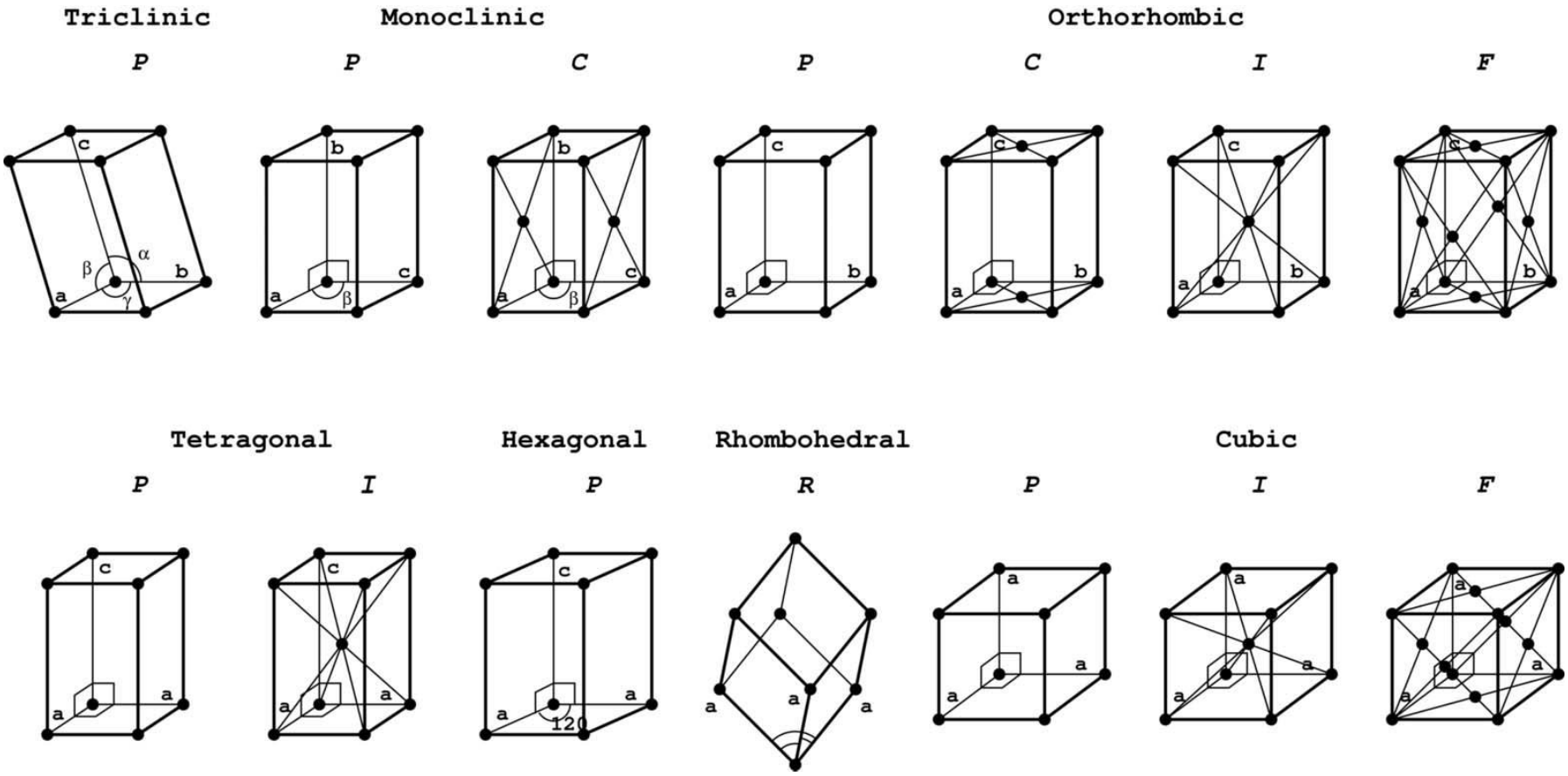

Institute for Chemical and Bioengineering, ETH Zurich, Zurich, Switzerland
Laboratory for Catalysis and Sustainable Chemistry, Paul Scherrer Institute, Villigen, Switzerland

Miller indices (hkl)

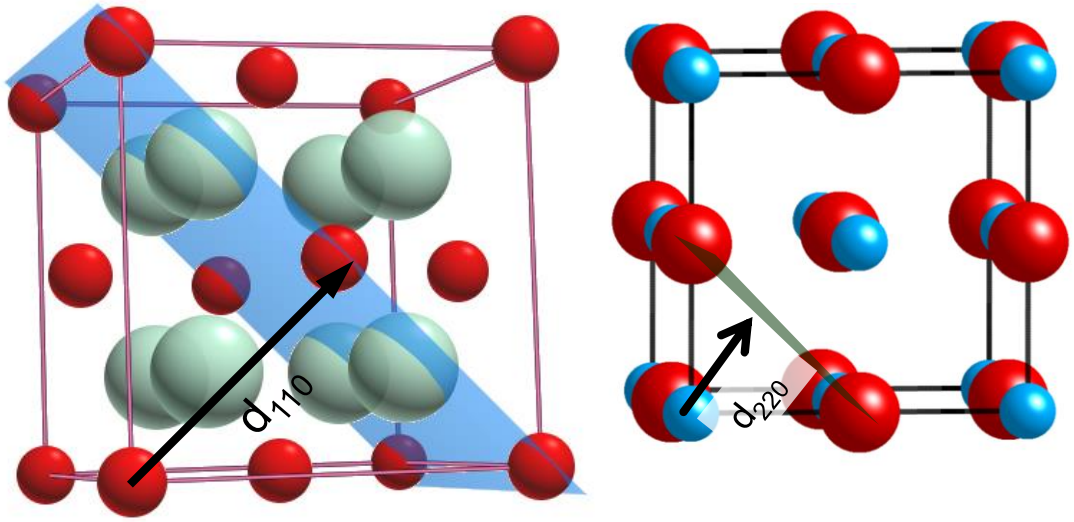

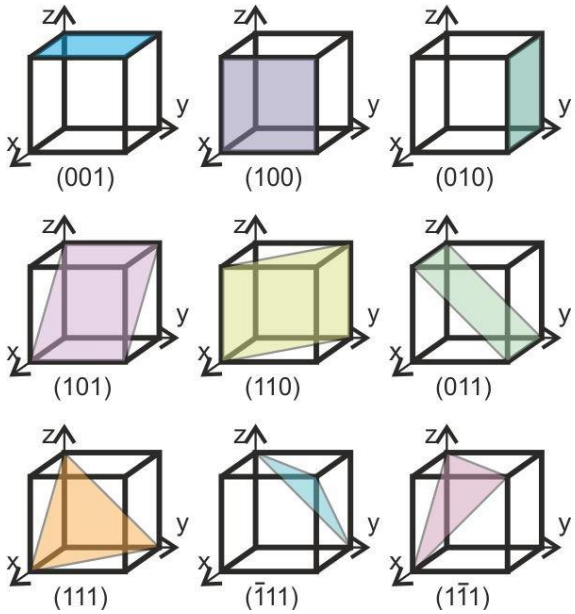

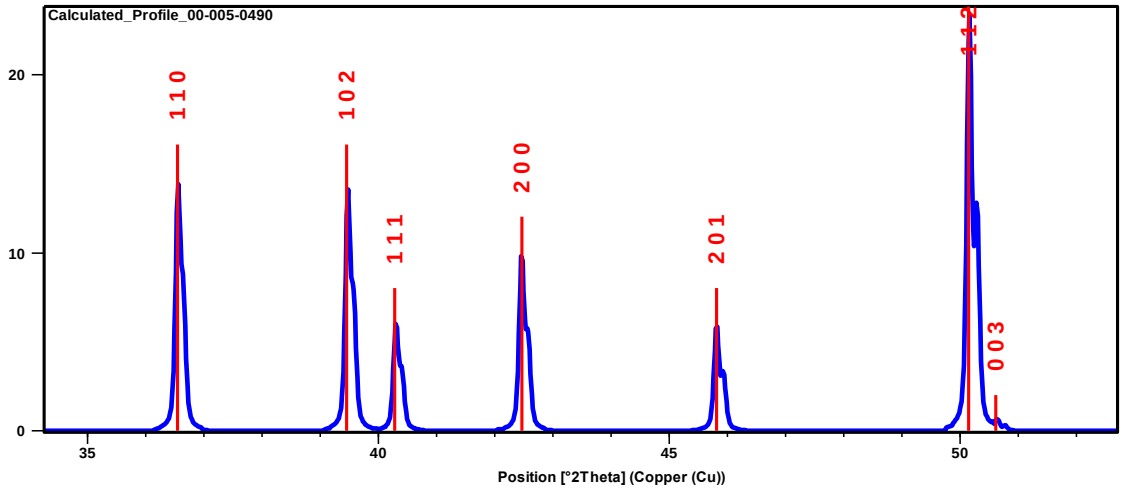

Miller indices represent the lattice planes. Peaks in a diffraction pattern can be assigned to planes of the crystal

Institute for Chemical and Bioengineering, ETH Zurich, Zurich, Switzerland
Laboratory for Catalysis and Sustainable Chemistry, Paul Scherrer Institute, Villigen, Switzerland

Reciprocal space

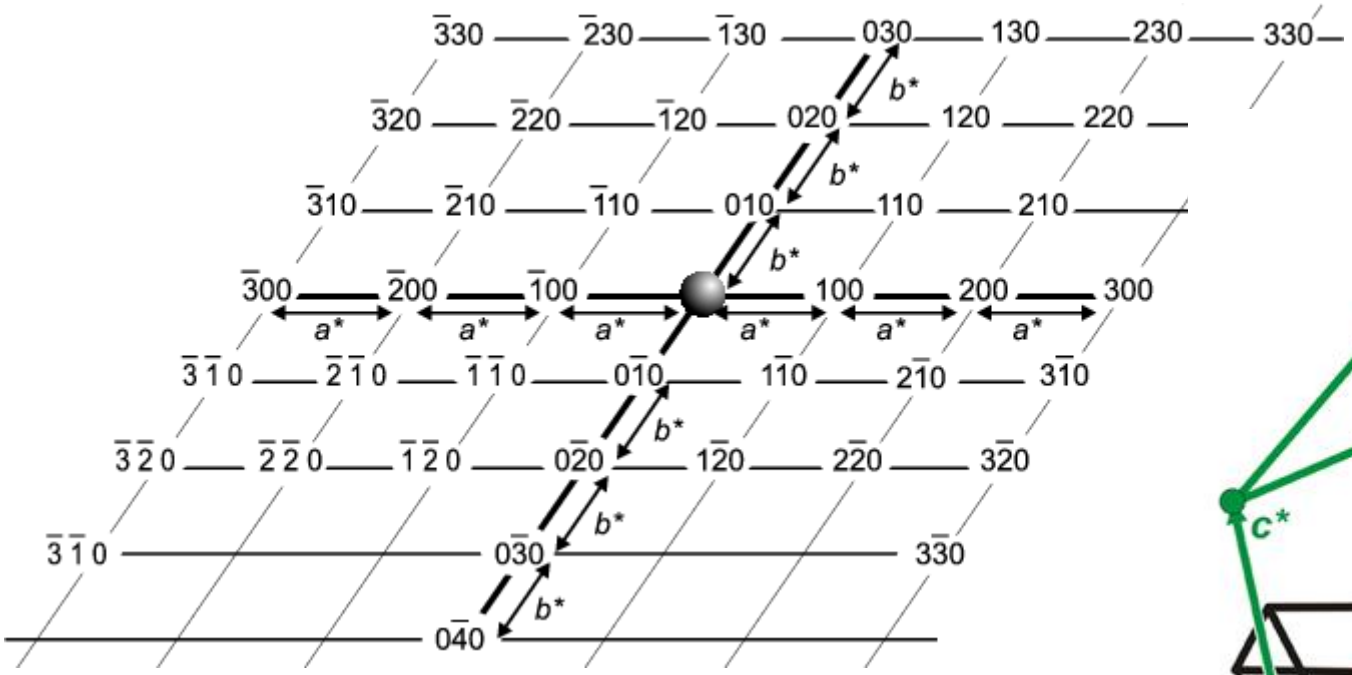

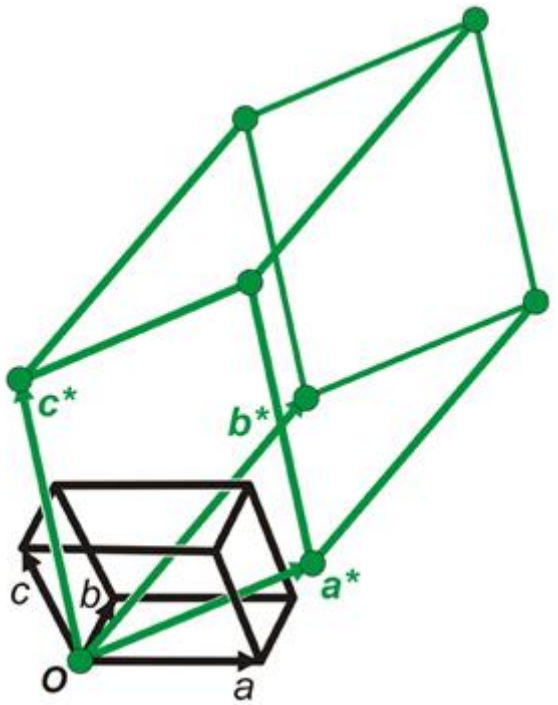

$$\mathbf{d}^* = h\mathbf{a}^* + k\mathbf{b}^* + l\mathbf{c}^*$$

$$1/d = d^*$$

$$a^* = \frac{b \times c}{V};\ b^* = \frac{c \times a}{V};\ c^* = \frac{a \times b}{V};$$

Institute for Chemical and Bioengineering, ETH Zurich, Zurich, Switzerland
Laboratory for Catalysis and Sustainable Chemistry, Paul Scherrer Institute, Villigen, Switzerland

Miller indices (hkl) and d-spacing

d-spacings in different crystal systems

Crystal system	d_{hkl} as a function of Miller indices and lattice parameters
Cubic	$\frac{1}{d^2} = \frac{h^2+k^2+l^2}{a^2}$
Tetragonal	$\frac{1}{d^2} = \frac{h^2+k^2}{a^2} + \frac{l^2}{c^2}$
Orthorhombic	$\frac{1}{d^2} = \frac{h^2}{a^2} + \frac{k^2}{b^2} + \frac{l^2}{c^2}$
Hexagonal	$\frac{1}{d^2} = \frac{4}{3}\left(\frac{h^2+hk+k^2}{a^2}\right) + \frac{l^2}{c^2}$
Monoclinic	$\frac{1}{d^2} = \frac{1}{\sin^2\beta}\left(\frac{h^2}{a^2} + \frac{k^2\sin^2\beta}{b^2} + \frac{l^2}{c^2} - \frac{2hl\cos\beta}{ac}\right)$

Systematic absences

Lattice Centering	Symmetry Operator(s)	Reflection Condition
P	-	None
A	$x,1/2+y,1/2+z$	hkl: $k + l = 2n$
B	$1/2+x,y,1/2+z$	hkl: $h + l = 2n$
C	$1/2+x,1/2+y,z$	hkl: $h + k = 2n$
F	$x,1/2+y,1/2+z$; $1/2+x,y,1/2+z$; $1/2+x,1/2+y,z$	hkl: $k + l$, $h + l$, $h + k = 2n$
I	$1/2+x,1/2+y,1/2+z$	hkl: $h + k + l = 2n$
R	$1/3+x,2/3+y,2/3+z$; $2/3+x,1/3+y,1/3+z$	hkl: $-h + k + l = 3n$

Rotary-Inversion Symmetry

Symmetry operation	Symmetry elements
Identity	----
Rotation by 360°/n	n-fold axis
Reflection	mirror plane
Inversion	point

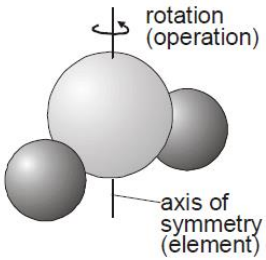

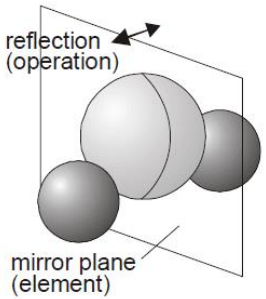

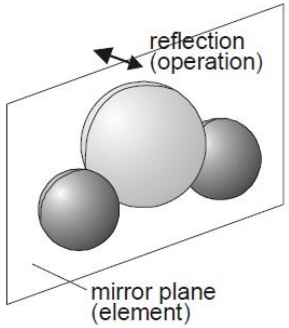

Translation
(Bravais lattice)

screw axis
glide plane

Institute for Chemical and Bioengineering, ETH Zurich, Zurich, Switzerland
Laboratory for Catalysis and Sustainable Chemistry, Paul Scherrer Institute, Villigen, Switzerland

Rotary-Inversion Symmetry

Symmetry operation	Symmetry elements
Identity	----
Rotation by 360°/n	n-fold axis
Reflection	mirror plane
Inversion	point

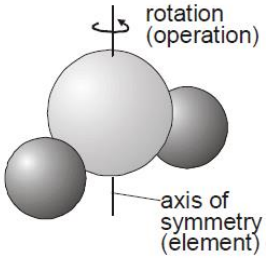

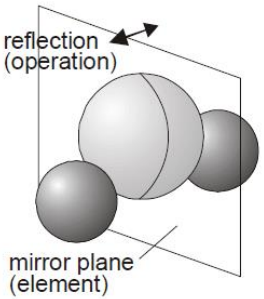

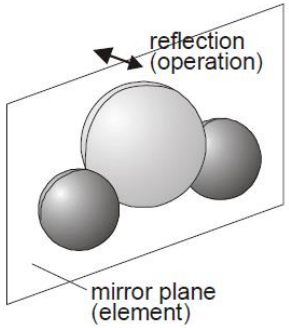

Translation
(Bravais lattice)

230 space groups
e.g. *Pm3m**

*http://img.chem.ucl.ac.uk/sgp/misc/notation.htm

Institute for Chemical and Bioengineering, ETH Zurich, Zurich, Switzerland
Laboratory for Catalysis and Sustainable Chemistry, Paul Scherrer Institute, Villigen, Switzerland
Przemyslaw Rzepka

Space groups

Triclinic: e.g. *P*-1

1. An inversion center (presence or absence)

Monoclinic: e.g. *P*2, *Pm*, *P*2/*m*

1. A symmetry with respect to the unique axis direction (b or c)

Orthorhombic: e.g. *P*222, *Pmm*2 (or *Pm*2*m* or *P*2*mm*), *Pmmm*

1. A symmetry with respect to the a axis
2. A symmetry with respect to the b axis
3. A symmetry with respect to the c axis

Tetragonal: e.g. *P*4, *P*-4, *P*4/*m*, *P*422, *P*4*mm*, *P*-42*m* (or *P*-4*m*2), *P*4/*mmm*

1. The 4-fold symmetry parallel to the *c* axis
2. The symmetry with respect to both the *x* and *y* axes
3. The symmetry with respect to the face diagonals [1 1 0]

Space groups

Trigonal & Rhombohedral: e.g. *P*3, *P*-3, *P*321, *P*312, *P*3*m*1, *P*31*m*, *P*-3*m*1, *P*-31*m*

1. The 3-fold symmetry parallel to the *c* axis
2. The symmetry with respect to the *a* and *b* axes
3. The additional symmetry elements with respect to [2 1 0]

Hexagonal: e.g. *P*6, *P*-6, *P*6/*m*, *P*622, *P*6*mm*, *P*-62*m* (or *P*-6*m*2), *P*6/*mmm*

1. The 6-fold symmetry parallel to the *c* axis
2. The symmetry with respect to the *a* and *b* axes
3. The additional symmetry elements with respect to [2 1 0]

Cubic: e.g. *P*23, *Pm*-3, *P*432, *P*-43*m*, *Pm*3*m*

1. The symmetry with respect to the *a*, *b*, and *c* axes
2. The 3-fold symmetry of the body diagonals [1 1 1]
3. The symmetry with respect to the face diagonals [1 1 0]

Tables for X-ray Crystallography

$P4_32_12$ D_4^8 422 Tetragonal

No. 96 $P4_32_12$ Patterson symmetry $P4/mmm$

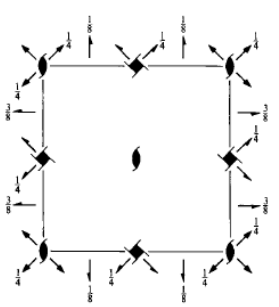

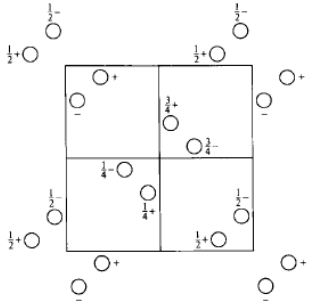

Origin on $2\,[1\,1\,0]$ at $2_1\,1\,(1,2)$

Asymmetric unit $0 \le x \le 1;\quad 0 \le y \le 1;\quad 0 \le z \le \frac{1}{8}$

Symmetry operations

(1) 1
(2) $2(0,0,\frac{1}{2})$ $0,0,z$
(3) $4^-(0,0,\frac{1}{4})$ $0,\frac{1}{2},z$
(4) $4\ (0,0,\frac{1}{2})$ $\frac{1}{2},0,z$
(5) $2(0,\frac{1}{2},0)$ $\frac{1}{4},y,\frac{3}{8}$
(6) $2(\frac{1}{2},0,0)$ $x,\frac{1}{4},\frac{1}{8}$
(7) 2 $x,x,0$
(8) 2 $x,\bar{x},\frac{1}{4}$

Generators selected (1); $t(1,0,0)$; $t(0,1,0)$; $t(0,0,1)$; (2); (3); (5)

Positions

Multiplicity, Wyckoff letter, Site symmetry		Coordinates				Reflection conditions
						General:
8	b	1	(1) x,y,z	(2) $\bar{x},\bar{y},z+\frac{1}{2}$	(3) $\bar{y}+\frac{1}{2},x+\frac{1}{2},z+\frac{3}{4}$	(4) $y+\frac{1}{2},\bar{x}+\frac{1}{2},z+\frac{1}{4}$
			(5) $\bar{x}+\frac{1}{2},y+\frac{1}{2},\bar{z}+\frac{1}{4}$	(6) $x+\frac{1}{2},\bar{y}+\frac{1}{2},\bar{z}+\frac{1}{4}$	(7) $y,x,\bar{z}$	(8) $\bar{y},\bar{x},\bar{z}+\frac{1}{2}$
						$00l:\ l=4n$
						$h00:\ h=2n$
						Special: as above, plus
4	a	$..2$	$x,x,0$	$\bar{x},\bar{x},\frac{1}{2}$	$\bar{x}+\frac{1}{2},x+\frac{1}{2},\frac{3}{4}$	$x+\frac{1}{2},\bar{x}+\frac{1}{2},\frac{1}{4}$
						$0kl:\ l=2n+1$ or $2k+l=4n$

Symmetry of special projections

Along [001] $p4gm$
$\mathbf{a}'=\mathbf{a}$ $\mathbf{b}'=\mathbf{b}$
Origin at $0,\frac{1}{2},z$

Along [100] $p2gg$
$\mathbf{a}'=\mathbf{b}$ $\mathbf{b}'=\mathbf{c}$
Origin at $x,\frac{1}{4},\frac{1}{8}$

Along [110] $p2gm$
$\mathbf{a}'=\frac{1}{2}(-\mathbf{a}+\mathbf{b})$ $\mathbf{b}'=\mathbf{c}$
Origin at $x,x,0$

Maximal non-isomorphic subgroups

I [2] $P4_32_12$ ($P4_32_12$, 78) 1; 2; 3; 4
[2] $P2_12_12$ ($C222_1$, 20) 1; 2; 7; 8
[2] $P2_12_12_1$ ($P2_12_12_1$, 19) 1; 2; 5; 6

IIa none

IIb none

Maximal isomorphic subgroups of lowest index

IIc [3] $P4_12_12$ ($\mathbf{c}'=3\mathbf{c}$) (92); [5] $P4_32_12$ ($\mathbf{c}'=5\mathbf{c}$) (96); [9] $P4_32_12$ ($\mathbf{a}'=3\mathbf{a}, \mathbf{b}'=3\mathbf{b}$) (96)

Minimal non-isomorphic supergroups

I [3] $P4_332$ (212)

II [2] $C4_322$ ($P4_322$, 95); [2] $I4_122$ (98); [2] $P4_22_12$ ($\mathbf{c}'=\frac{1}{2}\mathbf{c}$) (94)

Institute for Chemical and Bioengineering, ETH Zurich, Zurich, Switzerland
Laboratory for Catalysis and Sustainable Chemistry, Paul Scherrer Institute, Villigen, Switzerland
Przemyslaw Rzepka

Brief history of XRD

- 1895- Wilhelm Röntgen publishes the discovery of X-rays
- 1912- Maxwell von Laue observes diffraction of X-rays from a crystal
- 1913- Lawrence Bragg and William Henry Bragg solve the first crystal structure from X-ray diffraction data

Elastic scattering

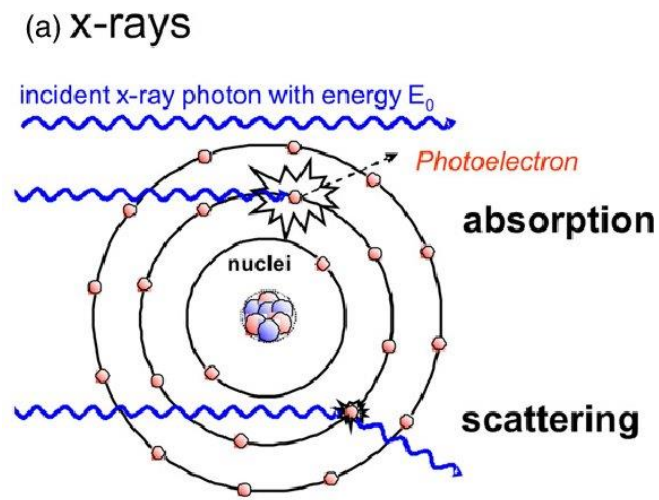

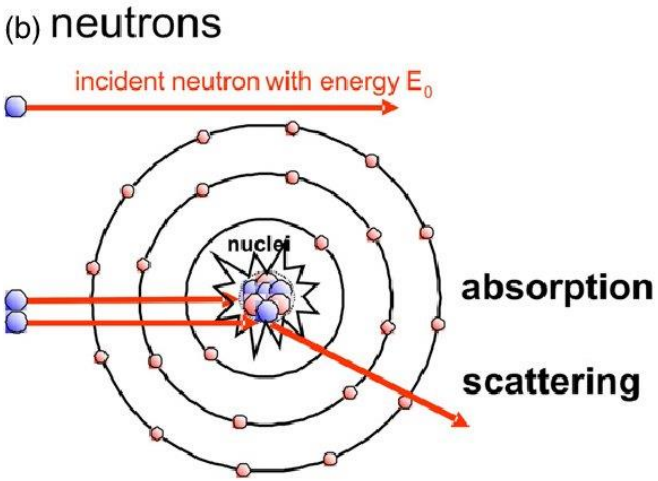

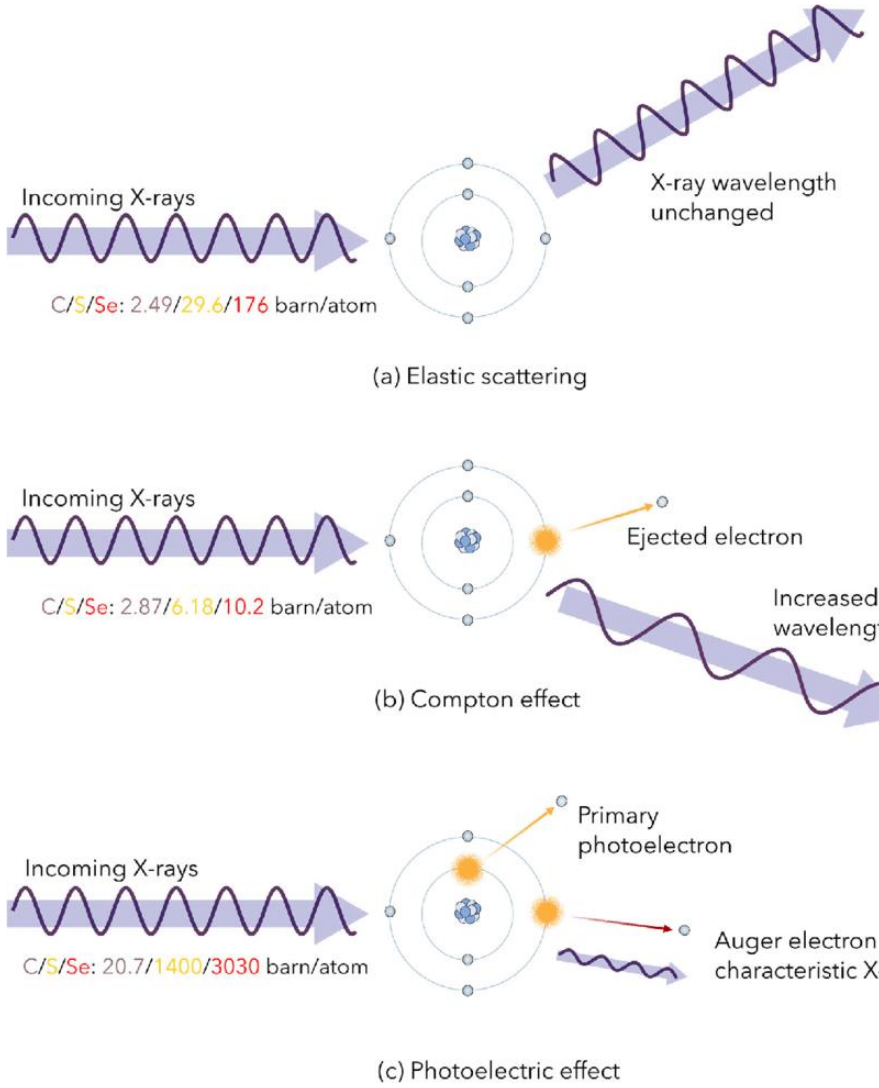

Bragg's Law

Elastic scattering phenomenon that occurs when a plane wave interacts with an obstacle or a slit whose size is approximately that of the wavelength

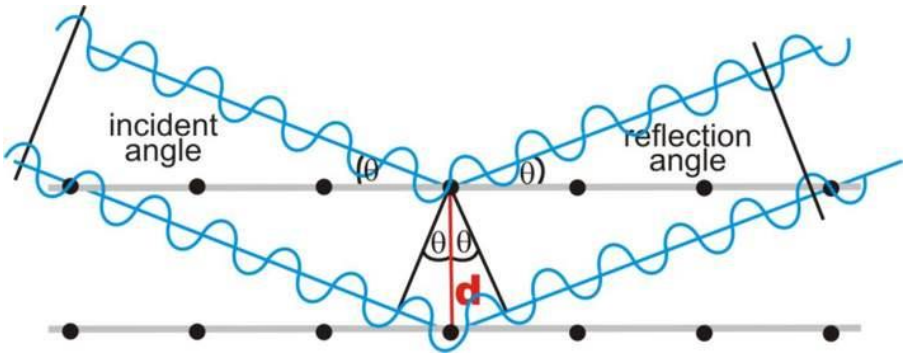

Destructive interference (out of phase).

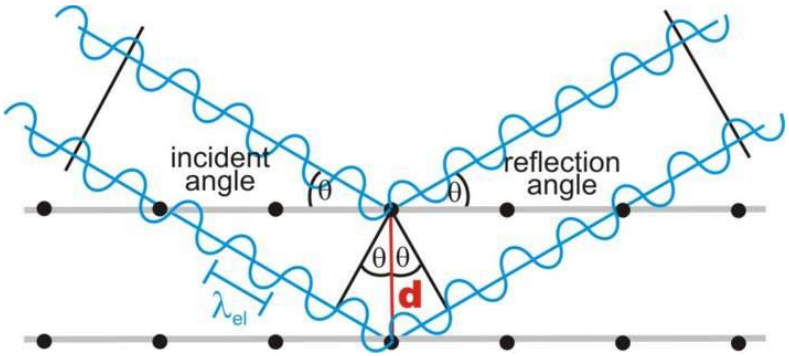

Constructive interference (in phase).

Bragg's Law $n\lambda = 2dsin\theta$

Institute for Chemical and Bioengineering, ETH Zurich, Zurich, Switzerland
Laboratory for Catalysis and Sustainable Chemistry, Paul Scherrer Institute, Villigen, Switzerland

X-ray light source

Particle accelerator (synchrotron source): Electrons accelerated at velocity close to the speed of light emit electromagnetic radiation in the region of X-rays.

- Tunable wavelength
- High brilliance (many photons of a given wavelength and direction)
- X-rays: very high resolution

In-house diffraction: Energy released when an electron from an outer shell “fills the gap” left by an inner shell electron that has been ionized. Kα Cu (1.5418 Å) is the most common

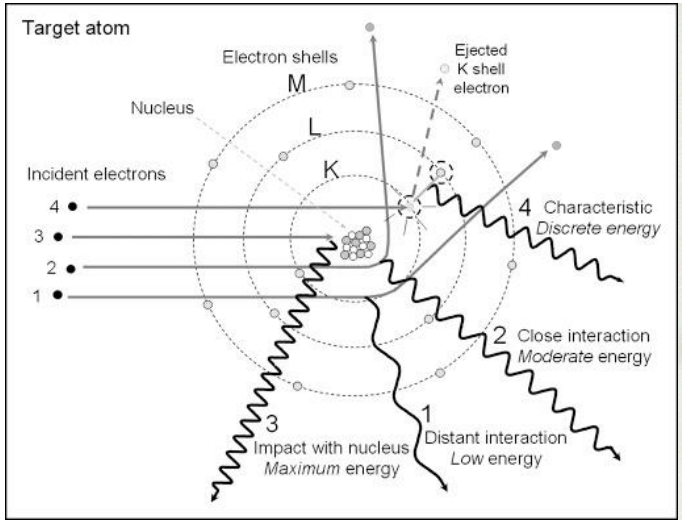

Institute for Chemical and Bioengineering, ETH Zurich, Zurich, Switzerland
Laboratory for Catalysis and Sustainable Chemistry, Paul Scherrer Institute, Villigen, Switzerland

Sources of neutrons

Neutrons for scattering experiments can be produced either by nuclear fission in a reactor (ILL Grenoble) or by spallation when high-energy protons strike a heavy metal target eg. W, Ta, or Pb (SINQ).

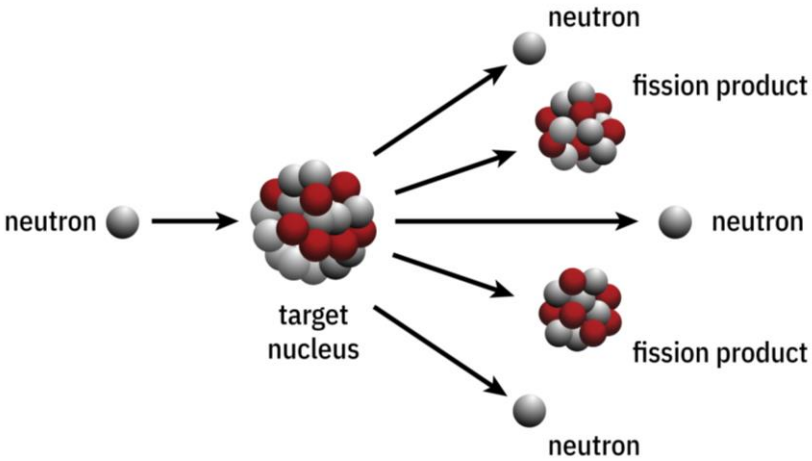

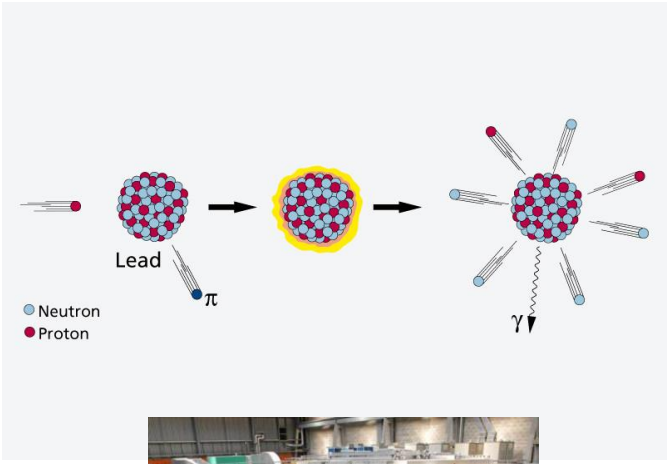

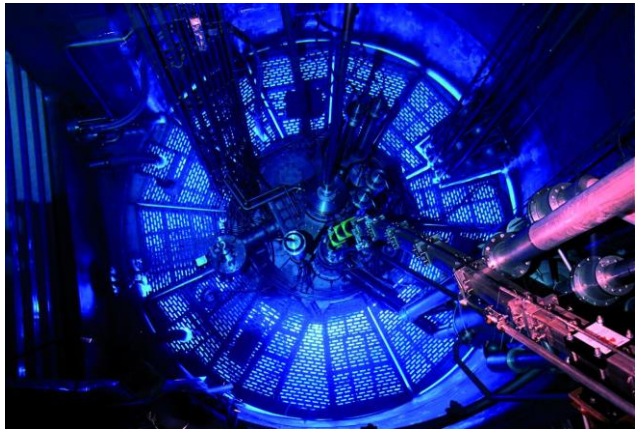

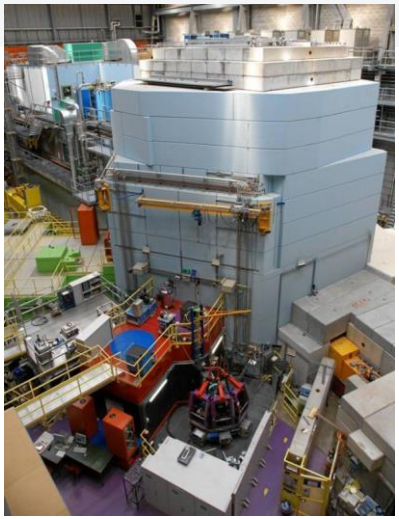

Institute for Chemical and Bioengineering, ETH Zurich, Zurich, Switzerland
Laboratory for Catalysis and Sustainable Chemistry, Paul Scherrer Institute, Villigen, Switzerland

Comparison of different radiations

	X-ray (powder)	Electrons	Neutrons (powder)
Data collection	easy	Less easy	difficult
Crystallite size	µm	nm	µm
Lattice parameters	precise	approximate	precise
Intensities	kinematical	dynamical	kinematical
Overlap	yes	no	yes
Image	no	yes	no
Magnetic moment	no	yes	yes
Scattering power against Z	smooth	smooth	irregular

Diffraction geometry

The Bragg-Brentano (reflection) geometry needs the simultaneous, equiaxial move of the anode and the detector (2θ) to provide the constant irradiated volume from a sample

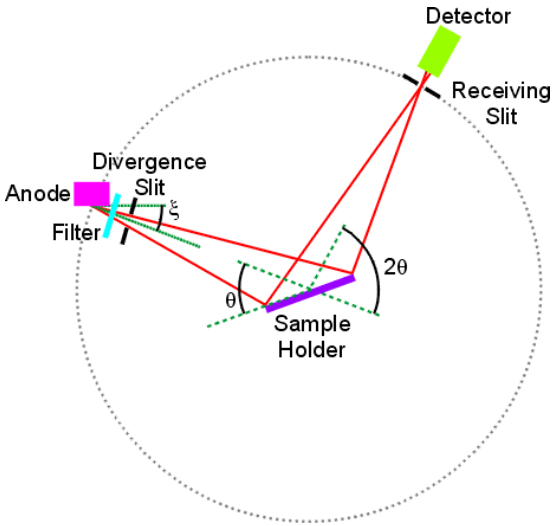

The Debye-Scherrer (transmission) geometry

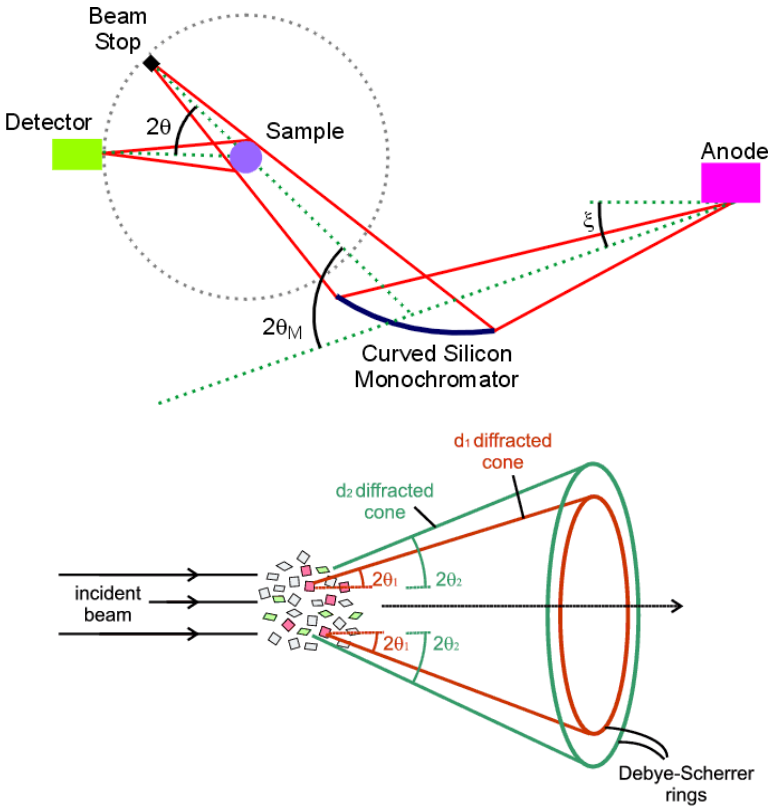

Institute for Chemical and Bioengineering, ETH Zurich, Zurich, Switzerland
Laboratory for Catalysis and Sustainable Chemistry, Paul Scherrer Institute, Villigen, Switzerland

Diffraction geometry

The Bragg-Brentano (reflection) geometry needs the simultaneous, equiaxial move of the anode and the detector (2θ) to provide the constant irradiated volume from a sample

The Debye-Scherrer (transmission) geometry

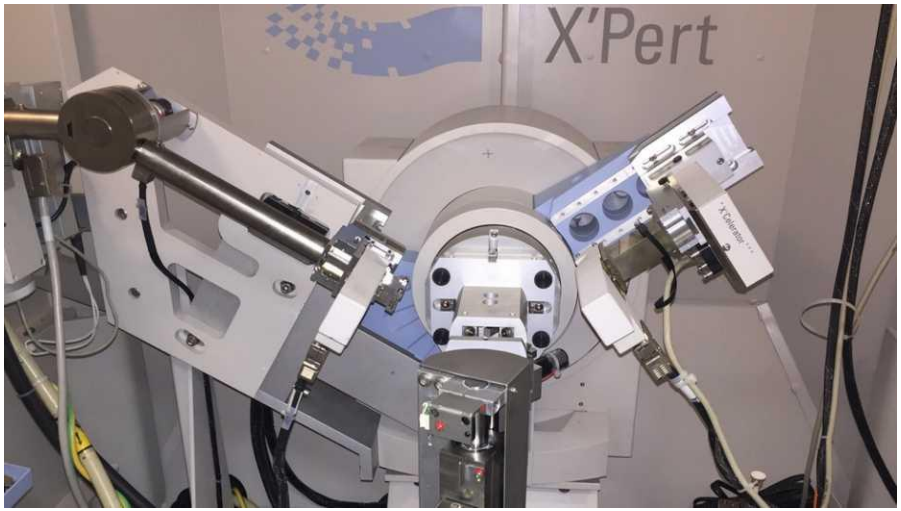

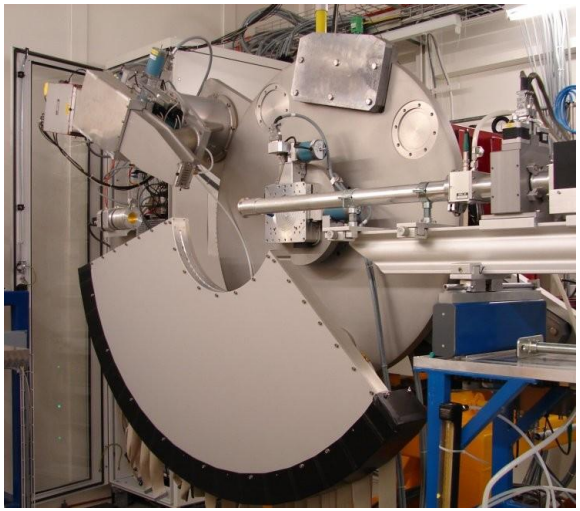

Institute for Chemical and Bioengineering, ETH Zurich, Zurich, Switzerland
Laboratory for Catalysis and Sustainable Chemistry, Paul Scherrer Institute, Villigen, Switzerland

X-ray Powder Diffraction

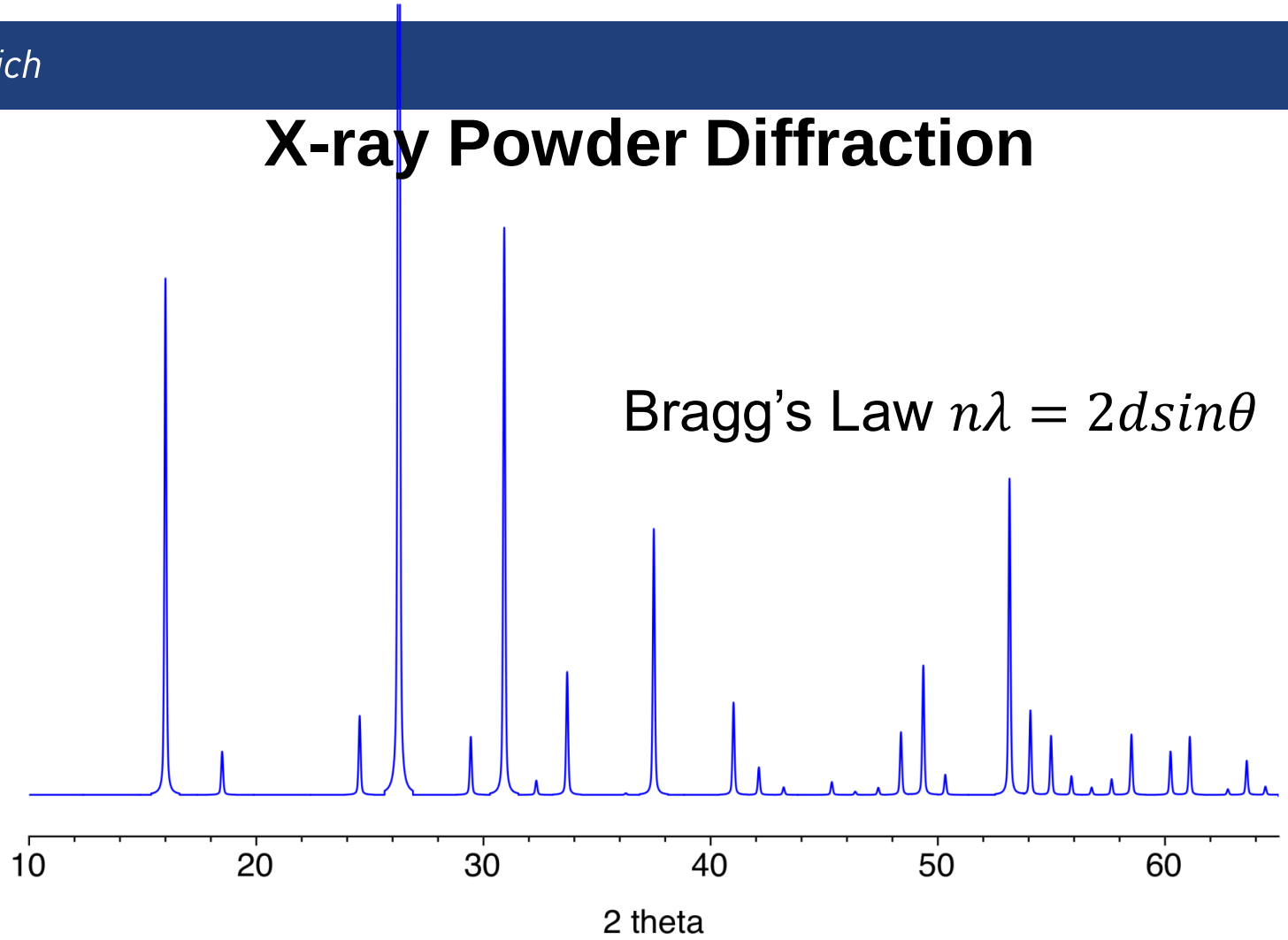

Peak positions: lattice planes (unit cell, symmetry)

Peak intensities: atoms on the planes

Peak shape: microstructure (crystal size, microstrain, lattice defects)

Institute for Chemical and Bioengineering, ETH Zurich, Zurich, Switzerland
Laboratory for Catalysis and Sustainable Chemistry, Paul Scherrer Institute, Villigen, Switzerland

Structure factor

$$F_{hkl} = \sum_j f_j \cdot e^{i2\pi(hx_j + ky_j + lz_j)} = \left|F_{hkl}\right| \cdot e^{i\phi_{hkl}}$$

Structure factor contains the amplitude and phase of the wave diffracted by each plane hkl

$$I_{obs}(hkl) = c\ j\ P\ L\ A \left|F_{obs}(hkl)\right|^2$$

- multiplicity, *j*
- the polarization factor, *P*
- the Lorentz factor, *L*
- X-ray absorption, *A*
- temperature

Structure factor

$$F_{hkl} = \sum_j f_j \cdot e^{i2\pi(hx_j + ky_j + lz_j)} = \left|F_{hkl}\right| \cdot e^{i\phi_{hkl}}$$

Structure factor phases are lost in diffraction data

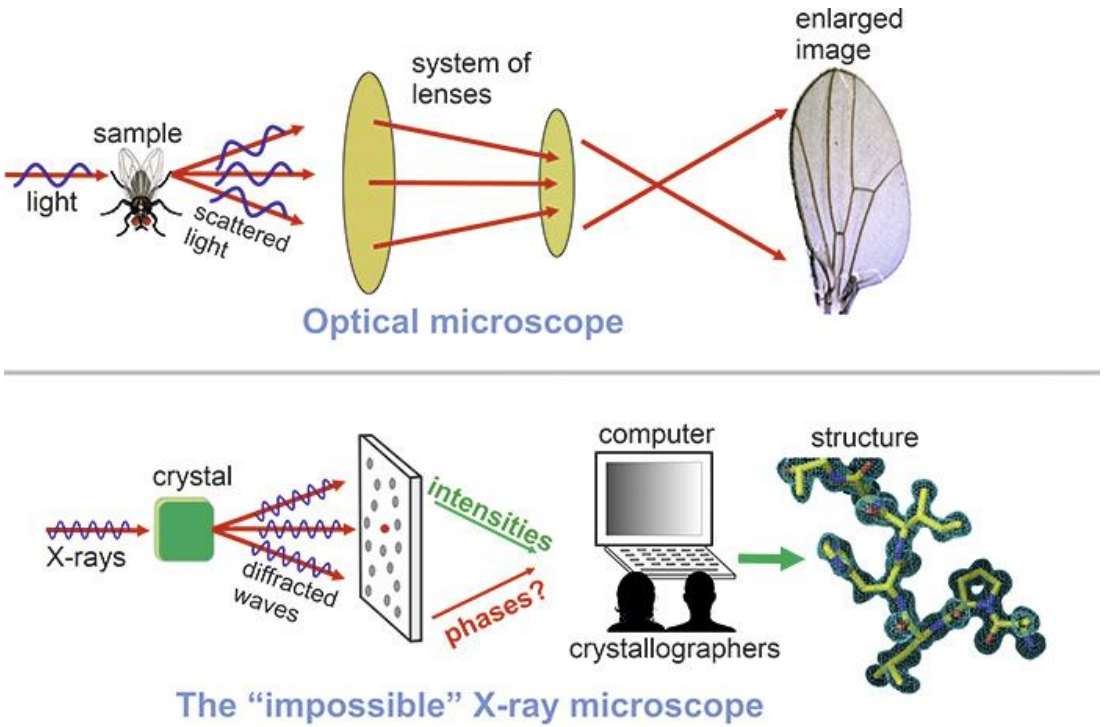

Institute for Chemical and Bioengineering, ETH Zurich, Zurich, Switzerland
Laboratory for Catalysis and Sustainable Chemistry, Paul Scherrer Institute, Villigen, Switzerland

Structure factor

$$F_{hkl} = \sum_j f_j \cdot e^{i2\pi(hx_j + ky_j + lz_j)} = \left|F_{hkl}\right| \cdot e^{i\phi_{hkl}}$$

From the electron densities calculated from structure factor for each plane to measured intensities

Crystal structure (3D)

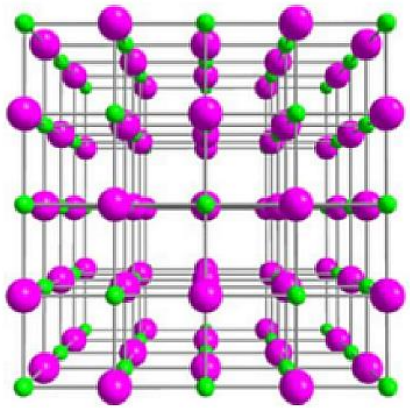

$$\mathbf{F}(\mathbf{h}) = \int_{cell} \rho(\mathbf{x}) \exp(2\pi i \mathbf{h}\cdot\mathbf{x}) d\mathbf{v}$$

Diffraction experiment

$$\rho(\mathbf{x}) = \frac{1}{V}\sum_{\mathbf{h}} \mathbf{F}(\mathbf{h}) \exp(-2\pi i \mathbf{h}\cdot\mathbf{x})$$

Structure solution

Diffraction pattern (1D)

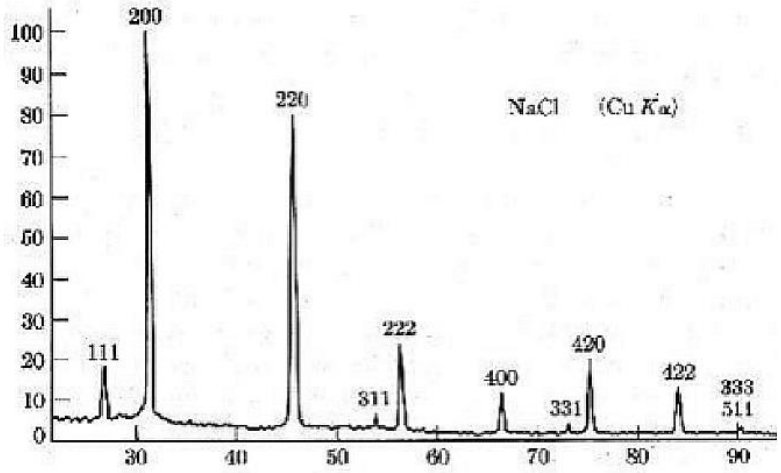

Institute for Chemical and Bioengineering, ETH Zurich, Zurich, Switzerland
Laboratory for Catalysis and Sustainable Chemistry, Paul Scherrer Institute, Villigen, Switzerland

Scattering power of an element

The amplitude of the scattered wave is called the atomic form factor f (X-rays) or scattering length b (neutrons).

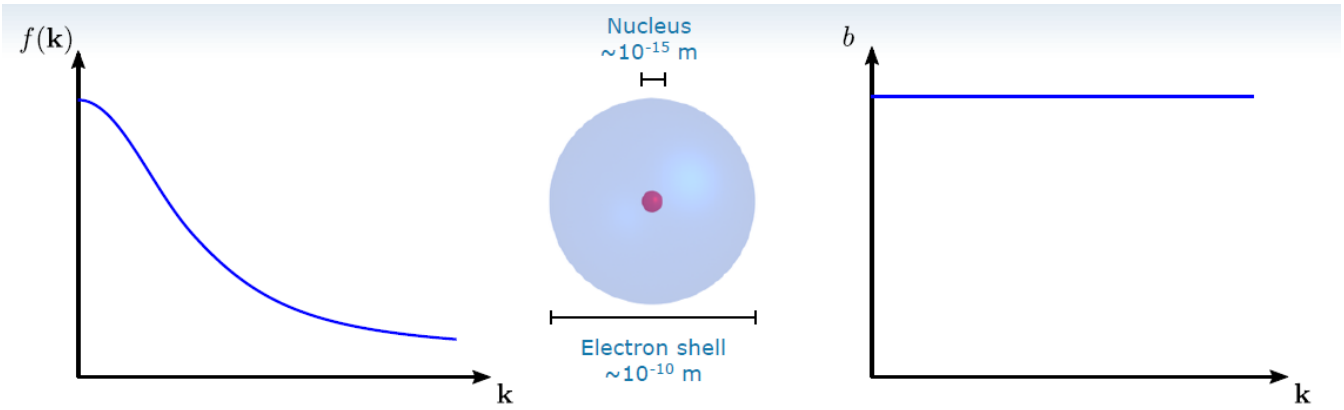

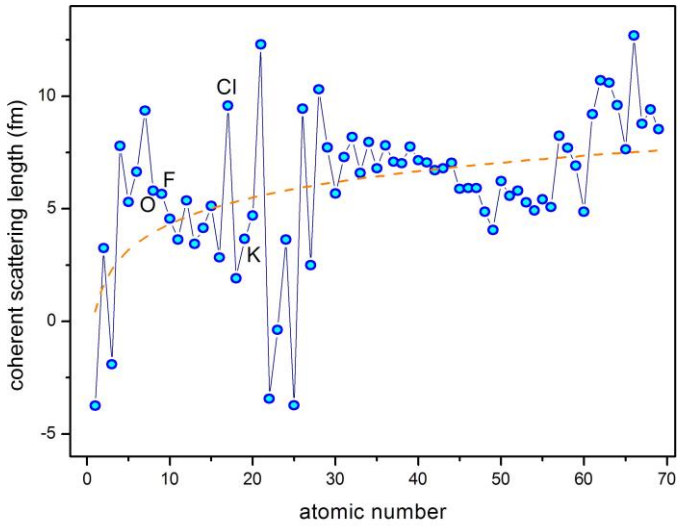

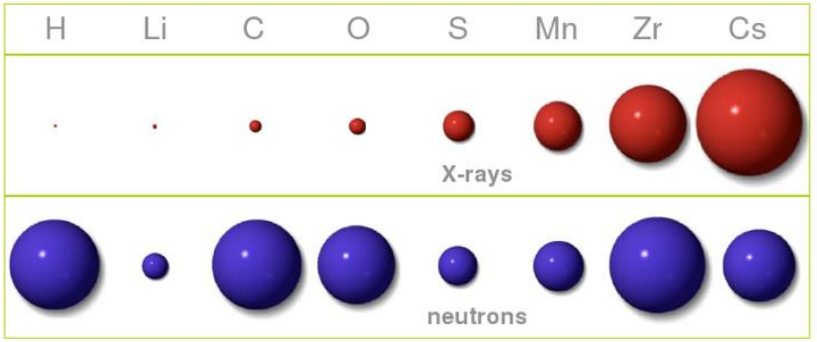

Institute for Chemical and Bioengineering, ETH Zurich, Zurich, Switzerland
Laboratory for Catalysis and Sustainable Chemistry, Paul Scherrer Institute, Villigen, Switzerland

X-ray Atomic Form Factor

Atomic form factor represents the scattering power of specific element regardless its positioning or symmetry. It depends only on number of electrons, radiation energy and Debye-Waller factor (2Θ)

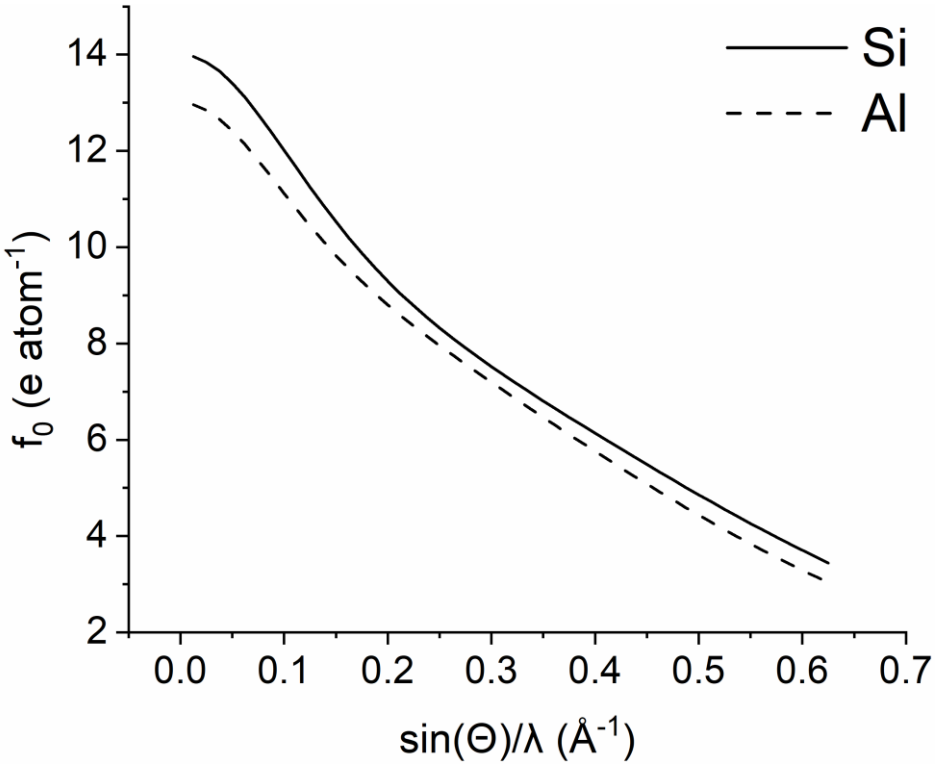

Silicon and aluminum demonstrate similar atomic number (Z=14 and 13) and are difficult to be distinguished

Institute for Chemical and Bioengineering, ETH Zurich, Zurich, Switzerland
Laboratory for Catalysis and Sustainable Chemistry, Paul Scherrer Institute, Villigen, Switzerland

X-ray Single-crystal Diffraction

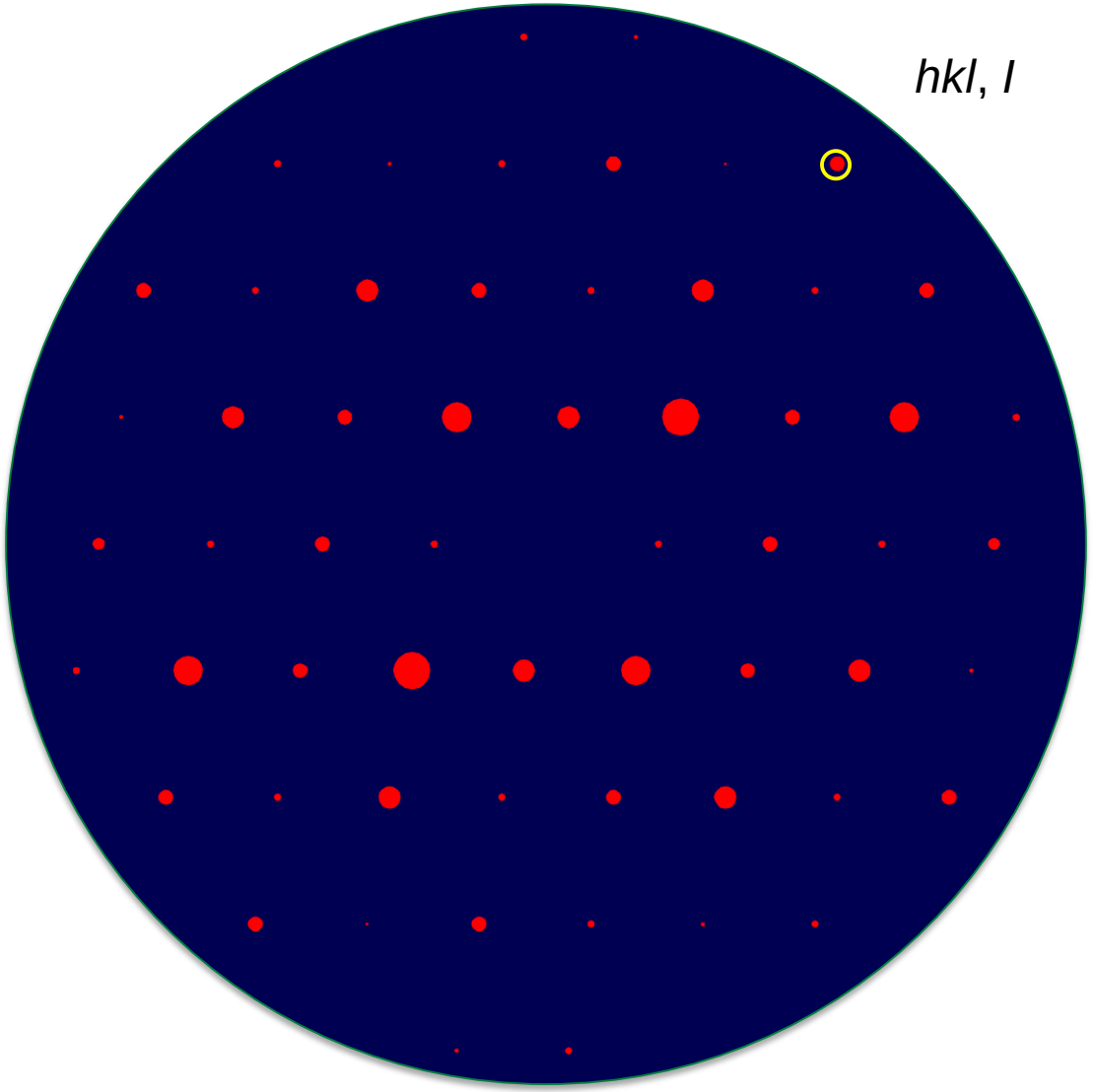

X-rays

$10^6\ \mu m^3$

Institute for Chemical and Bioengineering, ETH Zurich, Zurich, Switzerland
Laboratory for Catalysis and Sustainable Chemistry, Paul Scherrer Institute, Villigen, Switzerland

X-ray Powder Diffraction

X-rays

1 μm^3

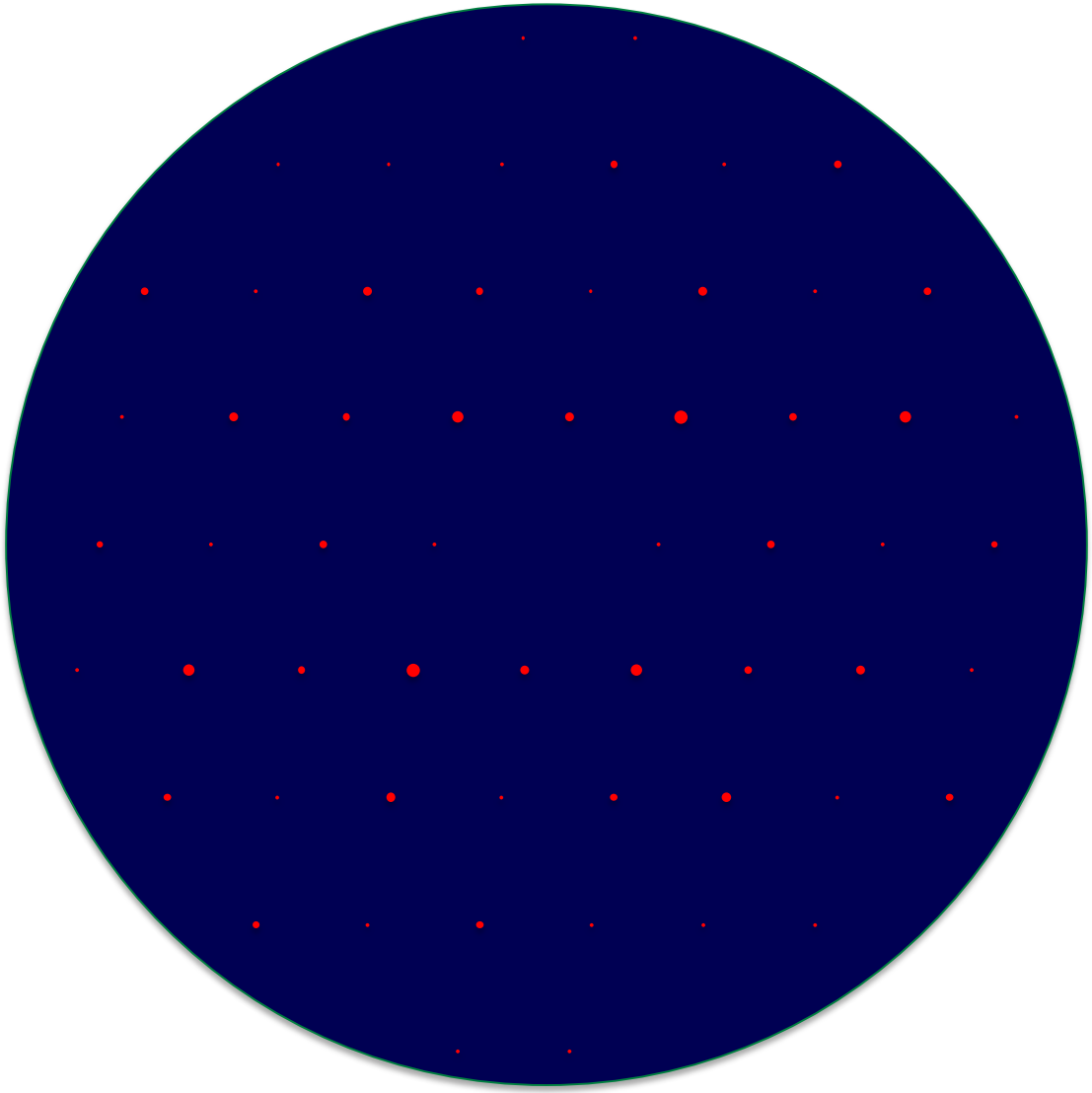

Institute for Chemical and Bioengineering, ETH Zurich, Zurich, Switzerland
Laboratory for Catalysis and Sustainable Chemistry, Paul Scherrer Institute, Villigen, Switzerland

X-ray Powder Diffraction

X-rays

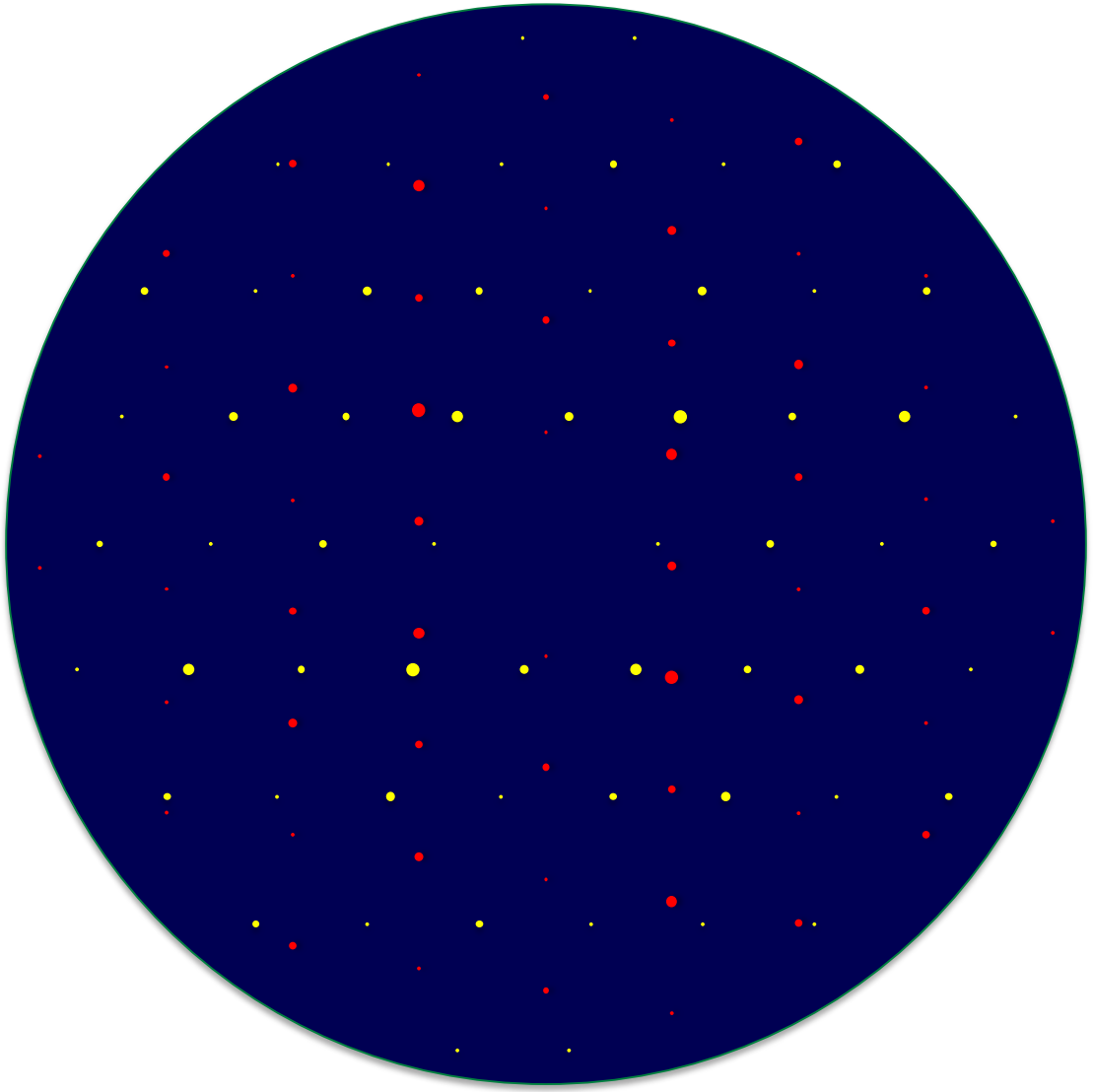

Institute for Chemical and Bioengineering, ETH Zurich, Zurich, Switzerland
Laboratory for Catalysis and Sustainable Chemistry, Paul Scherrer Institute, Villigen, Switzerland

X-ray Powder Diffraction

X-rays

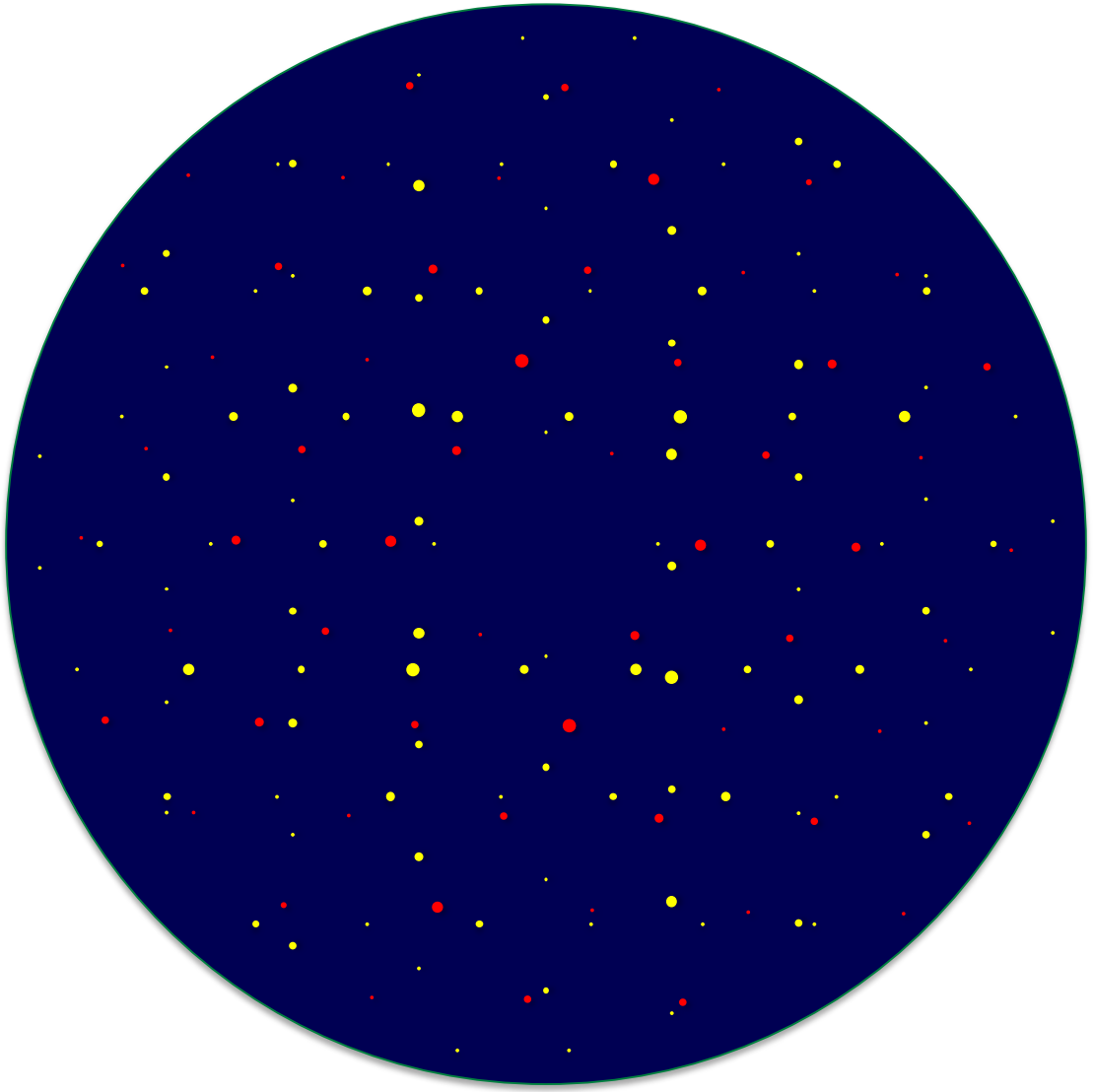

Institute for Chemical and Bioengineering, ETH Zurich, Zurich, Switzerland
Laboratory for Catalysis and Sustainable Chemistry, Paul Scherrer Institute, Villigen, Switzerland

X-ray Powder Diffraction

X-rays

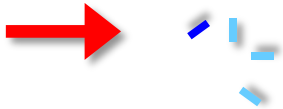

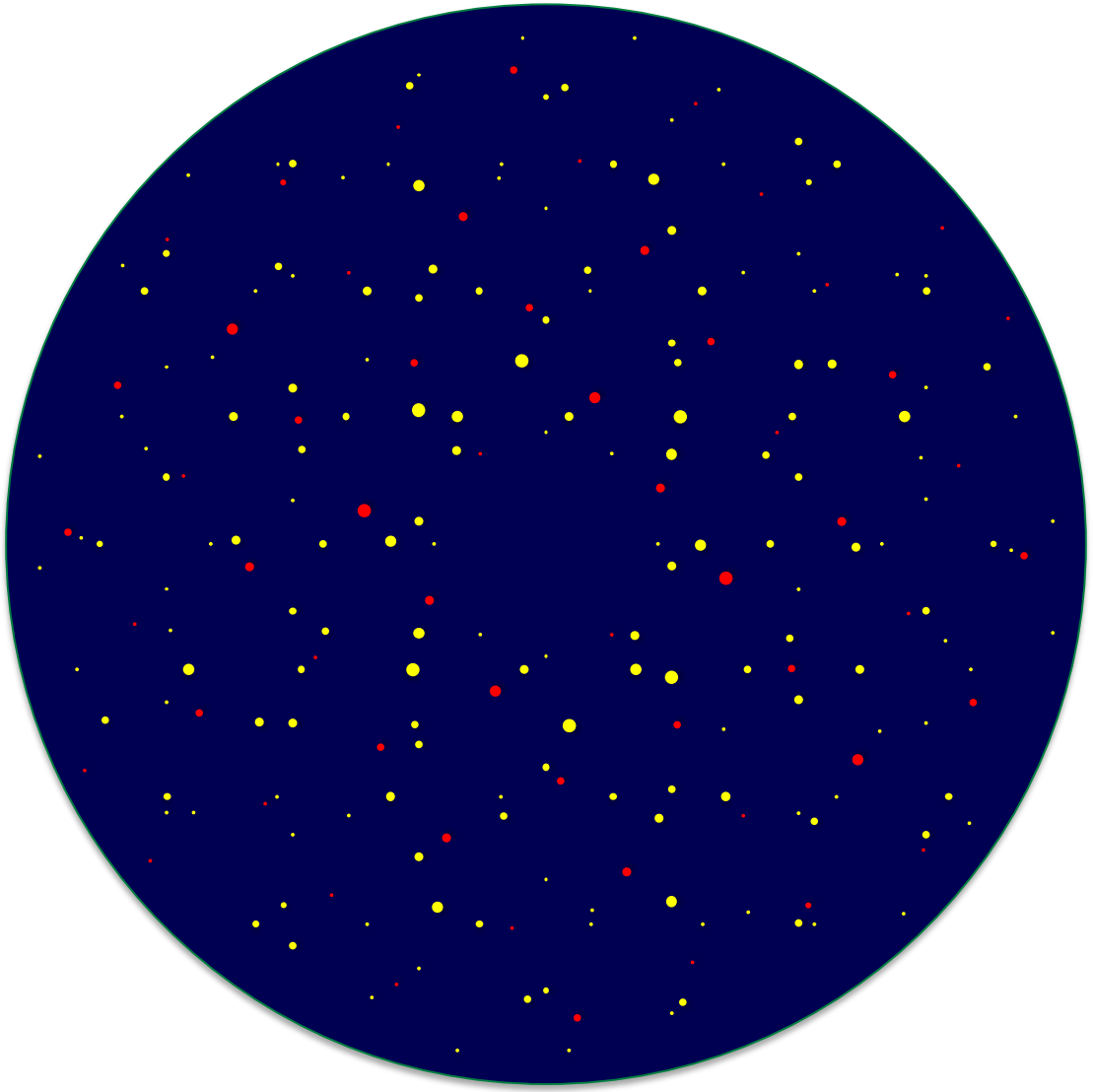

Institute for Chemical and Bioengineering, ETH Zurich, Zurich, Switzerland
Laboratory for Catalysis and Sustainable Chemistry, Paul Scherrer Institute, Villigen, Switzerland

X-ray Powder Diffraction

X-rays

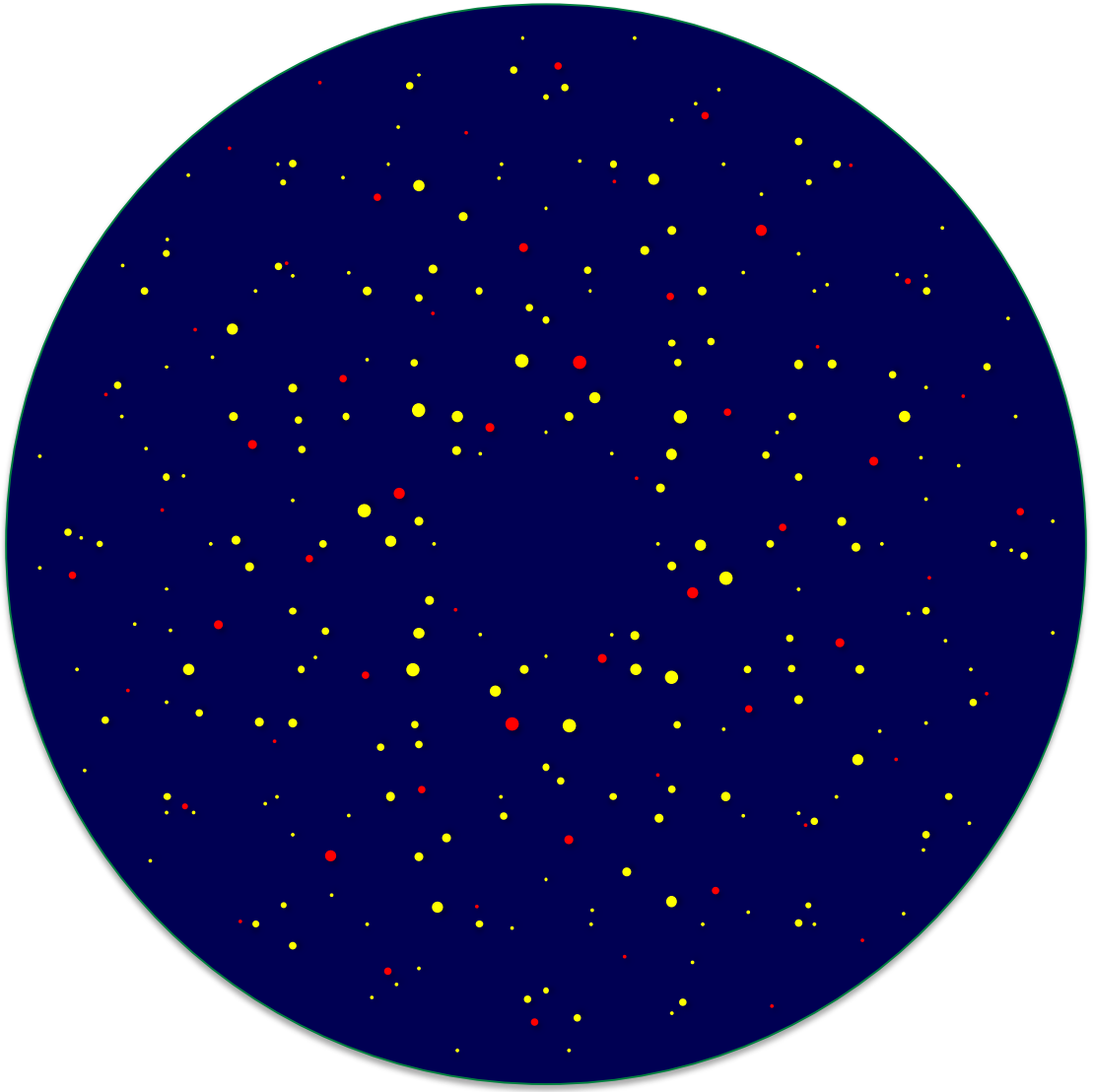

Institute for Chemical and Bioengineering, ETH Zurich, Zurich, Switzerland
Laboratory for Catalysis and Sustainable Chemistry, Paul Scherrer Institute, Villigen, Switzerland

X-ray Powder Diffraction

X-rays

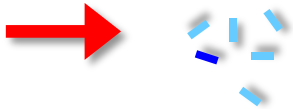

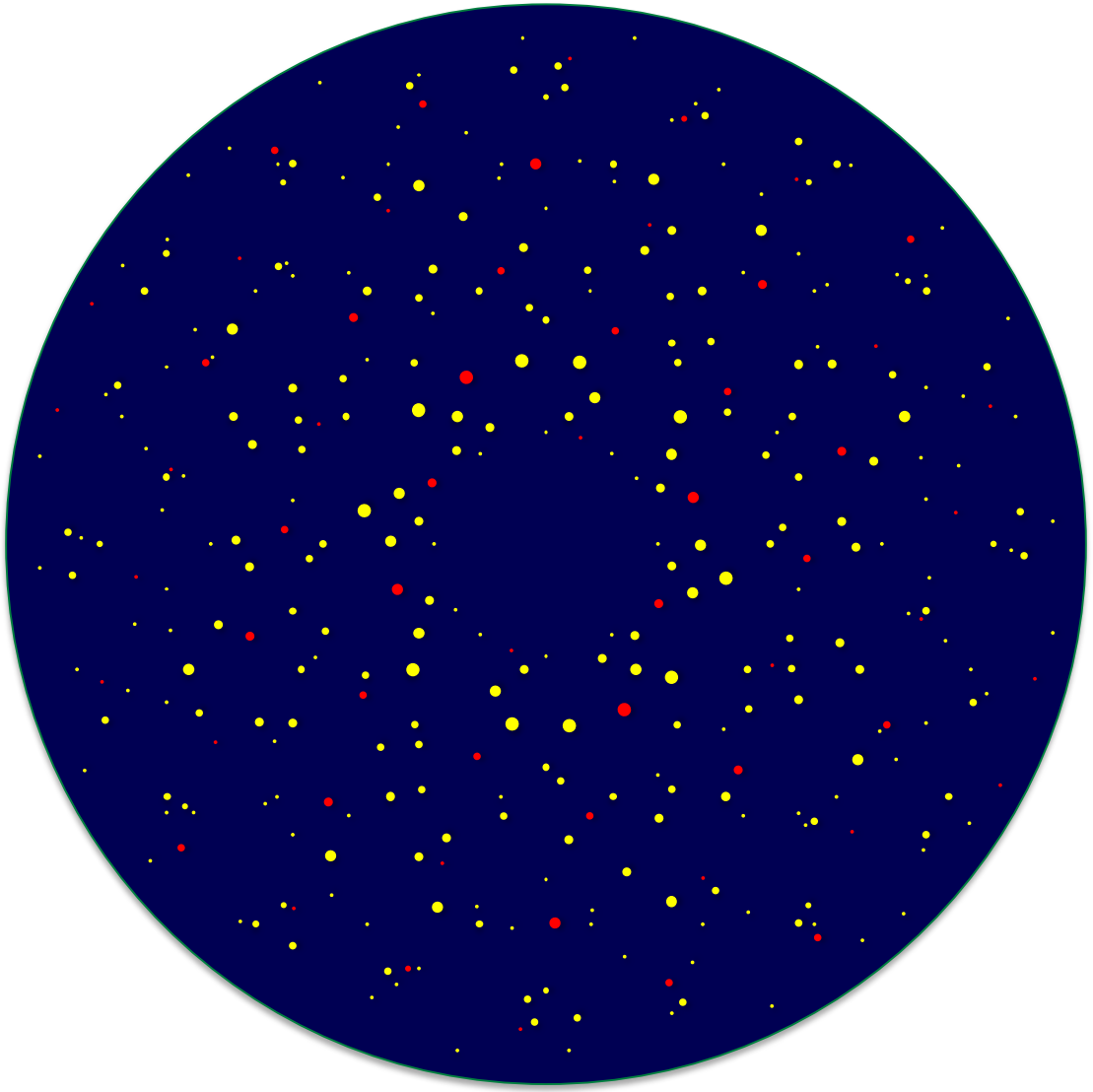

Institute for Chemical and Bioengineering, ETH Zurich, Zurich, Switzerland
Laboratory for Catalysis and Sustainable Chemistry, Paul Scherrer Institute, Villigen, Switzerland

X-ray Powder Diffraction

X-rays

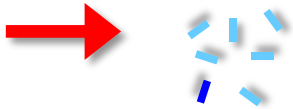

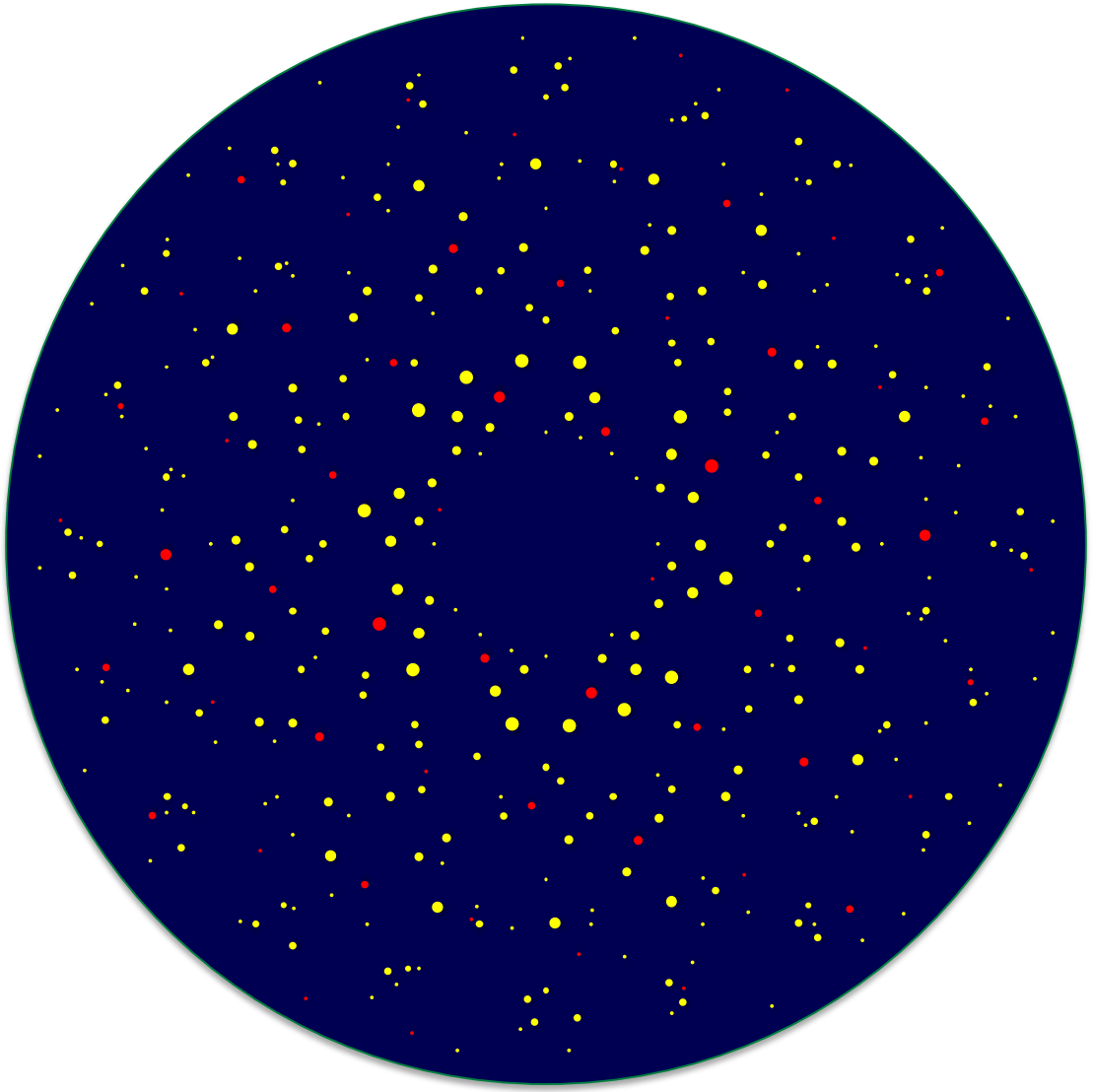

Institute for Chemical and Bioengineering, ETH Zurich, Zurich, Switzerland
Laboratory for Catalysis and Sustainable Chemistry, Paul Scherrer Institute, Villigen, Switzerland

X-ray Powder Diffraction

X-rays

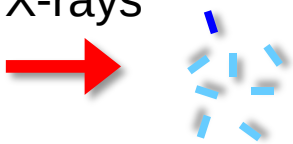

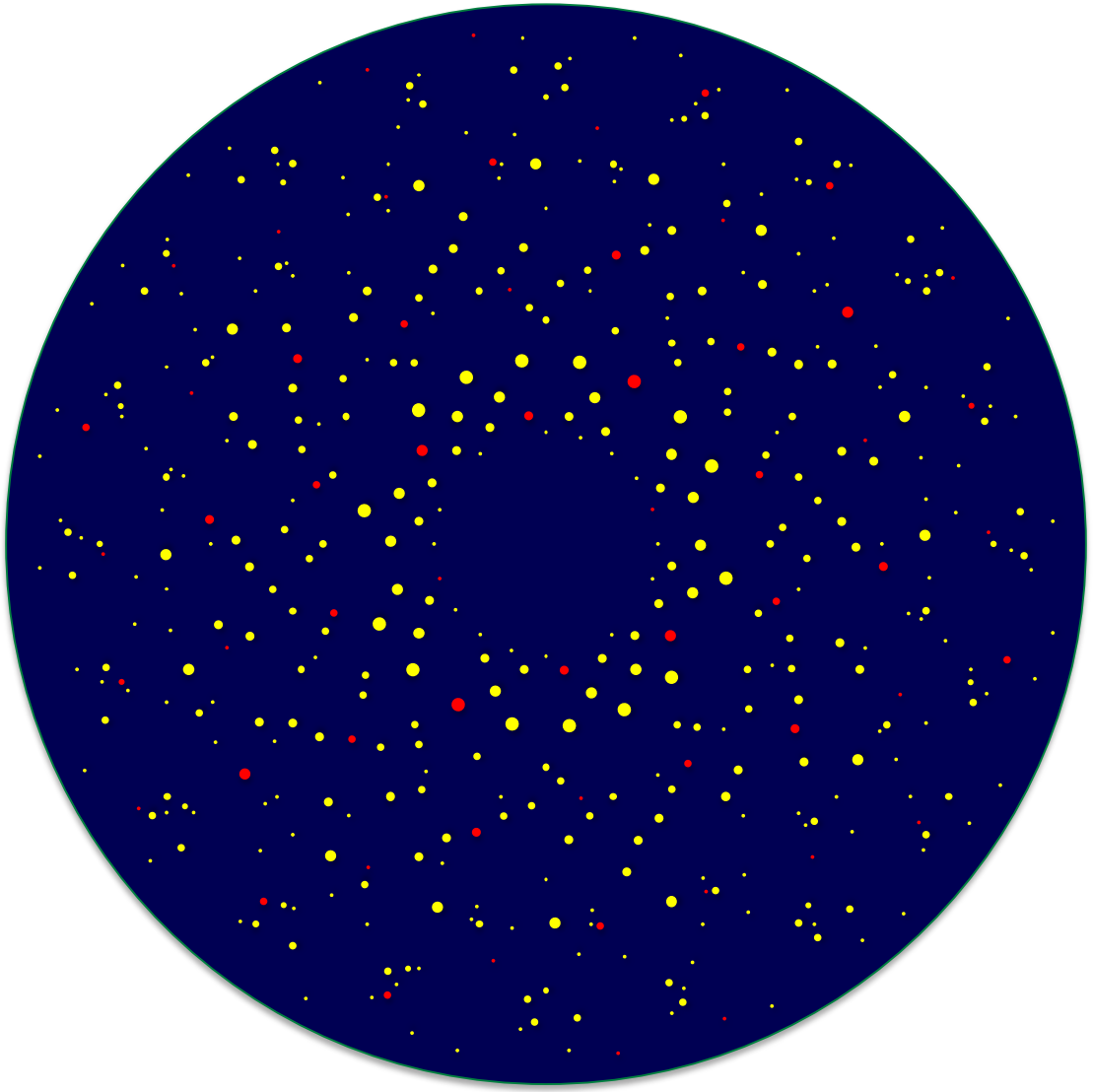

Institute for Chemical and Bioengineering, ETH Zurich, Zurich, Switzerland
Laboratory for Catalysis and Sustainable Chemistry, Paul Scherrer Institute, Villigen, Switzerland

X-ray Powder Diffraction

X-rays

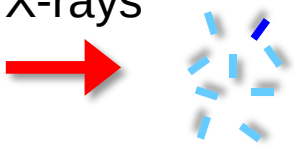

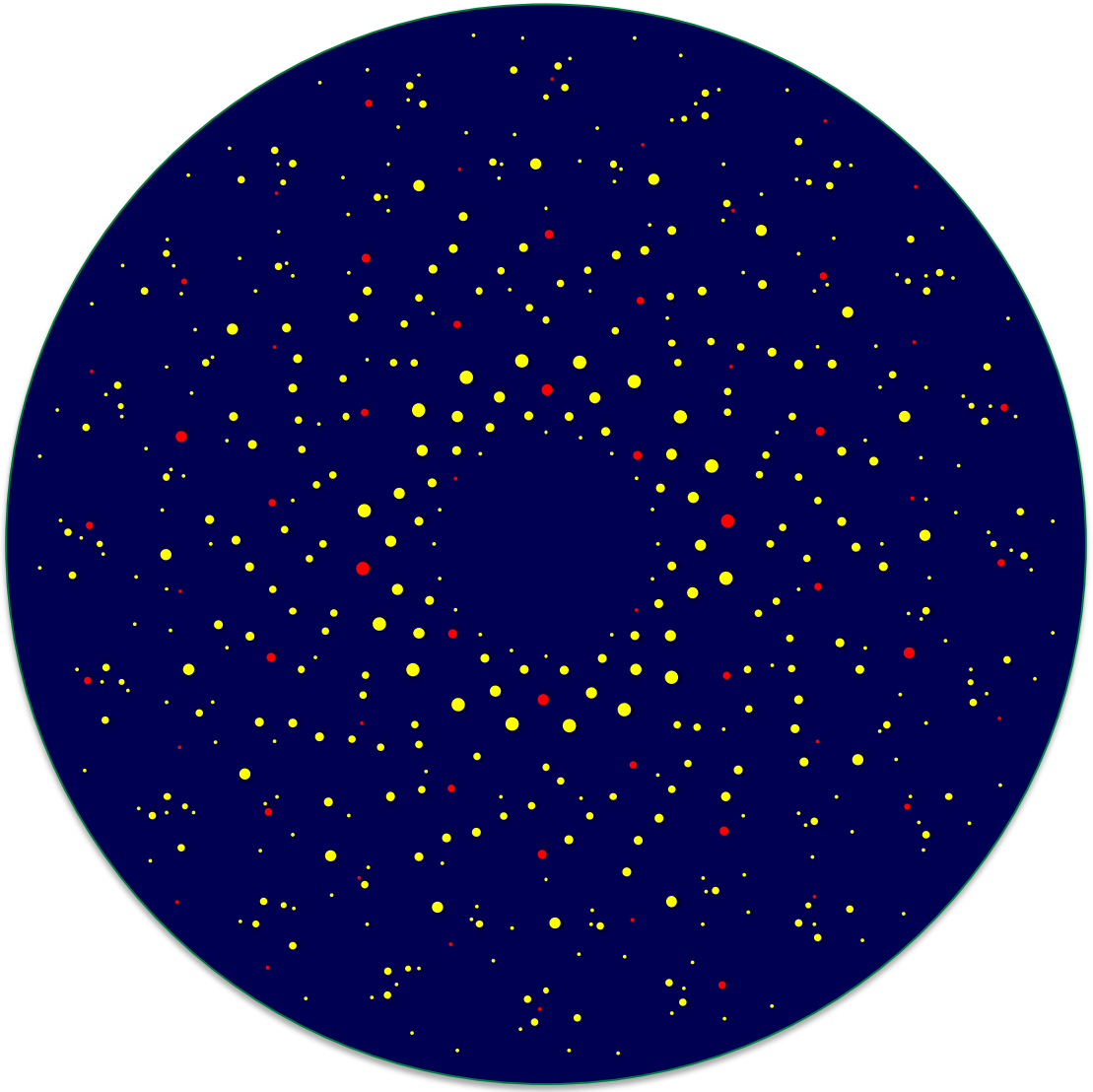

Institute for Chemical and Bioengineering, ETH Zurich, Zurich, Switzerland
Laboratory for Catalysis and Sustainable Chemistry, Paul Scherrer Institute, Villigen, Switzerland

X-ray Powder Diffraction

X-rays

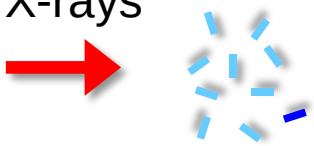

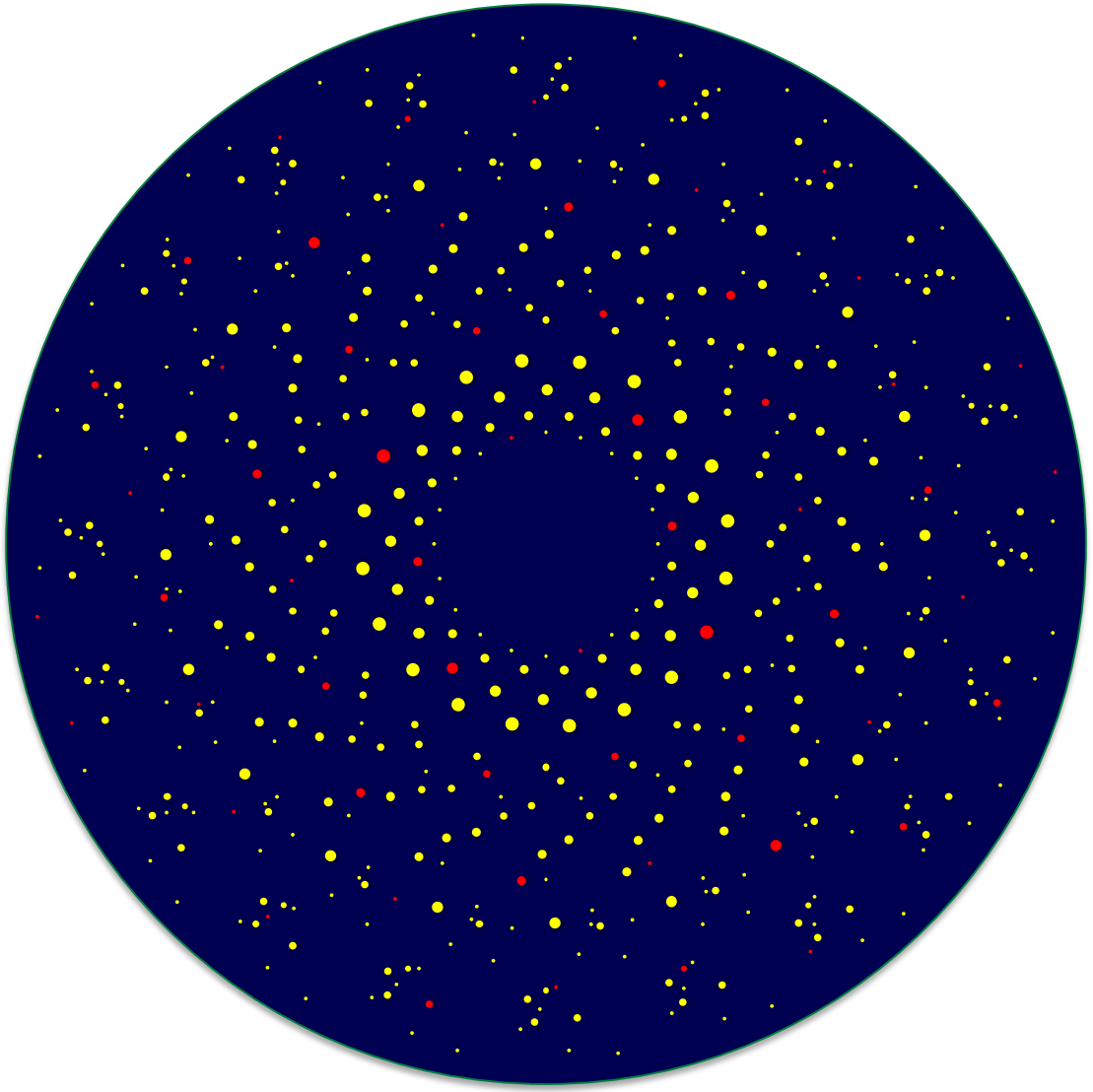

Institute for Chemical and Bioengineering, ETH Zurich, Zurich, Switzerland
Laboratory for Catalysis and Sustainable Chemistry, Paul Scherrer Institute, Villigen, Switzerland

X-ray Powder Diffraction

X-rays

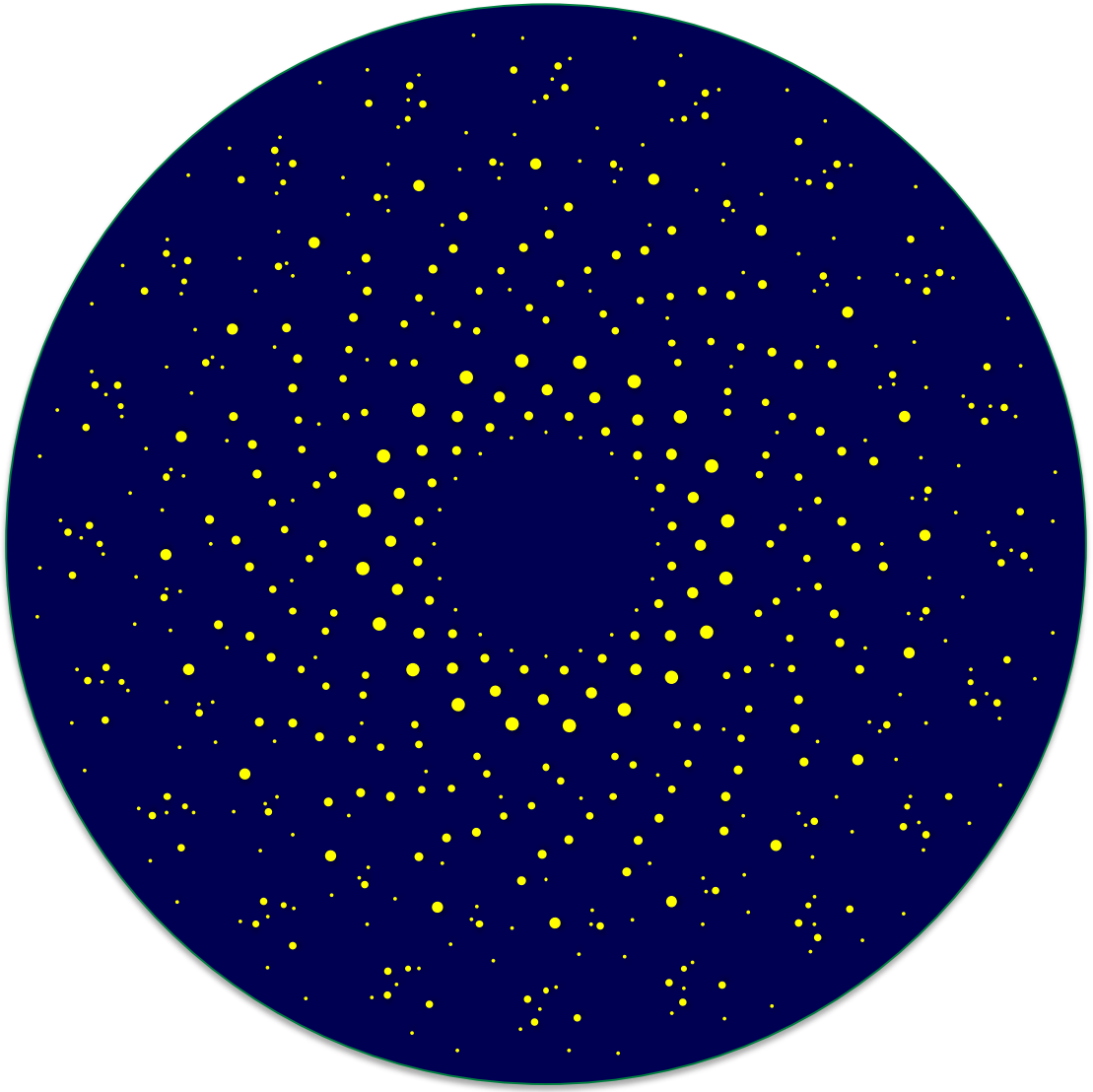

Institute for Chemical and Bioengineering, ETH Zurich, Zurich, Switzerland
Laboratory for Catalysis and Sustainable Chemistry, Paul Scherrer Institute, Villigen, Switzerland

X-ray Powder Diffraction

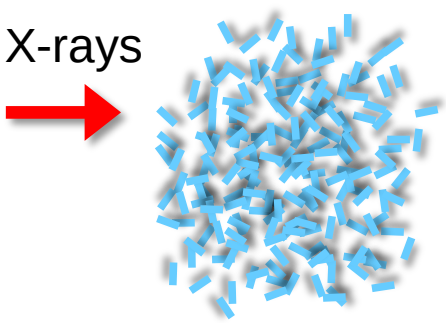

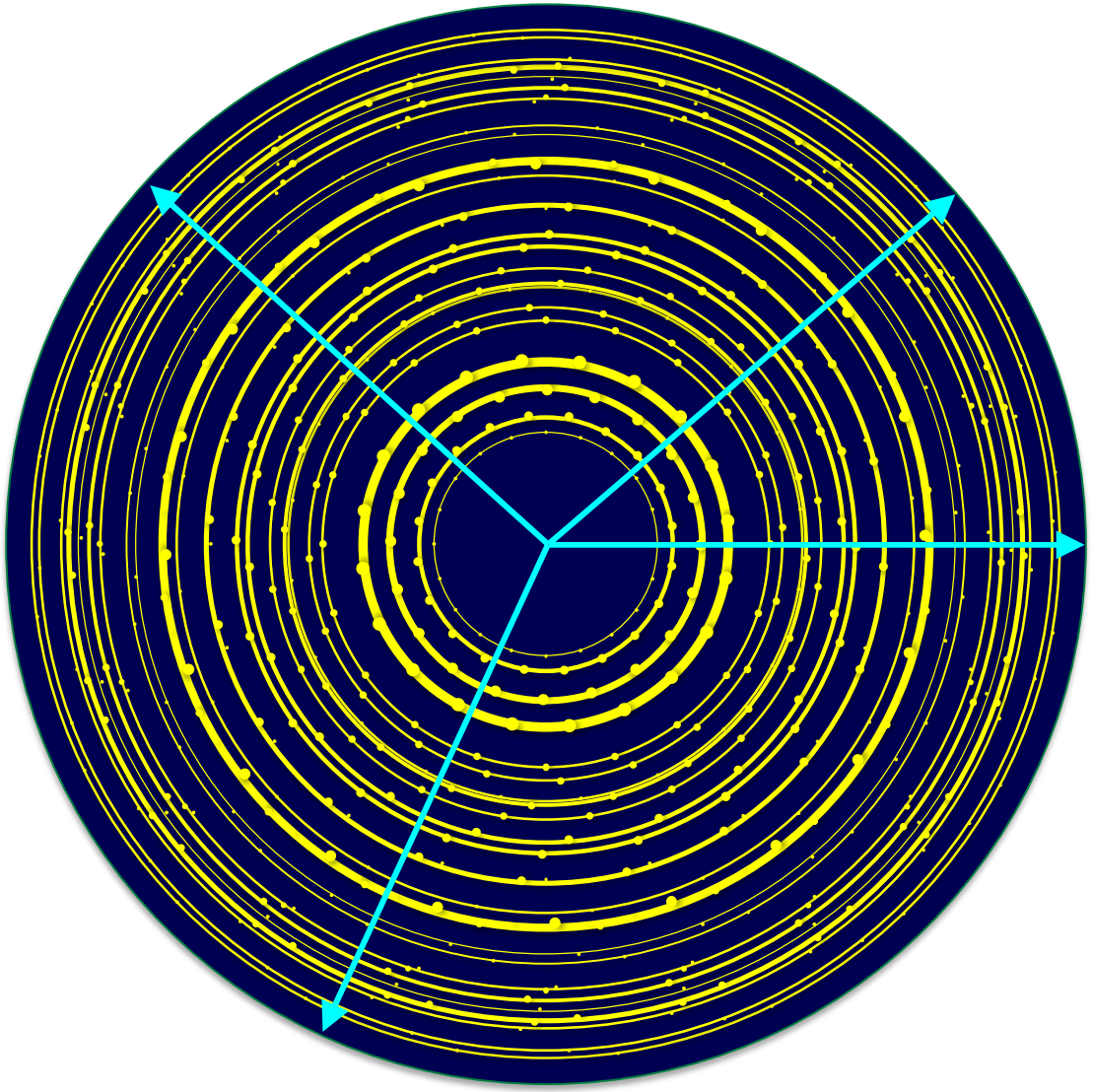

Institute for Chemical and Bioengineering, ETH Zurich, Zurich, Switzerland
Laboratory for Catalysis and Sustainable Chemistry, Paul Scherrer Institute, Villigen, Switzerland

X-ray Powder Diffraction

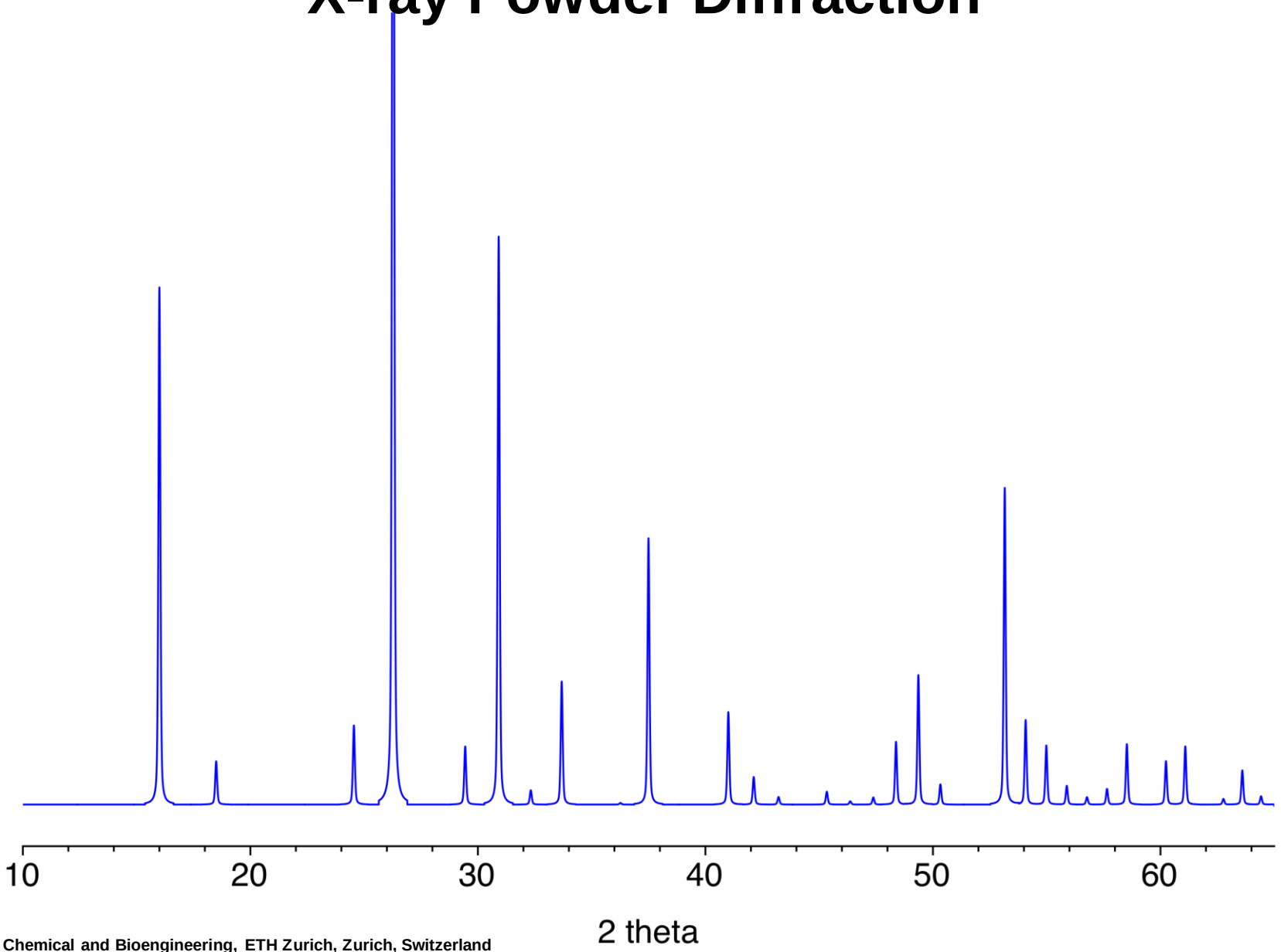

Institute for Chemical and Bioengineering, ETH Zurich, Zurich, Switzerland
Laboratory for Catalysis and Sustainable Chemistry, Paul Scherrer Institute, Villigen, Switzerland
Przemyslaw Rzepka

X-ray Powder Diffraction

Reflection Overlap Problem

X-rays

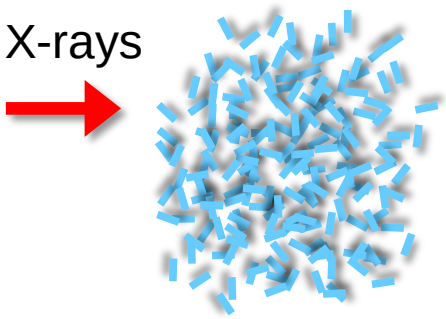

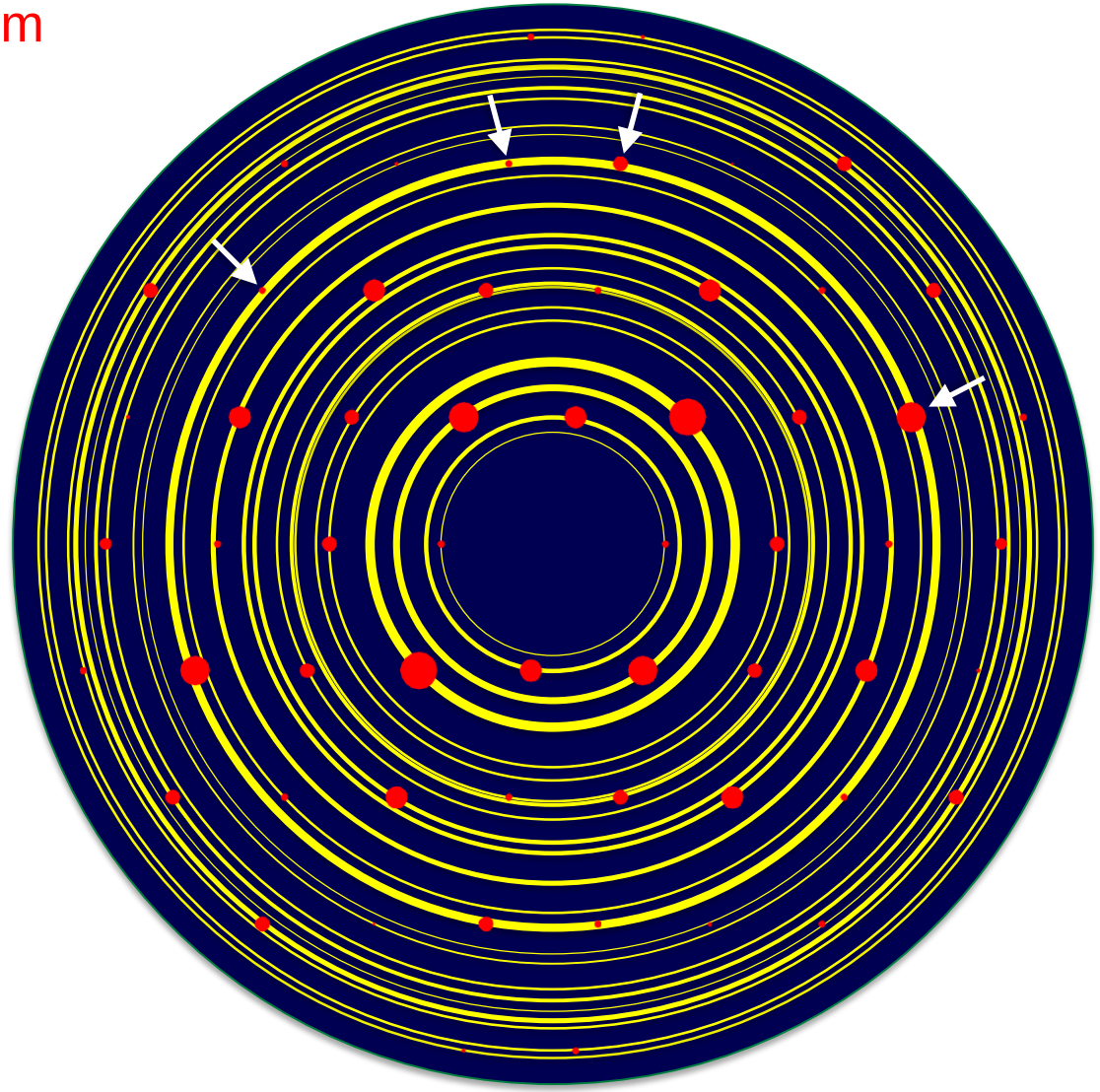

Institute for Chemical and Bioengineering, ETH Zurich, Zurich, Switzerland
Laboratory for Catalysis and Sustainable Chemistry, Paul Scherrer Institute, Villigen, Switzerland

Indexing an XPD Pattern

The determination of the background

- Assume flat background
- Measure an empty sample holder
- Estimate points and interpolate between them
- Fit a function

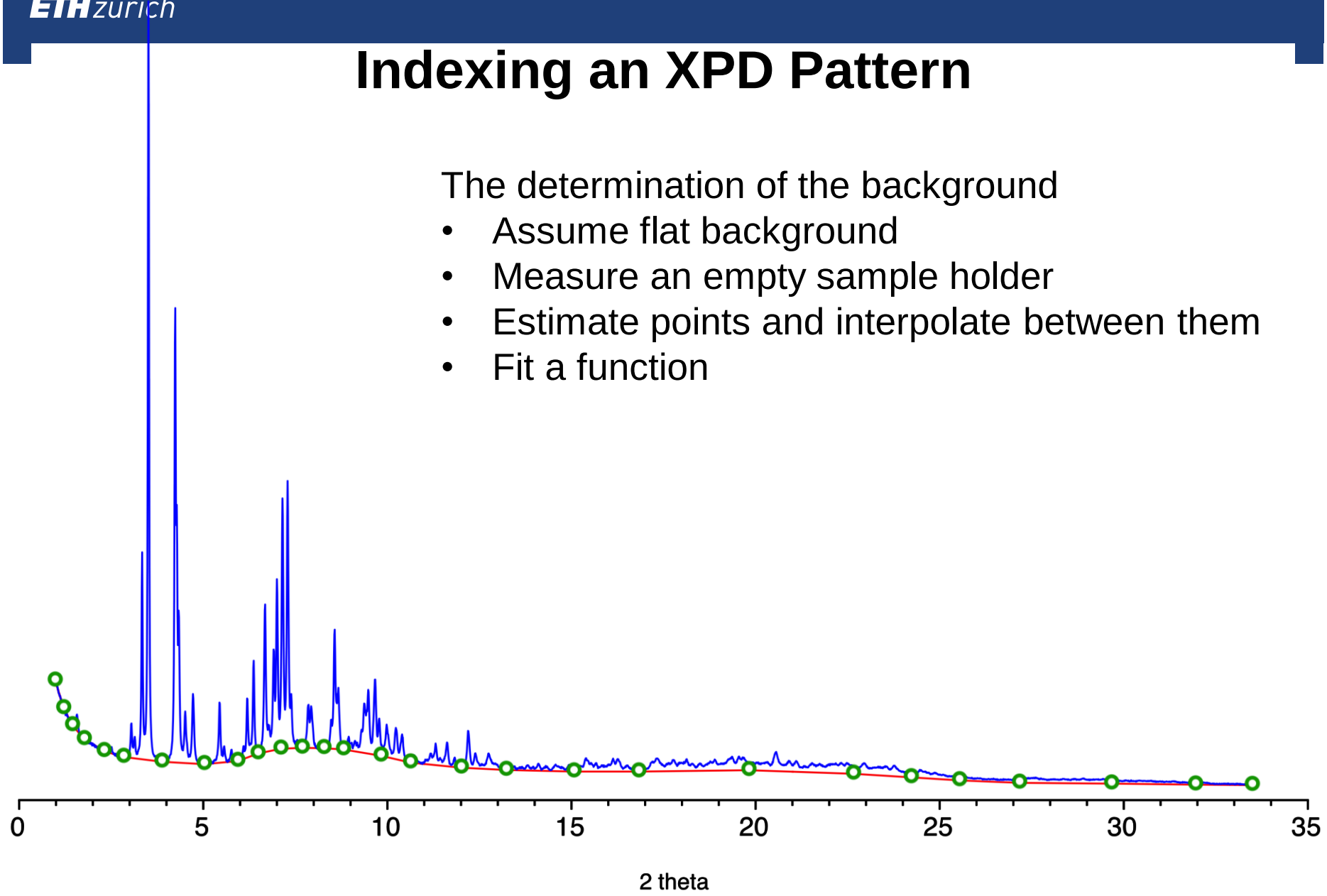

Institute for Chemical and Bioengineering, ETH Zurich, Zurich, Switzerland
Laboratory for Catalysis and Sustainable Chemistry, Paul Scherrer Institute, Villigen, Switzerland

Indexing an XPD Pattern

Peak positions search

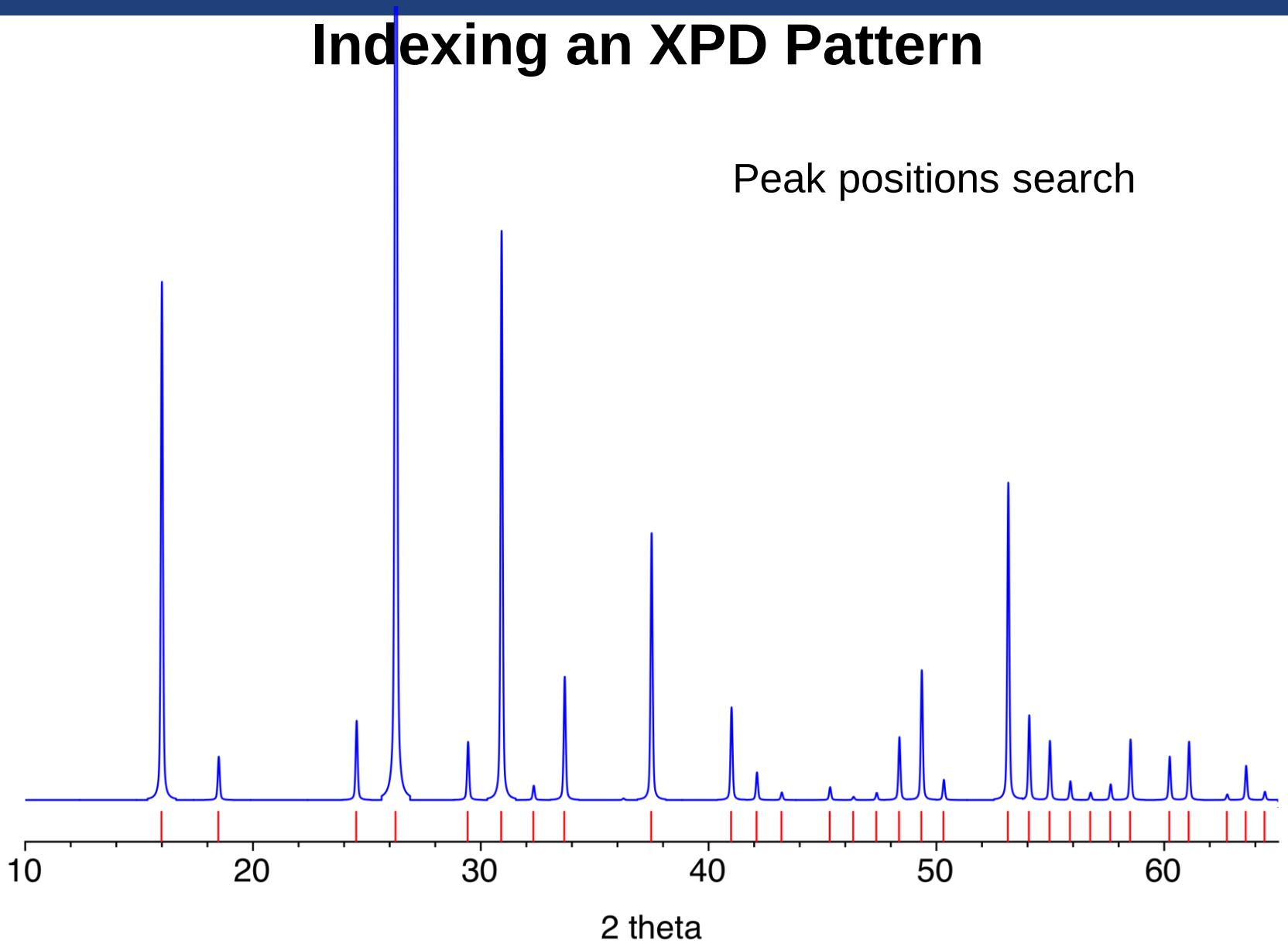

Institute for Chemical and Bioengineering, ETH Zurich, Zurich, Switzerland
Laboratory for Catalysis and Sustainable Chemistry, Paul Scherrer Institute, Villigen, Switzerland

Indexing an XPD Pattern

Relationship between 2θ and *d*-spacing

Bragg's Law $\lambda = 2d_{hkl}\sin\theta_{hkl}$

$$d_{hkl} = \lambda / 2\sin\theta_{hkl}$$

Relationship between *d*-spacing and lattice parameters

Cubic example $d_{hkl}^2 = \frac{a^2}{h^2 + k^2 + l^2}$

Institute for Chemical and Bioengineering, ETH Zurich, Zurich, Switzerland
Laboratory for Catalysis and Sustainable Chemistry, Paul Scherrer Institute, Villigen, Switzerland

Indexing an XPD Pattern

Peak positions search

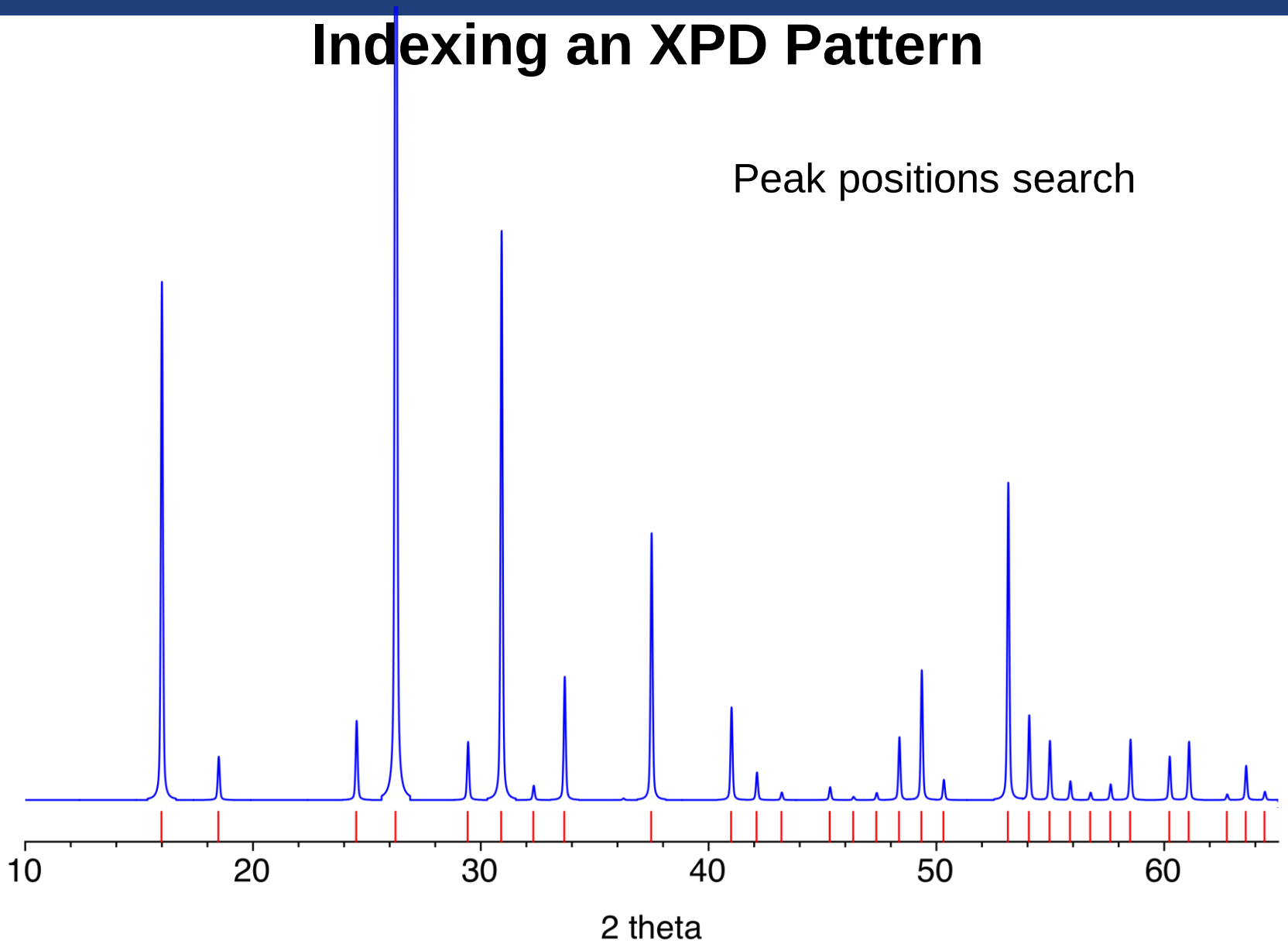

Institute for Chemical and Bioengineering, ETH Zurich, Zurich, Switzerland
Laboratory for Catalysis and Sustainable Chemistry, Paul Scherrer Institute, Villigen, Switzerland

Indexing an XPD Pattern

$$d_{hkl}^2 = \frac{\lambda^2}{4\sin^2\theta_{hkl}} = \frac{a^2}{h^2+k^2+l^2} \quad \rightarrow \quad \sin^2\theta_{hkl} = \left(\frac{\lambda^2}{4a^2}\right)\left(h^2+k^2+l^2\right)$$

Institute for Chemical and Bioengineering, ETH Zurich, Zurich, Switzerland
Laboratory for Catalysis and Sustainable Chemistry, Paul Scherrer Institute, Villigen, Switzerland

Indexing an XPD Pattern

$$d_{hkl}^2 = \frac{\lambda^2}{4\sin^2\theta_{hkl}} = \frac{a^2}{h^2+k^2+l^2} \quad \rightarrow \quad \sin^2\theta_{hkl} = \left(\frac{\lambda^2}{4a^2}\right)\left(h^2+k^2+l^2\right)$$

2θ (˚)
16.00
18.50
24.55
26.28
29.44
30.91
32.33
33.68
37.50
41.01
42.12
43.22
45.34

Institute for Chemical and Bioengineering, ETH Zurich, Zurich, Switzerland
Laboratory for Catalysis and Sustainable Chemistry, Paul Scherrer Institute, Villigen, Switzerland

Indexing an XPD Pattern

$$d_{hkl}^2 = \frac{\lambda^2}{4\sin^2\theta_{hkl}} = \frac{a^2}{h^2+k^2+l^2} \quad \rightarrow \quad \sin^2\theta_{hkl} = \left(\frac{\lambda^2}{4a^2}\right)\left(h^2+k^2+l^2\right)$$

2θ (˚)	sin²θ
16.00	0.01937
18.50	0.02583
24.55	0.04520
26.28	0.05166
29.44	0.06457
30.91	0.07103
32.33	0.07749
33.68	0.08395
37.50	0.10332
41.01	0.12269
42.12	0.12915
43.22	0.13561
45.34	0.14852

$$\frac{\sin^2\theta_2}{\sin^2\theta_1} = \frac{\left(h_2^2+k_2^2+l_2^2\right)}{\left(h_1^2+k_1^2+l_1^2\right)}$$

Institute for Chemical and Bioengineering, ETH Zurich, Zurich, Switzerland
Laboratory for Catalysis and Sustainable Chemistry, Paul Scherrer Institute, Villigen, Switzerland

Indexing an XPD Pattern

$$d_{hkl}^2 = \frac{\lambda^2}{4\sin^2\theta_{hkl}} = \frac{a^2}{h^2+k^2+l^2} \rightarrow \sin^2\theta_{hkl} = \left(\frac{\lambda^2}{4a^2}\right)\left(h^2+k^2+l^2\right)$$

2θ (°)	$\sin^2\theta$	ratio
16.00	0.01937	1.00
18.50	0.02583	1.33
24.55	0.04520	2.33
26.28	0.05166	2.67
29.44	0.06457	3.33
30.91	0.07103	3.66
32.33	0.07749	4.00
33.68	0.08395	4.33
37.50	0.10332	5.33
41.01	0.12269	6.33
42.12	0.12915	6.67
43.22	0.13561	7.00
45.34	0.14852	7.66

Indexing an XPD Pattern

$$d_{hkl}^2 = \frac{\lambda^2}{4\sin^2\theta_{hkl}} = \frac{a^2}{h^2+k^2+l^2} \quad \rightarrow \quad \sin^2\theta_{hkl} = \left(\frac{\lambda^2}{4a^2}\right)\left(h^2+k^2+l^2\right)$$

2θ (°)	$\sin^2\theta$	ratio	integers
16.00	0.01937	1.00	3
18.50	0.02583	1.33	4
24.55	0.04520	2.33	7
26.28	0.05166	2.67	8
29.44	0.06457	3.33	10
30.91	0.07103	3.66	11
32.33	0.07749	4.00	12
33.68	0.08395	4.33	13
37.50	0.10332	5.33	16
41.01	0.12269	6.33	19
42.12	0.12915	6.67	20
43.22	0.13561	7.00	21
45.34	0.14852	7.66	23

Institute for Chemical and Bioengineering, ETH Zurich, Zurich, Switzerland
Laboratory for Catalysis and Sustainable Chemistry, Paul Scherrer Institute, Villigen, Switzerland

Indexing an XPD Pattern

$$d_{hkl}^2 = \frac{\lambda^2}{4\sin^2\theta_{hkl}} = \frac{a^2}{h^2+k^2+l^2} \quad \rightarrow \quad \sin^2\theta_{hkl} = \left(\frac{\lambda^2}{4a^2}\right)\left(h^2+k^2+l^2\right)$$

2θ (°)	sin²θ	ratio	integers	$h^2 + k^2 + l^2$
16.00	0.01937	1.00	3	6
18.50	0.02583	1.33	4	8
24.55	0.04520	2.33	7	14
26.28	0.05166	2.67	8	16
29.44	0.06457	3.33	10	20
30.91	0.07103	3.66	11	22
32.33	0.07749	4.00	12	24
33.68	0.08395	4.33	13	26
37.50	0.10332	5.33	16	32
41.01	0.12269	6.33	19	38
42.12	0.12915	6.67	20	40
43.22	0.13561	7.00	21	42
45.34	0.14852	7.66	23	46

Institute for Chemical and Bioengineering, ETH Zurich, Zurich, Switzerland
Laboratory for Catalysis and Sustainable Chemistry, Paul Scherrer Institute, Villigen, Switzerland

Indexing an XPD Pattern

$$d_{hkl}^2 = \frac{\lambda^2}{4\sin^2\theta_{hkl}} = \frac{a^2}{h^2+k^2+l^2} \rightarrow \sin^2\theta_{hkl} = \left(\frac{\lambda^2}{4a^2}\right)\left(h^2+k^2+l^2\right)$$

2θ (°)	$\sin^2\theta$	ratio	integers	$h^2 + k^2 + l^2$	*hkl*
16.00	0.01937	1.00	3	6	211
18.50	0.02583	1.33	4	8	220
24.55	0.04520	2.33	7	14	321
26.28	0.05166	2.67	8	16	400
29.44	0.06457	3.33	10	20	420
30.91	0.07103	3.66	11	22	332
32.33	0.07749	4.00	12	24	422
33.68	0.08395	4.33	13	26	431
37.50	0.10332	5.33	16	32	440
41.01	0.12269	6.33	19	38	532, 611
42.12	0.12915	6.67	20	40	620
43.22	0.13561	7.00	21	42	541
45.34	0.14852	7.66	23	46	631

Institute for Chemical and Bioengineering, ETH Zurich, Zurich, Switzerland
Laboratory for Catalysis and Sustainable Chemistry, Paul Scherrer Institute, Villigen, Switzerland

Indexing an XPD Pattern

$$d_{hkl}^2 = \frac{\lambda^2}{4\sin^2\theta_{hkl}} = \frac{a^2}{h^2+k^2+l^2} \quad \rightarrow \quad \sin^2\theta_{hkl} = \left(\frac{\lambda^2}{4a^2}\right)\left(h^2+k^2+l^2\right)$$

2θ (°)	$\sin^2\theta$	ratio	integers	$h^2 + k^2 + l^2$	*hkl*	*a* (Å)
16.00	0.01937	1.00	3	6	211	13.5567
18.50	0.02583	1.33	4	8	220	13.5564
24.55	0.04520	2.33	**7**	14	321	13.5567
26.28	0.05166	2.67	8	16	400	13.5563
29.44	0.06457	3.33	10	20	420	13.5566
30.91	0.07103	3.66	11	22	332	13.5566
32.33	0.07749	4.00	12	24	422	13.5563
33.68	0.08395	4.33	13	26	431	13.5565
37.50	0.10332	5.33	16	32	440	13.5565
41.01	0.12269	6.33	19	38	532, 611	13.5564
42.12	0.12915	6.67	20	40	620	13.5565
43.22	0.13561	7.00	21	42	541	13.5565
45.34	0.14852	7.66	23	46	631	13.5565

Indexing an XPD Pattern

$$d_{hkl}^2 = \frac{\lambda^2}{4\sin^2\theta_{hkl}} = \frac{a^2}{h^2+k^2+l^2} \quad \rightarrow \quad \sin^2\theta_{hkl} = \left(\frac{\lambda^2}{4a^2}\right)\left(h^2+k^2+l^2\right)$$

2θ (°)	*hkl*
16.00	211
18.50	220
24.55	321
26.28	400
29.44	420
30.91	332
32.33	422
33.68	431
37.50	440
41.01	532, 611
42.12	620
43.22	541
45.34	631

Lattice parameter

a = 13.5565 Å

Centered?

P: *no conditions on hkl*

I: $h + k + l = 2n$

F: $h + k = 2n$, $h + l = 2n$, $k + l = 2n$ } *hkl* all even or all odd

Institute for Chemical and Bioengineering, ETH Zurich, Zurich, Switzerland
Laboratory for Catalysis and Sustainable Chemistry, Paul Scherrer Institute, Villigen, Switzerland

Indexing an XPD Pattern

$$d_{hkl}^2 = \frac{\lambda^2}{4\sin^2\theta_{hkl}} = \frac{a^2}{h^2+k^2+l^2} \quad \rightarrow \quad \sin^2\theta_{hkl} = \left(\frac{\lambda^2}{4a^2}\right)\left(h^2+k^2+l^2\right)$$

2θ (°)	*hkl*
16.00	211
18.50	220
24.55	321
26.28	400
29.44	420
30.91	332
32.33	422
33.68	431
37.50	440
41.01	532, 611
42.12	620
43.22	541
45.34	631

Lattice parameter

a = 13.5565 Å

Centered?

P: *no conditions on hkl*

→ *I:* $h + k + l = 2n$

F: $h + k = 2n$, $h + l = 2n$, $k + l = 2n$ } *hkl* all even or all odd

Institute for Chemical and Bioengineering, ETH Zurich, Zurich, Switzerland
Laboratory for Catalysis and Sustainable Chemistry, Paul Scherrer Institute, Villigen, Switzerland

Indexing an XPD Pattern

$$d_{hkl}^2 = \frac{\lambda^2}{4\sin^2\theta_{hkl}} = \frac{a^2}{h^2+k^2+l^2} \rightarrow \sin^2\theta_{hkl} = \left(\frac{\lambda^2}{4a^2}\right)\left(h^2+k^2+l^2\right)$$

2θ (˚)
38.46
55.54
69.58
82.46
94.94
107.64
121.36

Exercise 1 (send answers to przepka@ethz.ch):

1. Index listed peaks if you know the structure is cubic
2. What is lattice parameter a if λ=1.54Å?
3. What is centering?

Institute for Chemical and Bioengineering, ETH Zurich, Zurich, Switzerland
Laboratory for Catalysis and Sustainable Chemistry, Paul Scherrer Institute, Villigen, Switzerland

Reflection position

Parameters affecting reflection positions

- unit cell parameters
- zero point of the detector
- sample displacement

$$\lambda = 2d_{hkl}\sin\theta_{hkl}$$

smaller d ➡ larger 2θ

larger d ➡ smaller 2θ

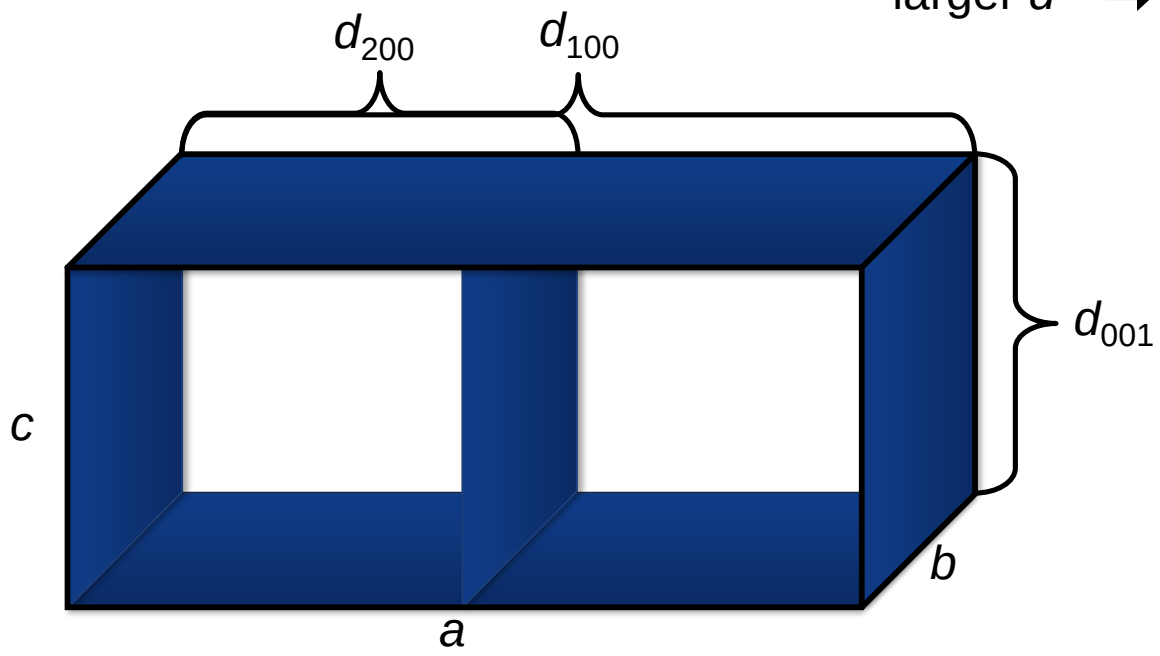

Institute for Chemical and Bioengineering, ETH Zurich, Zurich, Switzerland
Laboratory for Catalysis and Sustainable Chemistry, Paul Scherrer Institute, Villigen, Switzerland

Reflection position

Parameters affecting reflection positions

- unit cell parameters
- zero point of the detector
- sample displacement (Bragg-Brentano)

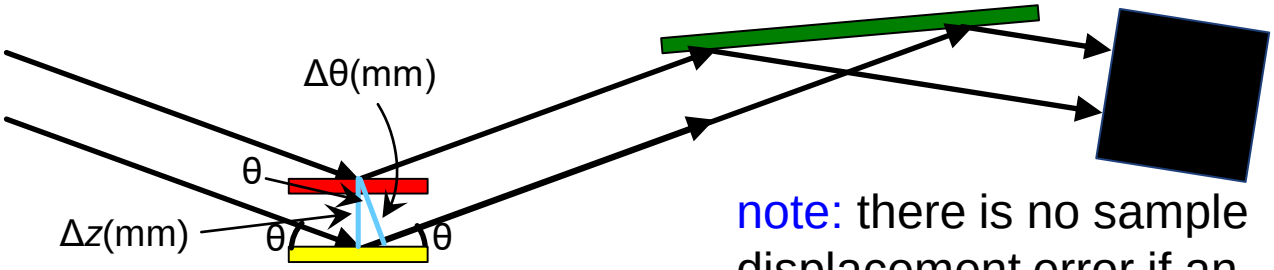

note: there is no sample displacement error if an analyzer crystal is used

$\cos(2\theta) = \Delta 2\theta / \Delta z$

$\Delta\theta = \Delta z \cos(\theta)$

Institute for Chemical and Bioengineering, ETH Zurich, Zurich, Switzerland
Laboratory for Catalysis and Sustainable Chemistry, Paul Scherrer Institute, Villigen, Switzerland

Reflection position

Parameters affecting reflection positions

- unit cell parameters
- zero point of the detector
- sample displacement (Debye-Scherrer)

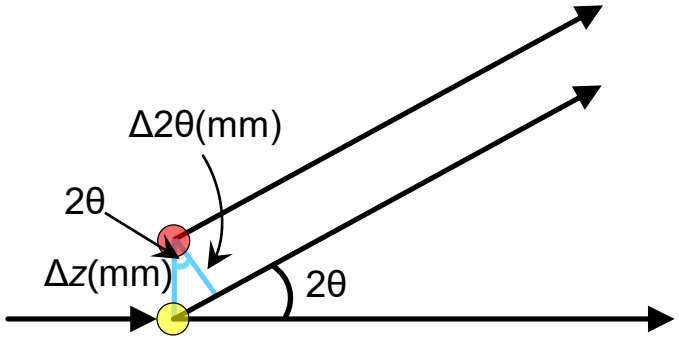

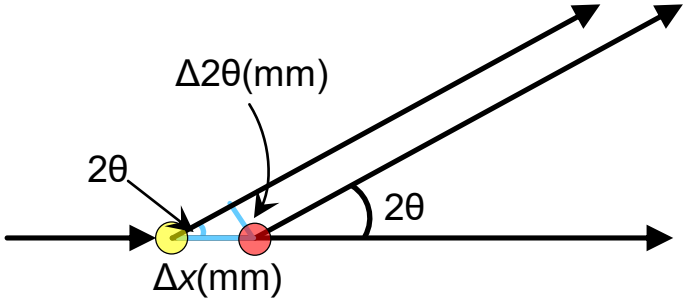

$\cos(2\theta) = \Delta 2\theta / \Delta z$

$\Delta 2\theta = \Delta z \cos(2\theta)$

$\sin(2\theta) = \Delta 2\theta / \Delta x$

$\Delta 2\theta = \Delta x \sin(2\theta)$

Institute for Chemical and Bioengineering, ETH Zurich, Zurich, Switzerland
Laboratory for Catalysis and Sustainable Chemistry, Paul Scherrer Institute, Villigen, Switzerland
Przemyslaw Rzepka

Crystalline size

Peak width (B) is inversely proportional to crystallite size (L)

Scherrer equation $D = \frac{K\lambda}{FWHM\ cos\theta}$

D – crystalline size, K=0.9 - shape factor, λ – wavelength, FWHM – the line broadening at half the maximum intensity, θ – Bragg angle

The Laue Equations describe the intensity of a diffracted peak from an **infinitely large (> 1um)** and **perfectly ordered** crystal. Deviations from the ideal (nano-sizing) create peak broadening

Crystalline size

Peak width (B) is inversely proportional to crystallite size (L)

Scherrer equation $D = \frac{K\lambda}{FWHM\ cos\theta}$

D – crystalline size, K=0.9 - shape factor, λ – wavelength, FWHM – the line broadening at half the maximum intensity, θ – Bragg angle

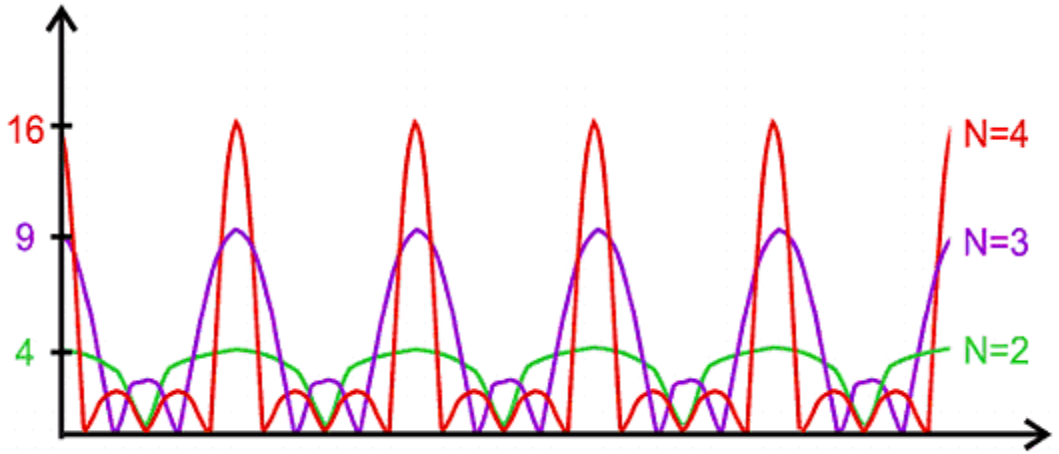

The interference from n = 2, 3, 4 scattering centers

Institute for Chemical and Bioengineering, ETH Zurich, Zurich, Switzerland
Laboratory for Catalysis and Sustainable Chemistry, Paul Scherrer Institute, Villigen, Switzerland

Crystalline size

Peak width (B) is inversely proportional to crystallite size (L)

Scherrer equation $D = \frac{K\lambda}{FWHM\ cos\theta}$

D – crystalline size, K=0.9 - shape factor, λ – wavelength, FWHM – the line broadening at half the maximum intensity, θ – Bragg angle

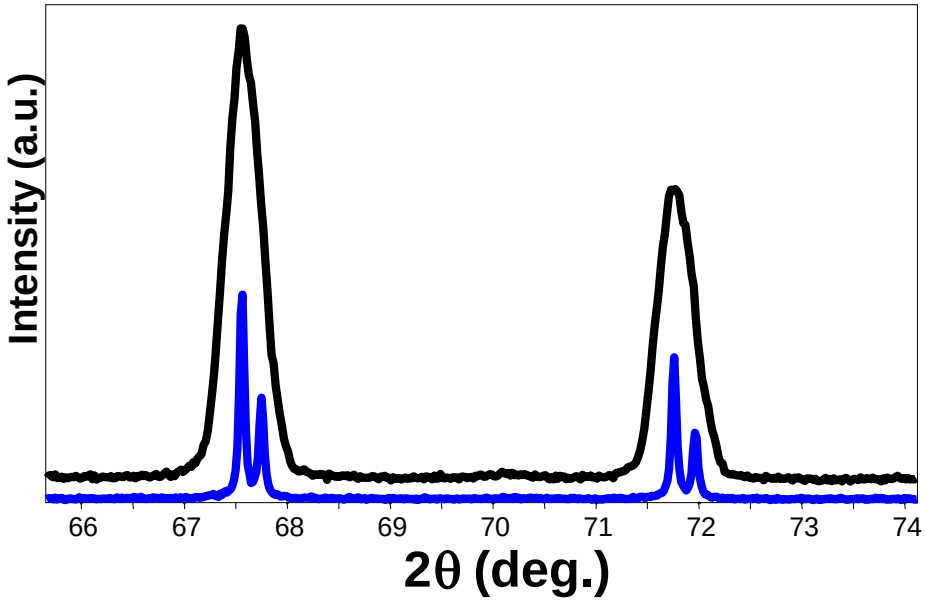

Note the instrumental contribution. Left: the same sample, different instruments

Institute for Chemical and Bioengineering, ETH Zurich, Zurich, Switzerland
Laboratory for Catalysis and Sustainable Chemistry, Paul Scherrer Institute, Villigen, Switzerland

Crystalline size

Peak width (B) is inversely proportional to crystallite size (L)

Scherrer equation $D = \frac{K\lambda}{FWHM\ cos\theta}$

Microstrain (ε) analysis

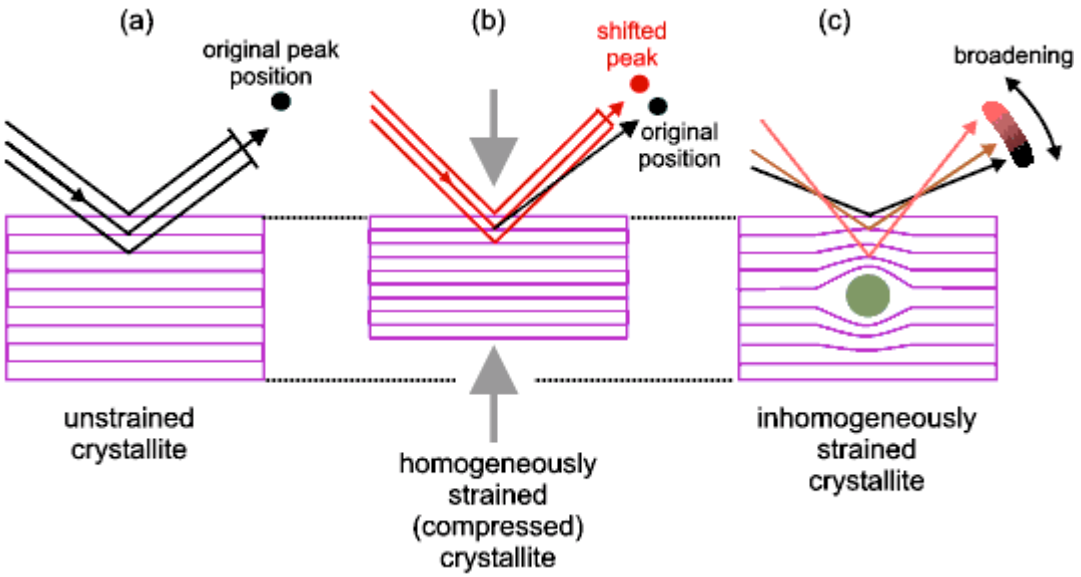

$FWHM = C\ \varepsilon\ tan\theta$

Institute for Chemical and Bioengineering, ETH Zurich, Zurich, Switzerland
Laboratory for Catalysis and Sustainable Chemistry, Paul Scherrer Institute, Villigen, Switzerland

Anisotropic Size Broadening

The broadening of a single diffraction peak is the product of the crystallite dimensions in the direction perpendicular to the planes that produced the diffraction peak

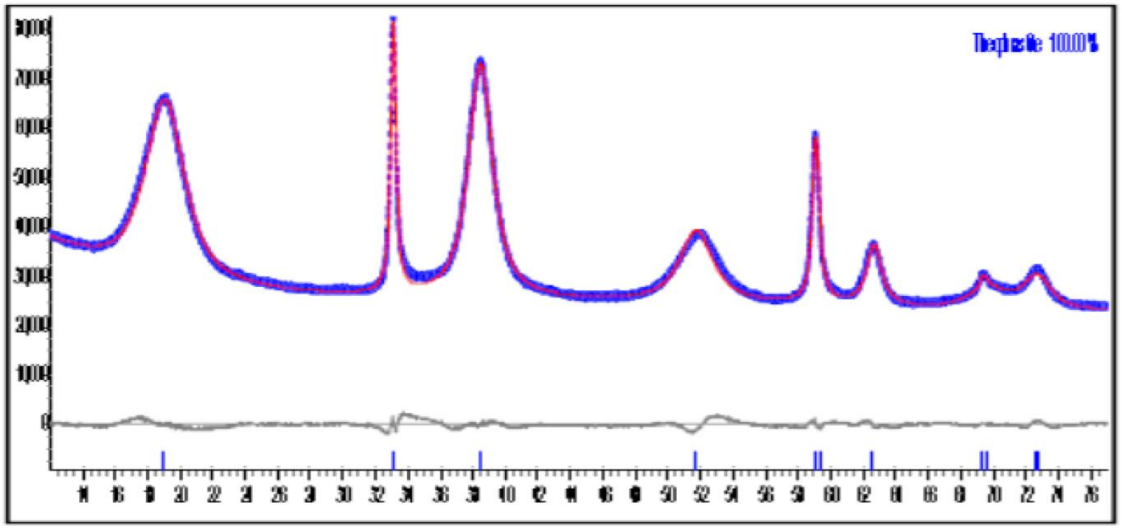

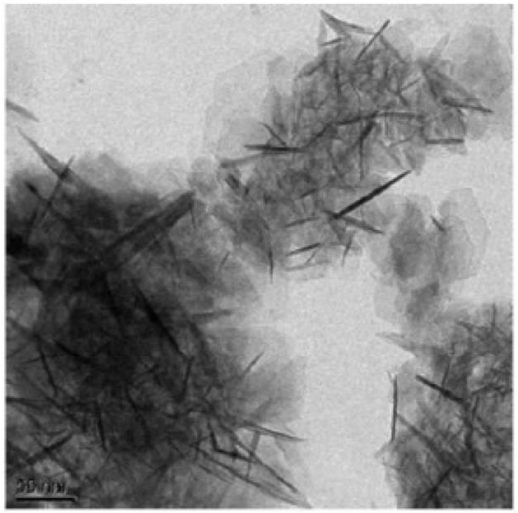

Anisotropic broadening in the PXRD pattern of $Ni(OH)_2$

Institute for Chemical and Bioengineering, ETH Zurich, Zurich, Switzerland
Laboratory for Catalysis and Sustainable Chemistry, Paul Scherrer Institute, Villigen, Switzerland

Anisotropic Size Broadening

The broadening of a single diffraction peak is the product of the crystallite dimensions in the direction perpendicular to the planes that produced the diffraction peak

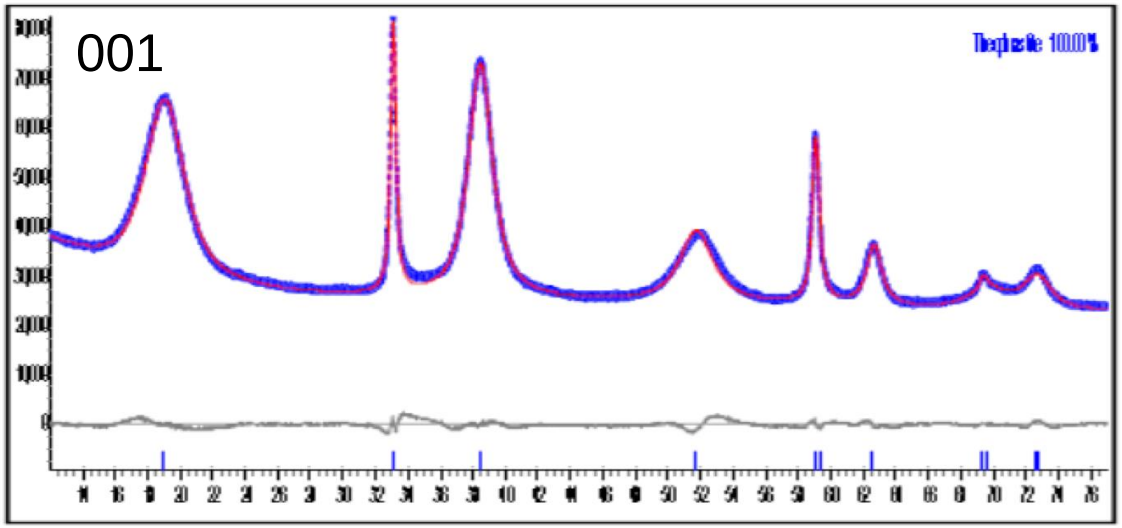

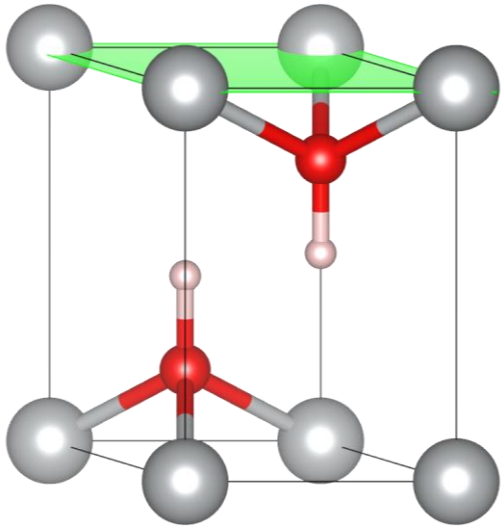

Anisotropic broadening in the PXRD pattern of $Ni(OH)_2$

Institute for Chemical and Bioengineering, ETH Zurich, Zurich, Switzerland
Laboratory for Catalysis and Sustainable Chemistry, Paul Scherrer Institute, Villigen, Switzerland

Anisotropic Size Broadening

The broadening of a single diffraction peak is the product of the crystallite dimensions in the direction perpendicular to the planes that produced the diffraction peak

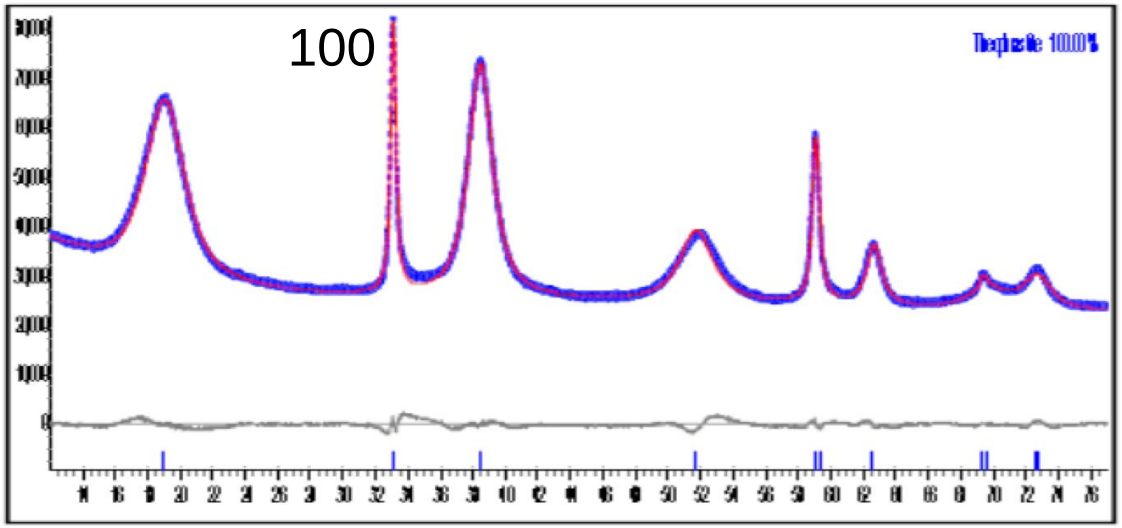

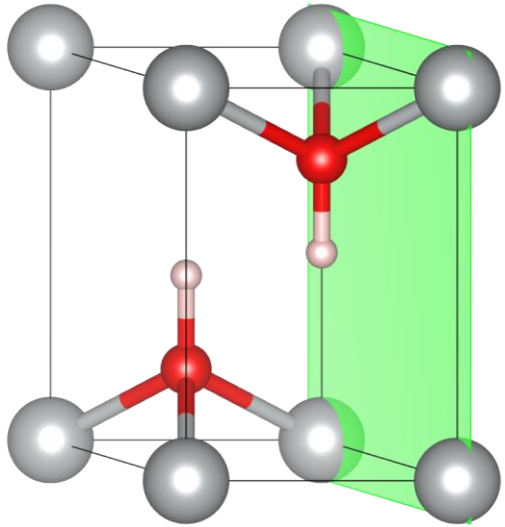

Anisotropic broadening in the PXRD pattern of $Ni(OH)_2$

Institute for Chemical and Bioengineering, ETH Zurich, Zurich, Switzerland
Laboratory for Catalysis and Sustainable Chemistry, Paul Scherrer Institute, Villigen, Switzerland

The Rietveld analysis

The Rietveld method refines user-selected parameters to minimize the difference between an experimental pattern (observed data) and a model based on the hypothesized crystal structure and instrumental parameters (calculated pattern)

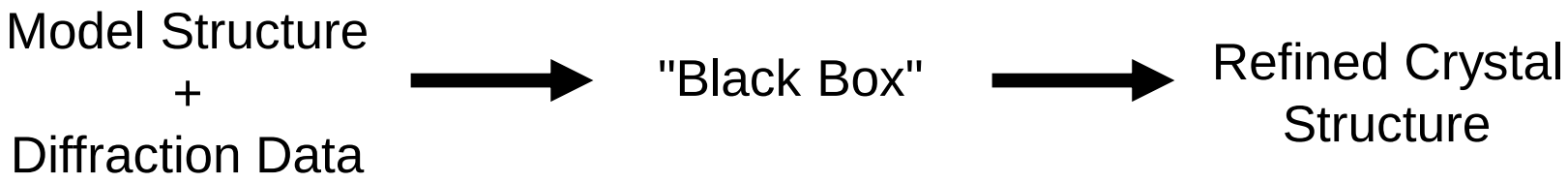

The Rietveld analysis

The Rietveld method refines user-selected parameters to minimize the difference between an experimental pattern (observed data) and a model based on the hypothesized crystal structure and instrumental parameters (calculated pattern)

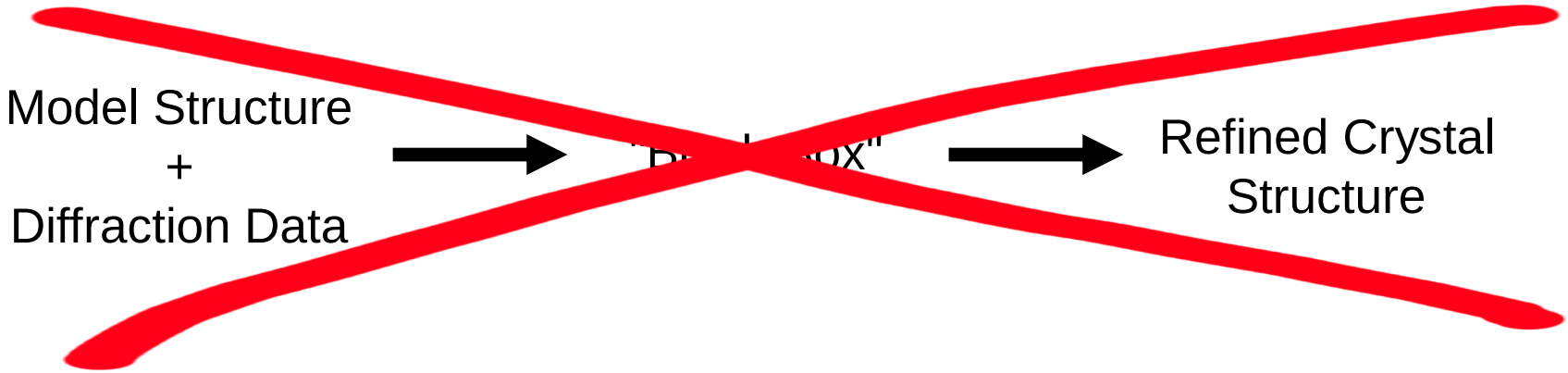

From intensities to structural parameters

$$\Delta = \sum_{n=1}^{N} \{ I_n(\text{obs}) - I_n(\text{calc})\}2$$

$$I(\text{calc}) = c\, j_{hkl}\, L(2\theta)\, P(2\theta)\, A(2\theta)\, F^2(hkl)$$

where L, P, A are the Lorentz, polarization, and absorption corrections, respectively. j is the multiplicity factor (symmetry), c is a scale factor and F is a structure factor.

$$F_{hkl} = \sum_j f_j \exp[\, 2\pi\, i(hx_j + hy_j + hz_j)]$$

where f_i is atomic form factor.

bkg @ 0 0 0 0

Institute for Chemical and Bioengineering, ETH Zurich, Zurich, Switzerland
Laboratory for Catalysis and Sustainable Chemistry, Paul Scherrer Institute, Villigen, Switzerland

R-Factors

$$R_{wp} = \{\sum_i w_i\{y_i(obs) - y_i(calc)\}^2 / \{\sum_i w_i y_i(obs)^2\}^{1/2}$$

$$w_i^2 = 1/\sigma(y_i(obs))^2$$

$$R_{exp} = \{(M - P)/\{\sum_i w_i y_i(obs)^2\}^{1/2}$$

$$\chi^2 = (R_{wp}/R_{exp})^2 \text{ (goodness-of-fit)}$$

where w_i is weighting related to uncertainty σ. M – the number of data points, P – the number of parameters

Institute for Chemical and Bioengineering, ETH Zurich, Zurich, Switzerland
Laboratory for Catalysis and Sustainable Chemistry, Paul Scherrer Institute, Villigen, Switzerland

Pawley and LeBail profile fitting

Parameters:

- *I*(*hkl*) - Intensity of each reflection with indices *hkl* (only Pawley);
- *a,b,c,α,β,γ* - Unit-cell metric tensor parameters;
- $2\theta_{zero}$ - Instrumental zero error;
- *U,V,W* - Peak-width parameters;
- η, etc. - Other peak-shape parameters

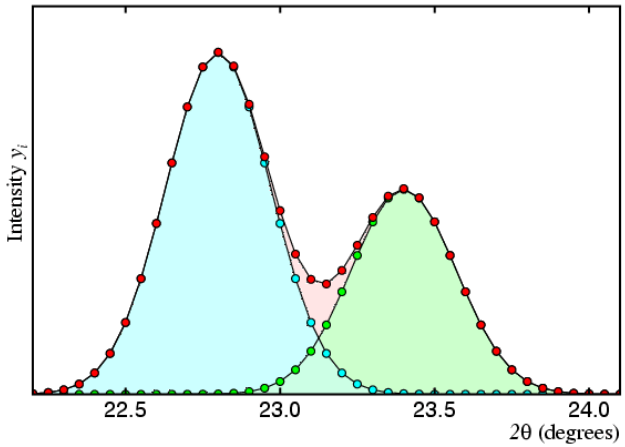

Pseudo-Voight peak shape function:

$$I(2\theta) = I_{hkl}\,[\eta\,\mathbf{L}\,(2\theta - 2\theta_0) + (1-\eta)\,\mathbf{G}\,(2\theta - 2\theta_0)\,]$$

where L (2θ − 2θ0) and G (2θ − 2θ0) represent Lorentz and Gaussian functions, and η - the "Lorentz fraction"

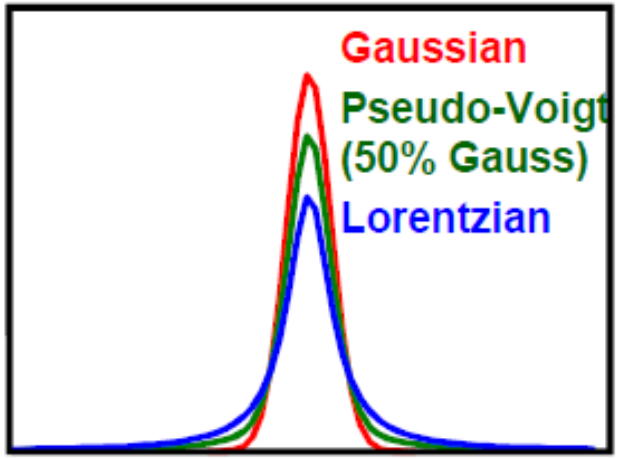

Institute for Chemical and Bioengineering, ETH Zurich, Zurich, Switzerland
Laboratory for Catalysis and Sustainable Chemistry, Paul Scherrer Institute, Villigen, Switzerland
Przemyslaw Rzepka

Pawley and LeBail profile fitting

Parameters:

- *I*(*hkl*) - Intensity of each reflection with indices *hkl* (only Pawley);
- *a,b,c,α,β,γ* - Unit-cell metric tensor parameters;
- $2\theta_{zero}$ - Instrumental zero error;
- *U,V,W* - Peak-width parameters;
- η, etc. - Other peak-shape parameters

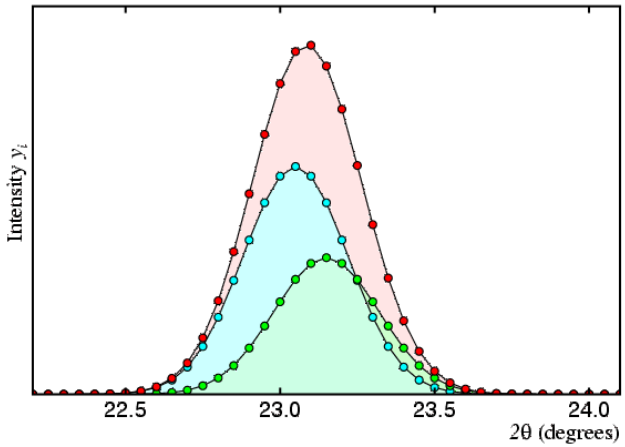

Pseudo-Voight peak shape function:

$$I(2\theta) = I_{hkl}\,[\eta\,\mathbf{L}\,(2\theta - 2\theta_0) + (1-\eta)\,\mathbf{G}\,(2\theta - 2\theta_0)\,]$$

where L (2θ − 2θ0) and G (2θ − 2θ0) represent Lorentz and Gaussian functions, and η - the "Lorentz fraction"

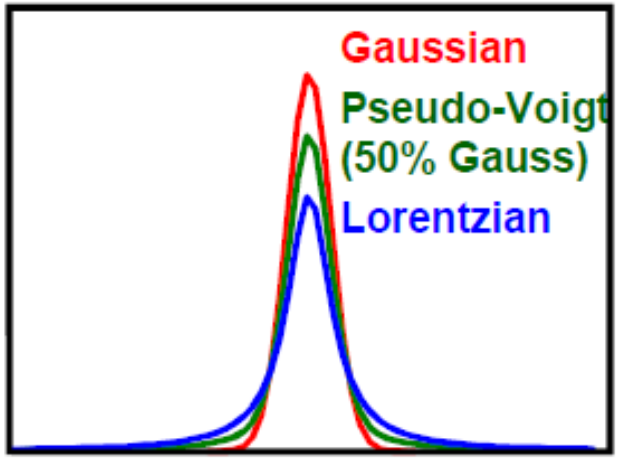

Institute for Chemical and Bioengineering, ETH Zurich, Zurich, Switzerland
Laboratory for Catalysis and Sustainable Chemistry, Paul Scherrer Institute, Villigen, Switzerland

Pawley and LeBail profile fitting

Parameters:

- *I*(*hkl*) - Intensity of each reflection with indices *hkl* (only Pawley);
- *a,b,c,α,β,γ* - Unit-cell metric tensor parameters;
- $2\theta_{zero}$ - Instrumental zero error;
- *U,V,W* - Peak-width parameters;
- η, etc. - Other peak-shape parameters

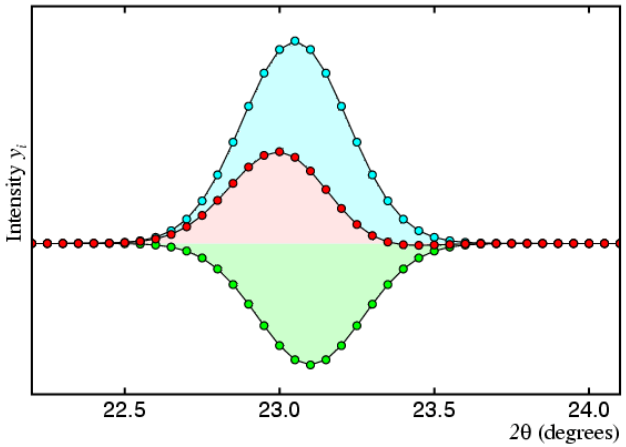

Pseudo-Voight peak shape function:

$$I(2\theta) = I_{hkl}\,[\eta\,\mathbf{L}\,(2\theta - 2\theta_0) + (1-\eta)\,\mathbf{G}\,(2\theta - 2\theta_0)\,]$$

where L (2θ − 2θ0) and G (2θ − 2θ0) represent Lorentz and Gaussian functions, and η - the "Lorentz fraction"

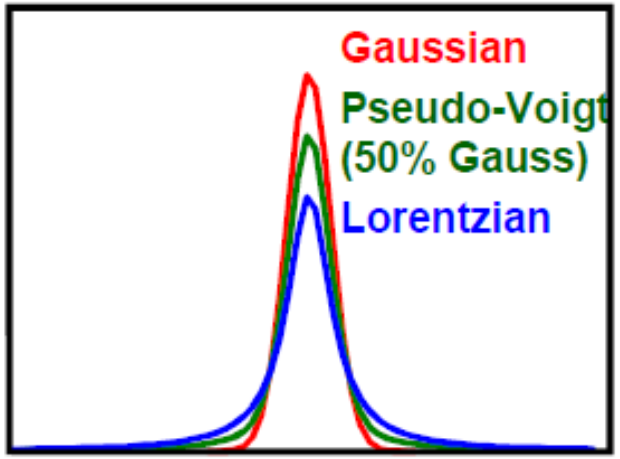

Rietveld profile fitting

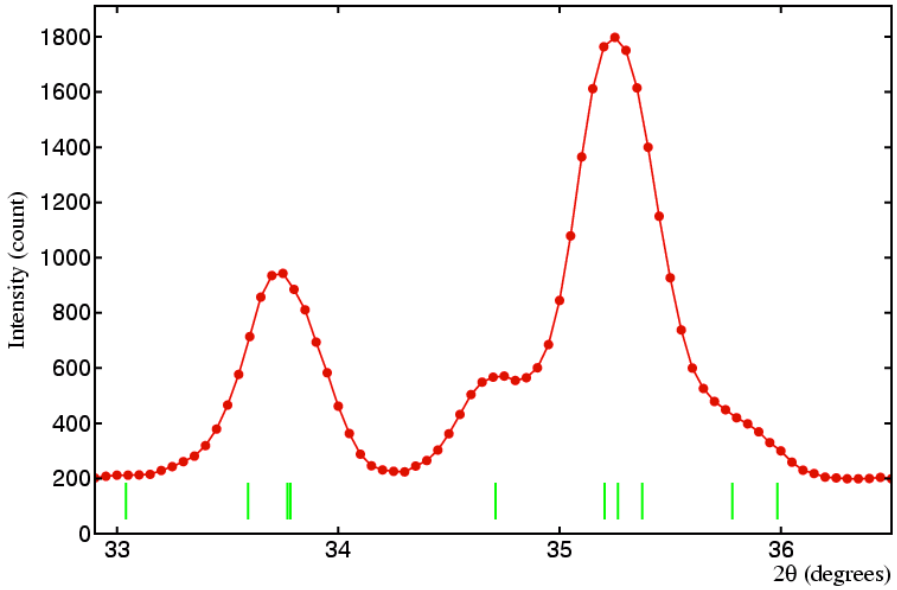

The detailed diffraction profile contained a lot more information than the extracted intensities of composite peaks

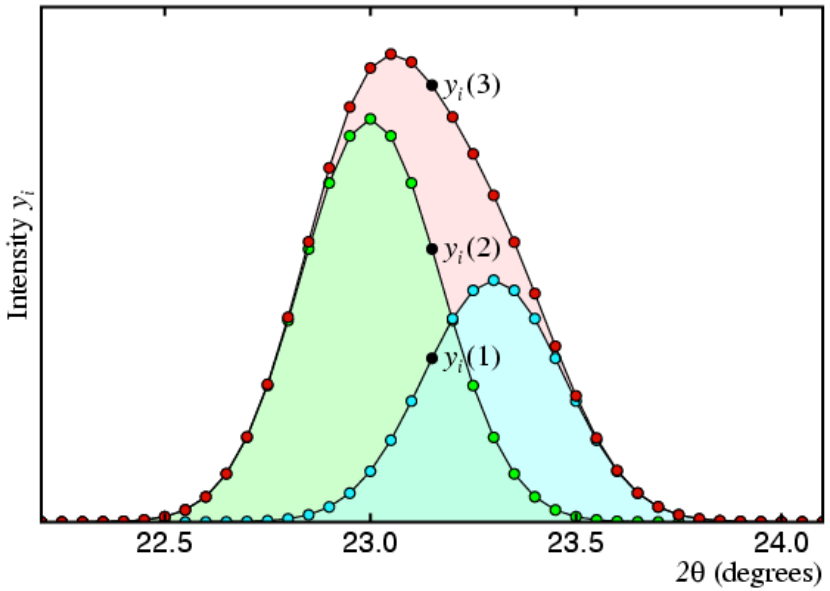

The detailed profile can be fitted on a point by point basis as the summation of the contribution of the profiles of all reflections to that point:

$$y_i(3) = yi(1) + yi(2)$$

Institute for Chemical and Bioengineering, ETH Zurich, Zurich, Switzerland
Laboratory for Catalysis and Sustainable Chemistry, Paul Scherrer Institute, Villigen, Switzerland

Instrumental function

Refinement in TOPAS

xdd {

! Lam profile (wavelength)

@ SD()

@ PV_Peak_Type()

@ Simple_Axial_Model()

@ @ Scale

}

Structure parameters

str {

@ Unit cell parameters

											Site Ocupp. Factor		Therm. Factor
			Fractional atomic coordinates										
site Si(1)	*num_posns*	*16*	*x*	*0.32281*	*y*	*0.19961*	*z*	*0.20804*	*occ Si*	*1.0*	*beq 1*
site Si(2)	*num_posns*	*8*	*x*	*0.08670*	*y*	*0.20129*	*z*	*0.00000*	*occ Si*	*1.0*	*beq 1*
site Si(3)	*num_posns*	*8*	*x*	*0.27374*	*y*	*0.00000*	*z*	*0.29371*	*occ Si*	*1.0*	*beq 1*
site Si(4)	*num_posns*	*4*	*x*	*0.15538*	*y*	*0.00000*	*z*	*0.00000*	*occ Si*	*1.0*	*beq 1*
site O(8)	*num_posns*	*4*	*x*	*0.25169*	*y*	*0.00000*	*z*	*0.50000*	*occ O*	*1.0*	*beq 1*
site O(7)	*num_posns*	*8*	*x*	*0.20342*	*y*	*0.00000*	*z*	*0.18745*	*occ O*	*1.0*	*beq 2*
site O(5)	*num_posns*	*8*	*x*	*0.10707*	*y*	*0.09088*	*z*	*0.00000*	*occ O*	*1.0*	*beq 2*
site O(3)	*num_posns*	*8*	*x*	*0.34246*	*y*	*0.21404*	*z*	*0.00000*	*occ O*	*1.0*	*beq 2*
site O(6)	*num_posns*	*4*	*x*	*0.00000*	*y*	*0.20890*	*z*	*0.00000*	*occ O*	*1.0*	*beq 2*
site O(4)	*num_posns*	*8*	*x*	*0.25000*	*y*	*0.25000*	*z*	*0.25000*	*occ O*	*1.0*	*beq 2*
site O(2)	*num_posns*	*16*	*x*	*0.38070*	*y*	*0.24571*	*z*	*0.32000*	*occ O*	*1.0*	*beq 2*
site O(1)	*num_posns*	*16*	*x*	*0.31646*	*y*	*0.09052*	*z*	*0.24720*	*occ O*	*1.0*	*beq 2*

}

The Rietveld analysis

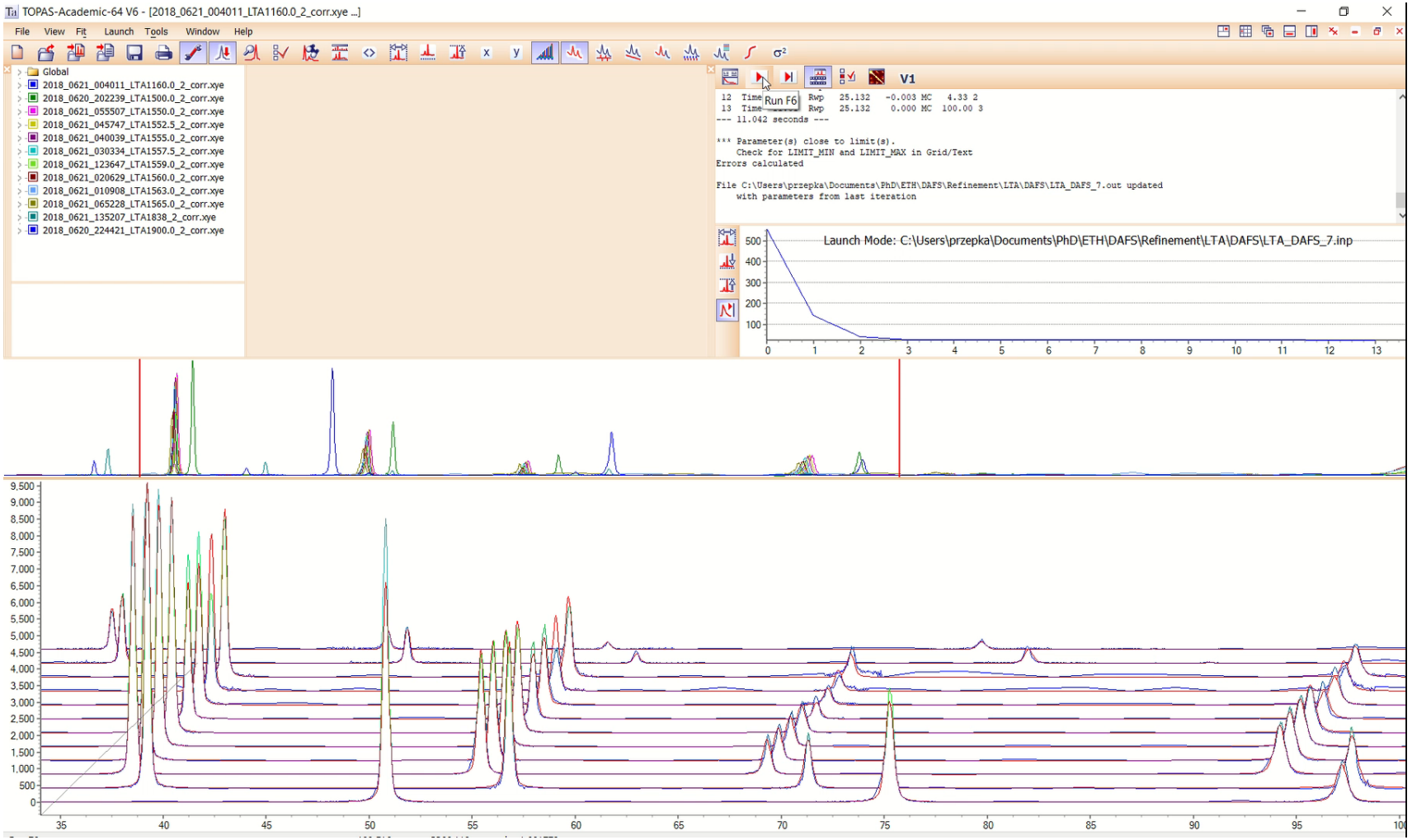

Institute for Chemical and Bioengineering, ETH Zurich, Zurich, Switzerland
Laboratory for Catalysis and Sustainable Chemistry, Paul Scherrer Institute, Villigen, Switzerland

Przemyslaw Rzepka

Phase identification

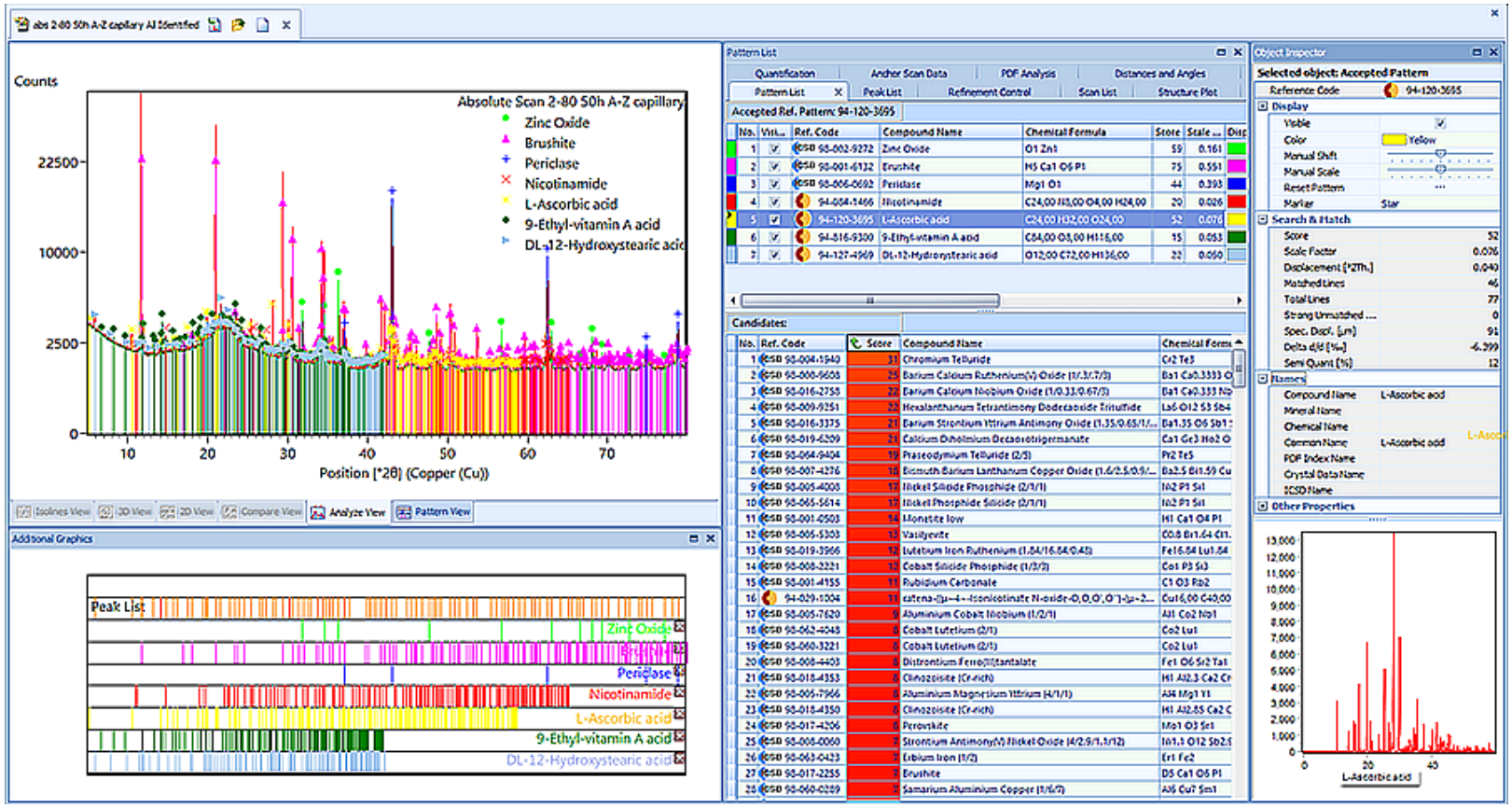

HighScore matches the peaks from collected data with database records

Institute for Chemical and Bioengineering, ETH Zurich, Zurich, Switzerland
Laboratory for Catalysis and Sustainable Chemistry, Paul Scherrer Institute, Villigen, Switzerland

Sample preparation. What happens when wrong?

1. Not all crystal lattice planes present (graininess)

2. Relative intensities distribution different from expected (preferred orientation)

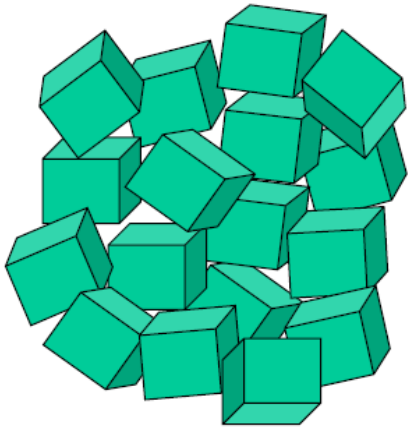

Random orientation of crystallites (e.g. isotropic powder)

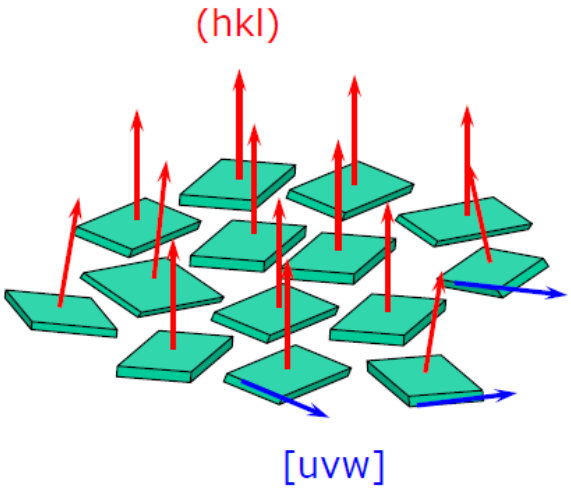

Preferred orientation of crystallites (typical for plate-like crystallites)

Sample preparation. What happens when wrong?

1. Not all crystal lattice planes present (graininess)

2. Relative intensities distribution different from expected (preferred orientation)

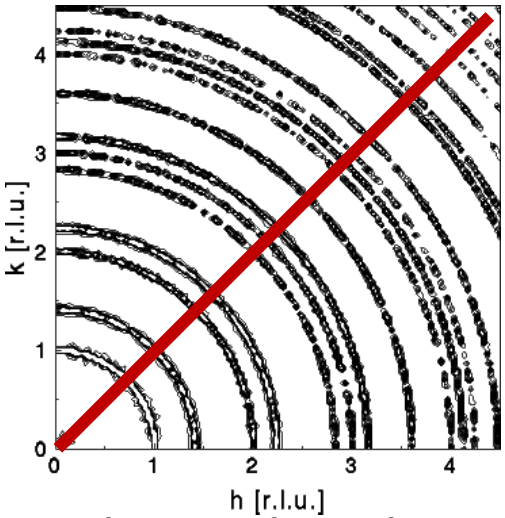

Random orientation of crystallites (e.g. isotropic powder)

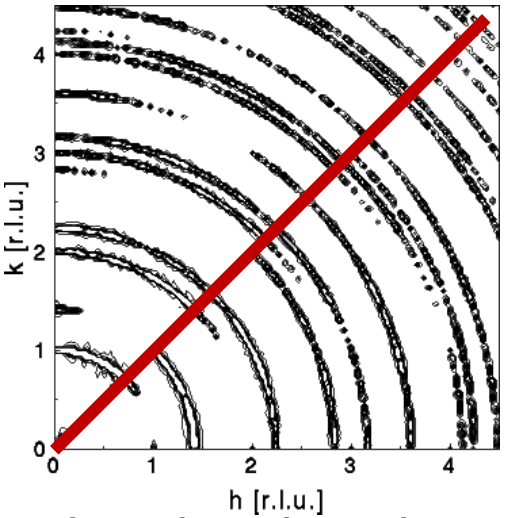

Preferred orientation of crystallites (typical for plate-like crystallites)

Sample preparation

Preferred orientation may be corrected by spherical harmonics function. It compromises however the structure refinement or quantitative phase identification

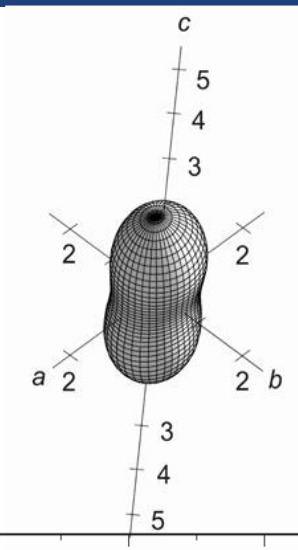

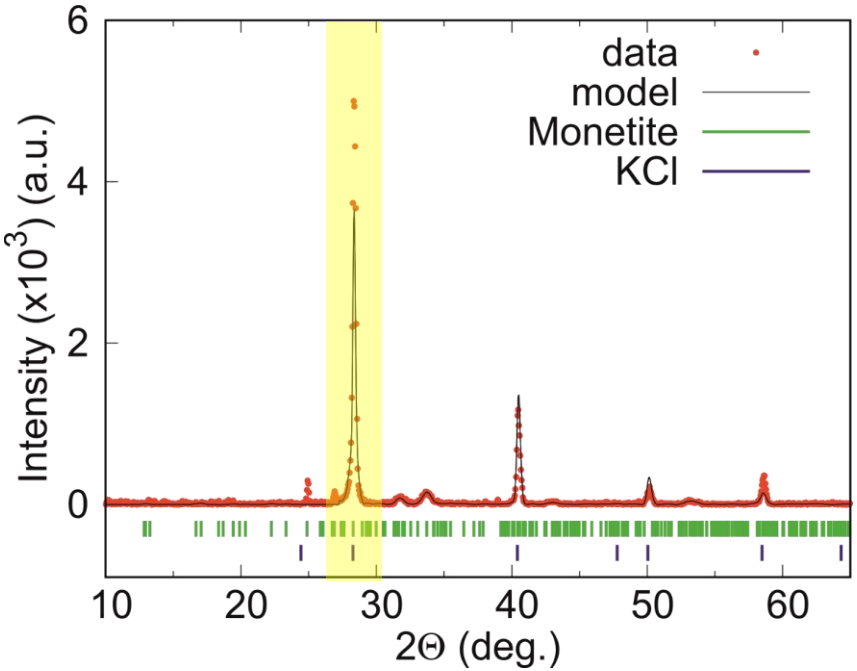

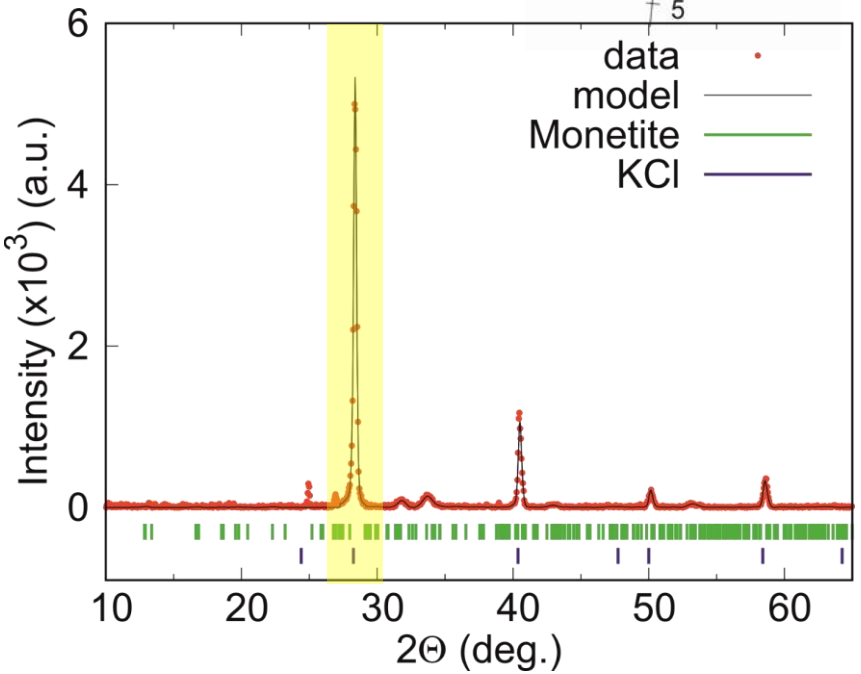

Institute for Chemical and Bioengineering, ETH Zurich, Zurich, Switzerland
Laboratory for Catalysis and Sustainable Chemistry, Paul Scherrer Institute, Villigen, Switzerland

Sample preparation for reflection XRD

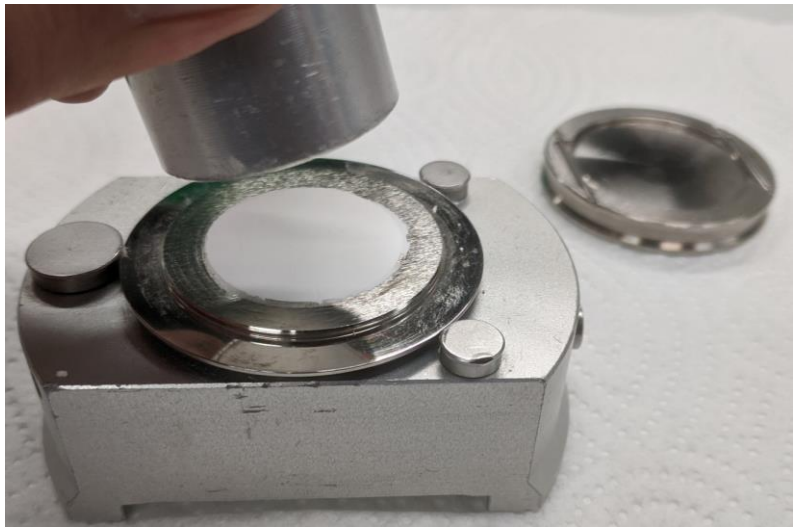

Sample preparation for reflection XRD

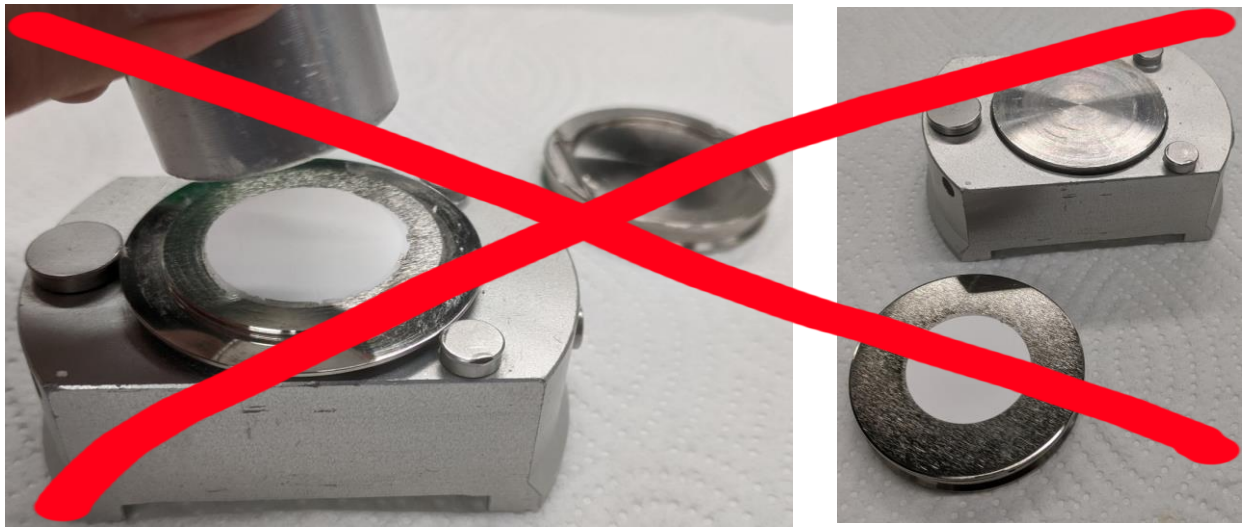

$$I/I_0 = e^{-(\mu_{tot}/\rho)x} < 1\% \; if \; x > 0.5mm$$

I_0(ph/s) – incident photon flux for Cu anode;
μ_{tot} – total absorption coefficient for a zeolite;
ρ – density of a zeolite;

Institute for Chemical and Bioengineering, ETH Zurich, Zurich, Switzerland
Laboratory for Catalysis and Sustainable Chemistry, Paul Scherrer Institute, Villigen, Switzerland

Sample preparation for reflection XRD

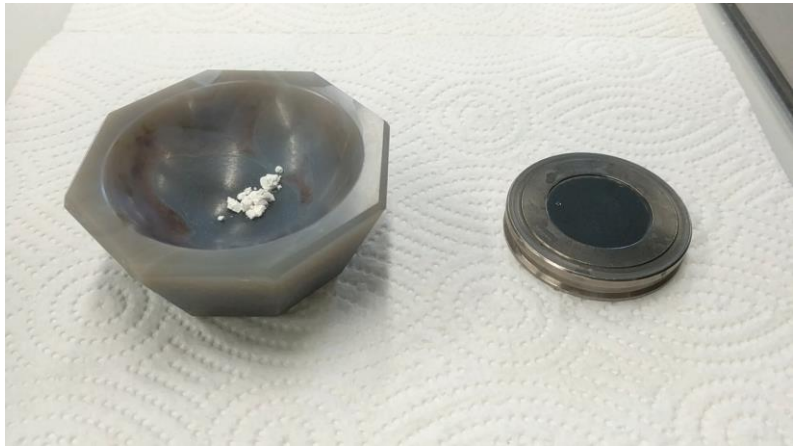

Institute for Chemical and Bioengineering, ETH Zurich, Zurich, Switzerland
Laboratory for Catalysis and Sustainable Chemistry, Paul Scherrer Institute, Villigen, Switzerland

Przemyslaw Rzepka

Sample preparation for transmission XRD

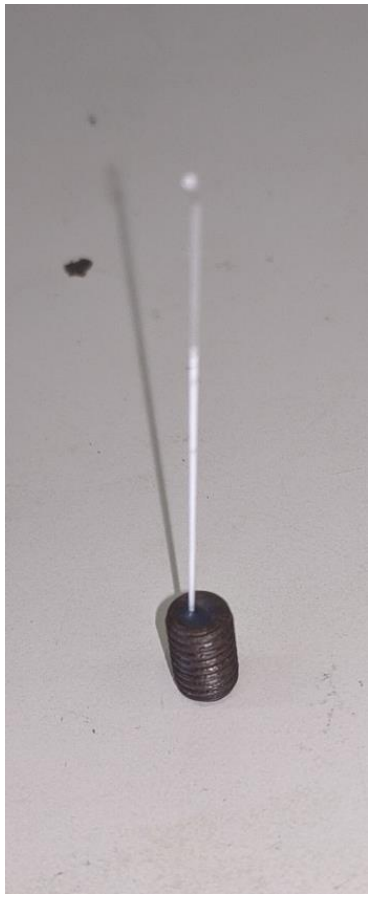

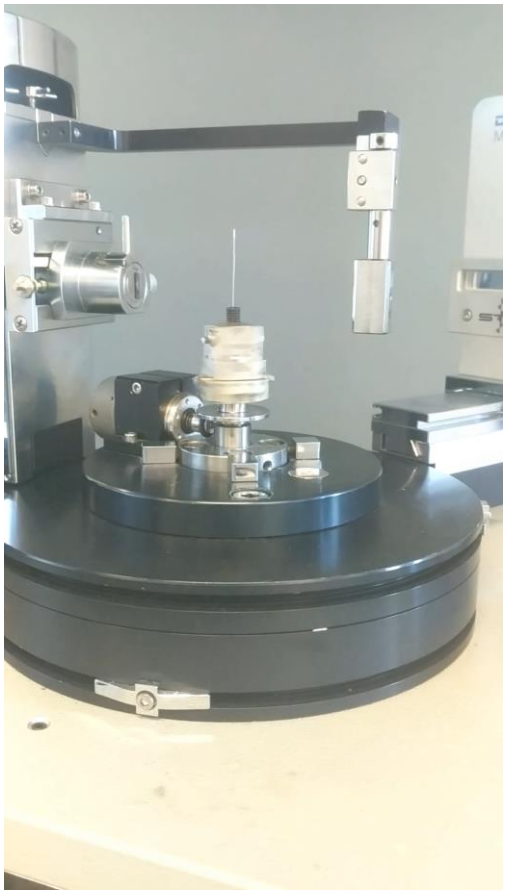

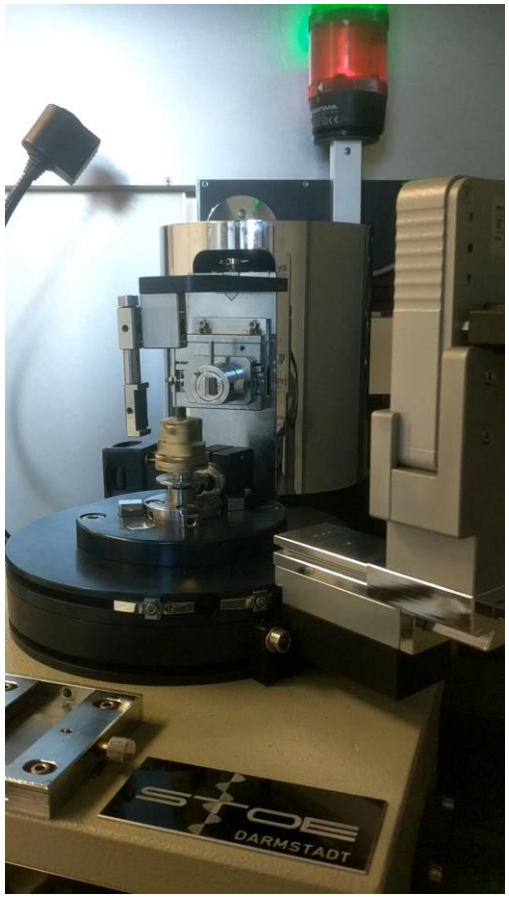

Stoe STADIP diffractometer working in Transmission-/Debye-Scherrer-geometry available for ex situ capillaries measurements

Institute for Chemical and Bioengineering, ETH Zurich, Zurich, Switzerland
Laboratory for Catalysis and Sustainable Chemistry, Paul Scherrer Institute, Villigen, Switzerland

Si:Al distribution in zeolite framework

Protons and other light elements are poor scatterers and cannot be detected directly by X-ray diffraction methods

Brønsted acid sites or hydroxyl groups are balanced by framework charge associated to aluminum. Hence determination of Al positions allows on situating extra-framework entities

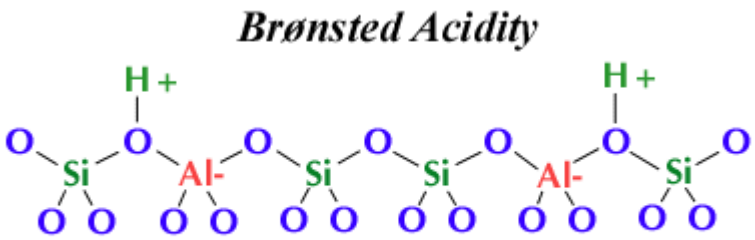

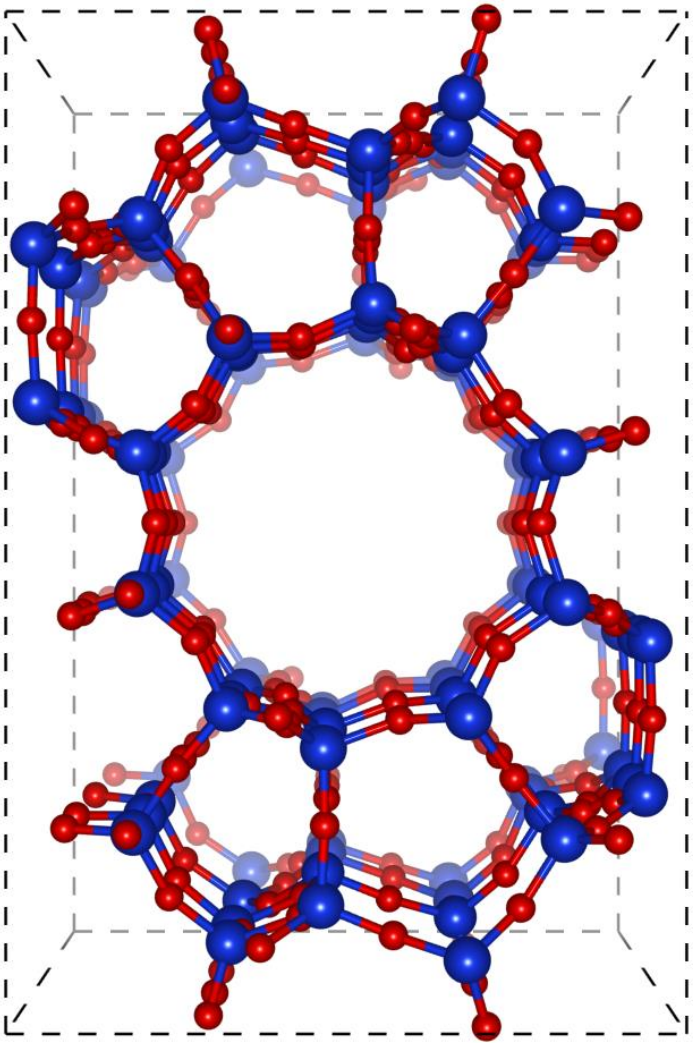

Institute for Chemical and Bioengineering, ETH Zurich, Zurich, Switzerland
Laboratory for Catalysis and Sustainable Chemistry, Paul Scherrer Institute, Villigen, Switzerland

Difference density maps

fourier_map_formula=Fobs-Fcalc(model);

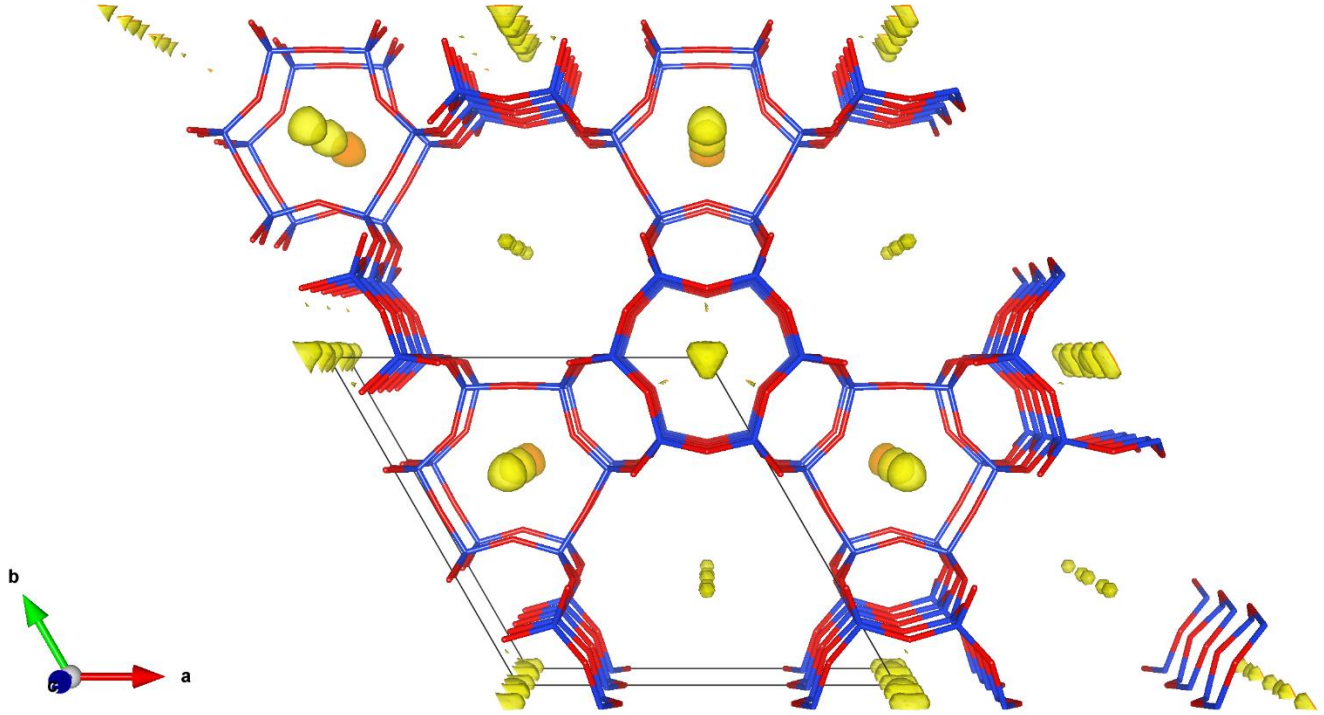

To investigate the positioning of the cations in Cu-OFF zeolite, the structure model containing only the framework atoms was subtracted from observed PXRD data

The refinement of extraframework cations

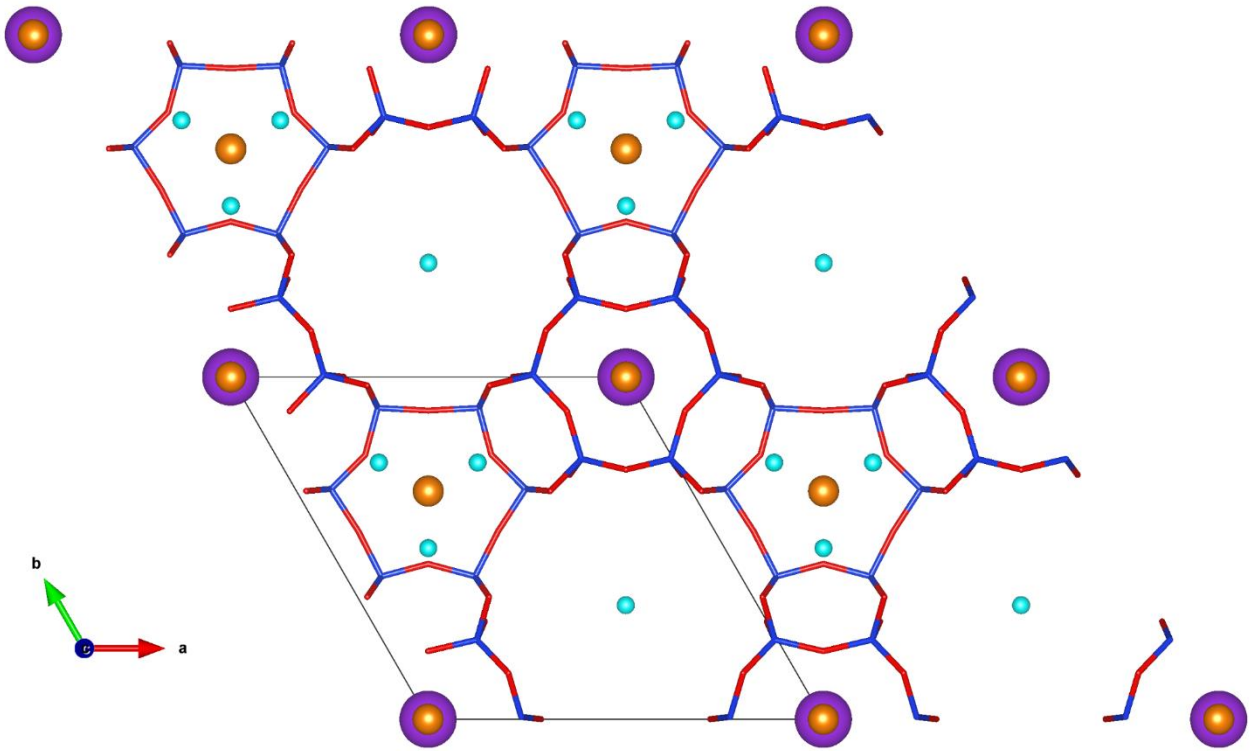

The structure of Cu-OFF with input positions of the extra-framework cations adopted from DDM was refined using Rietveld analysis

Institute for Chemical and Bioengineering, ETH Zurich, Zurich, Switzerland
Laboratory for Catalysis and Sustainable Chemistry, Paul Scherrer Institute, Villigen, Switzerland

Structure Determination by Simulated Annealing

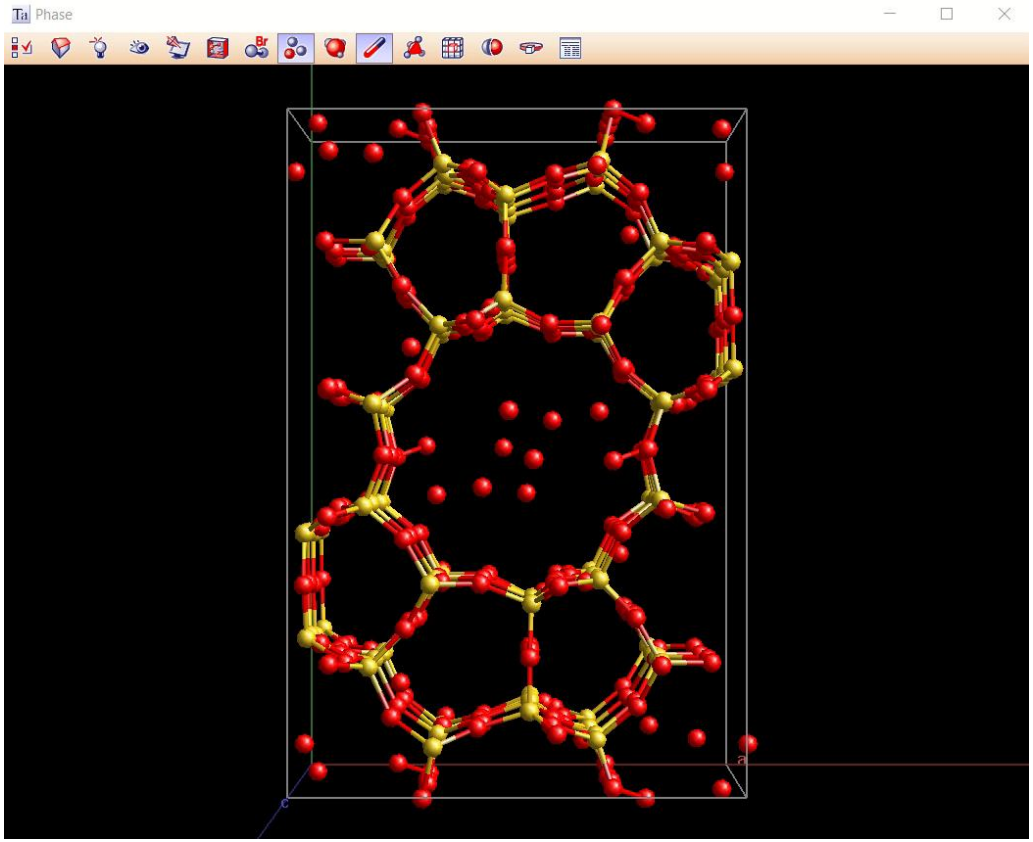


```
rigid
   load z_matrix {
      O1
      H2  1  0.9687
      H3  1  0.9687  2  104
   }

   translate
      tx @ 0 ty @ 0 tz @ 0
   rotate
      qa @ 0 qb @ 0 qc @ 0
```

The simulated annealing algorithm approximates the global optimum of a given parameter in an environment of a large number of local optima whereas least square methods are local optimization only

Simulated annealing vs least squares methods (Rietveld refinement)

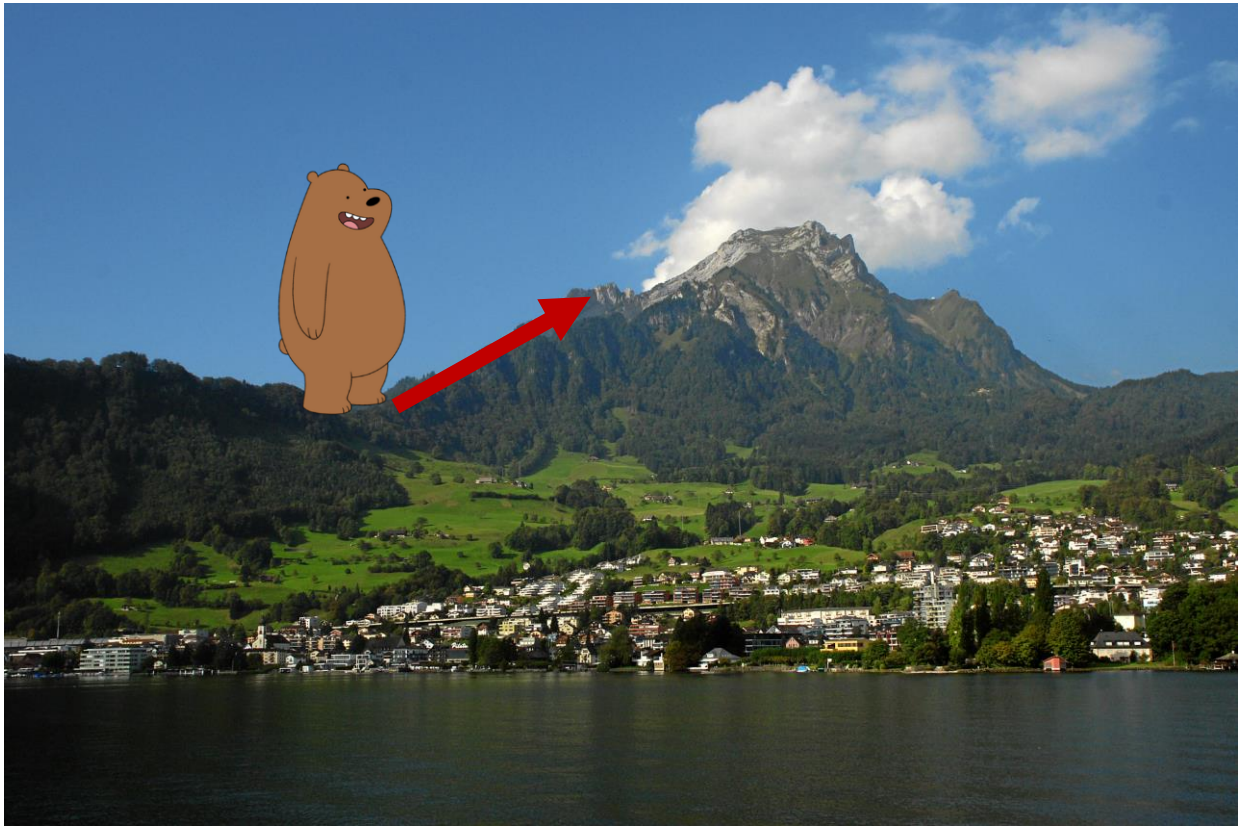

The simulated annealing algorithm approximates the global optimum of a given parameter in an environment of a large number of local optima whereas least square methods are local optimization only

Institute for Chemical and Bioengineering, ETH Zurich, Zurich, Switzerland
Laboratory for Catalysis and Sustainable Chemistry, Paul Scherrer Institute, Villigen, Switzerland

Simulated annealing vs least squares methods (Rietveld refinement)

The simulated annealing algorithm approximates the global optimum of a given parameter in an environment of a large number of local optima whereas least square methods are local optimization only

Institute for Chemical and Bioengineering, ETH Zurich, Zurich, Switzerland
Laboratory for Catalysis and Sustainable Chemistry, Paul Scherrer Institute, Villigen, Switzerland

Lattice parameters and particle size analysis

Formation of the strong metal support interaction (SMSI). Pt-Ti alloying

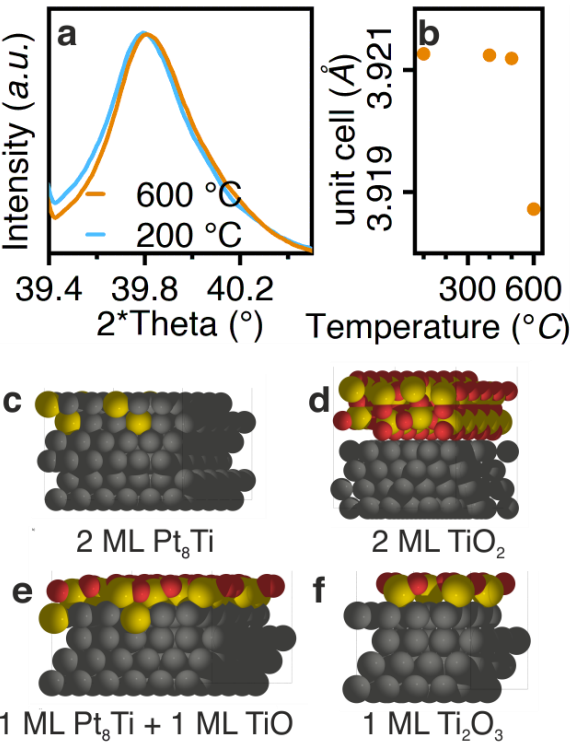

The annealing of carbon-supported Pt nanoparticles. The evolution of diffraction peaks

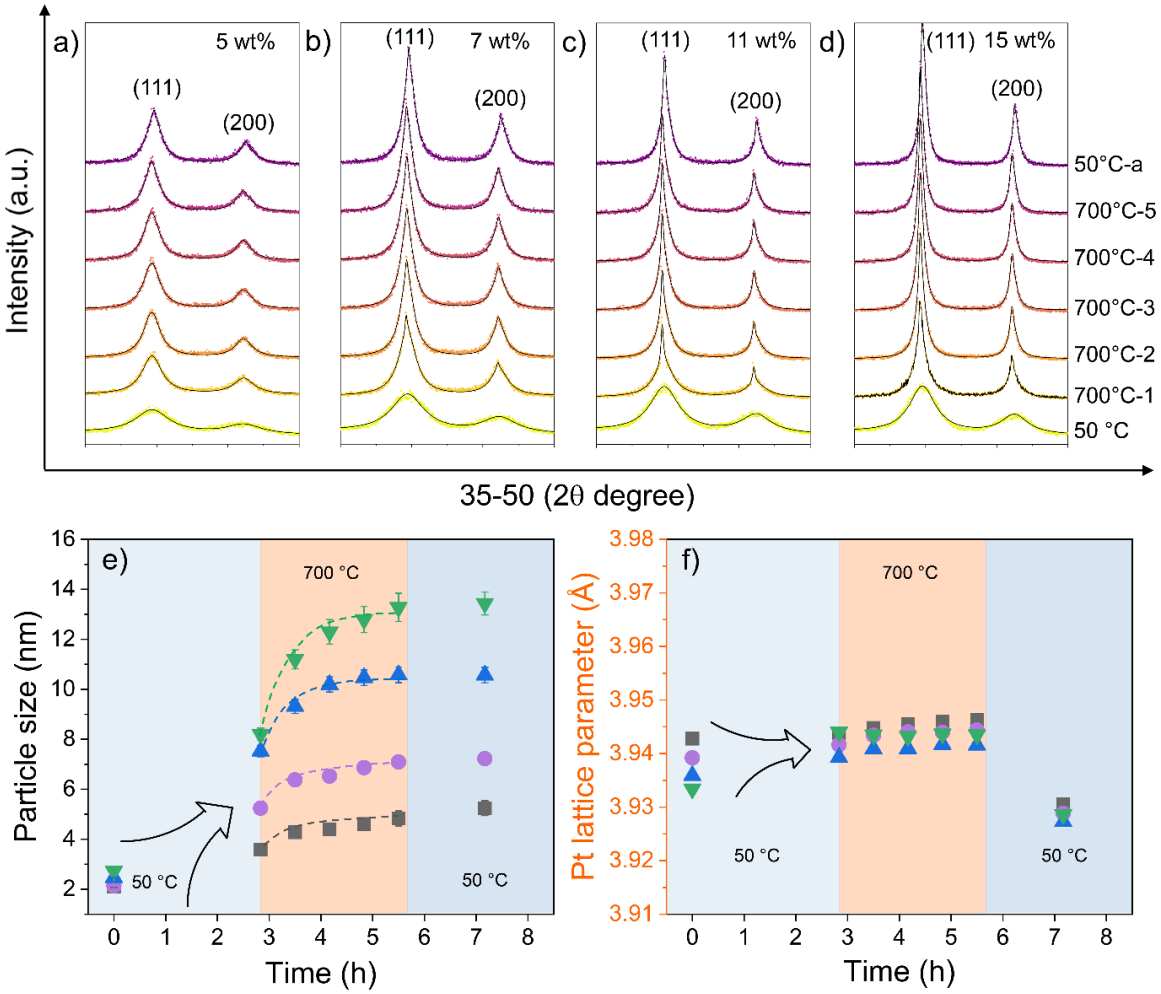

Institute for Chemical and Bioengineering, ETH Zurich, Zurich, Switzerland
Laboratory for Catalysis and Sustainable Chemistry, Paul Scherrer Institute, Villigen, Switzerland

ZSM5 structure upon MTH conversion

before

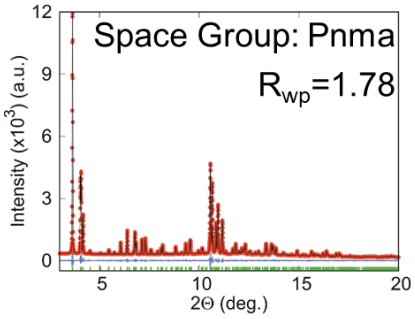

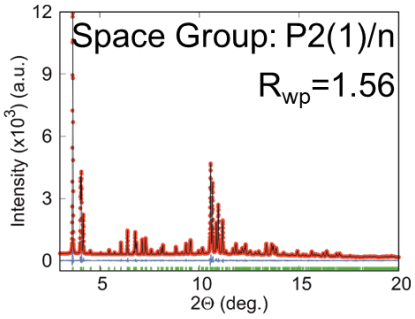

after

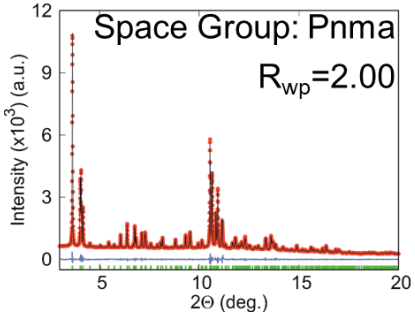

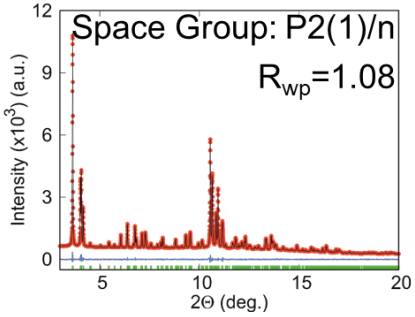

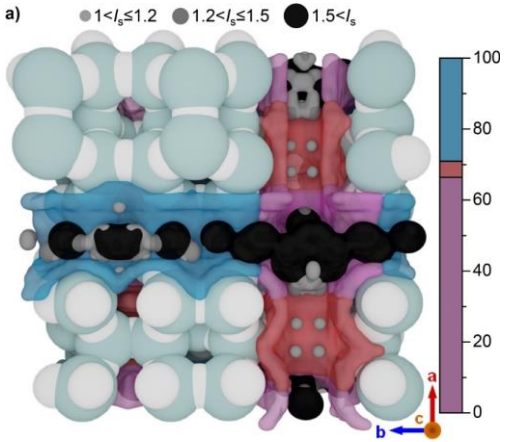

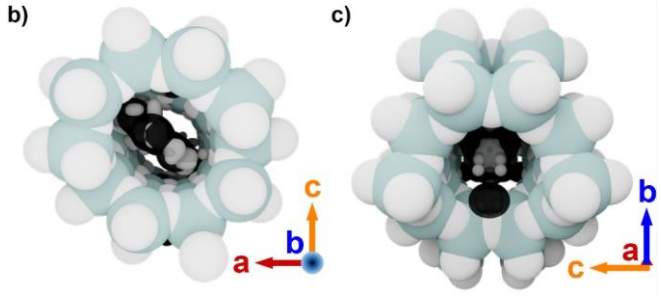

Clustering of coke in the intersection of ZSM-5 channels during methanol-to-hydrocarbons conversion (MTH) leads to lowering of the structure symmetry

Institute for Chemical and Bioengineering, ETH Zurich, Zurich, Switzerland
Laboratory for Catalysis and Sustainable Chemistry, Paul Scherrer Institute, Villigen, Switzerland

ZSM5 structure upon MTH conversion

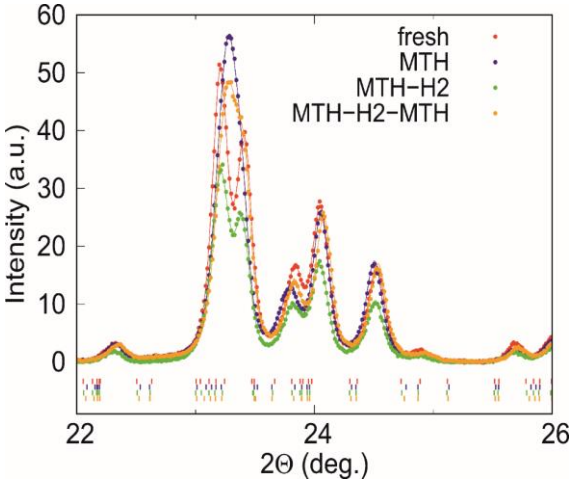

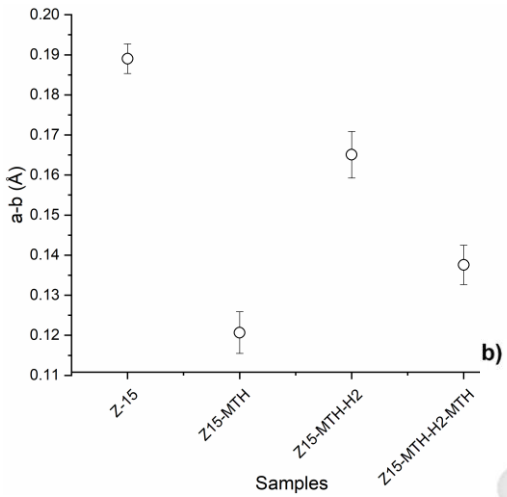

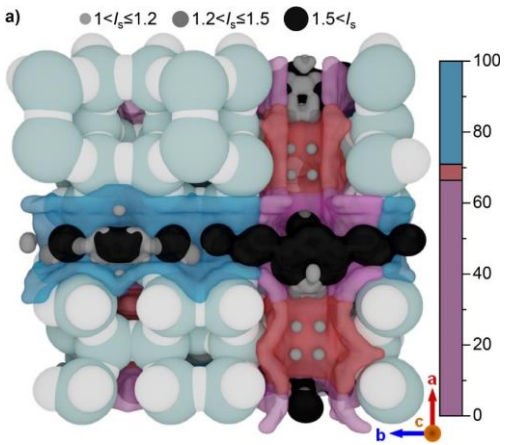

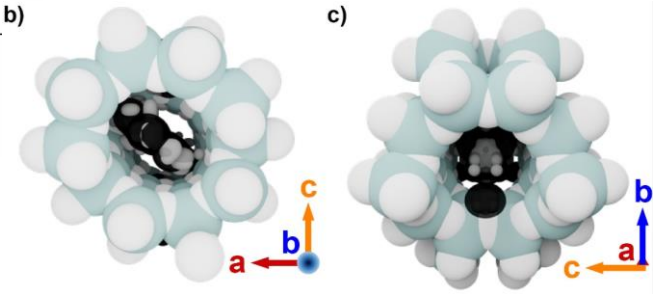

Clustering of coke in the intersection of ZSM-5 channels during methanol-to-hydrocarbons conversion (MTH) is correlated by a-b lattice parameters change

Institute for Chemical and Bioengineering, ETH Zurich, Zurich, Switzerland
Laboratory for Catalysis and Sustainable Chemistry, Paul Scherrer Institute, Villigen, Switzerland

Symmetry lowering with T-atoms alternations

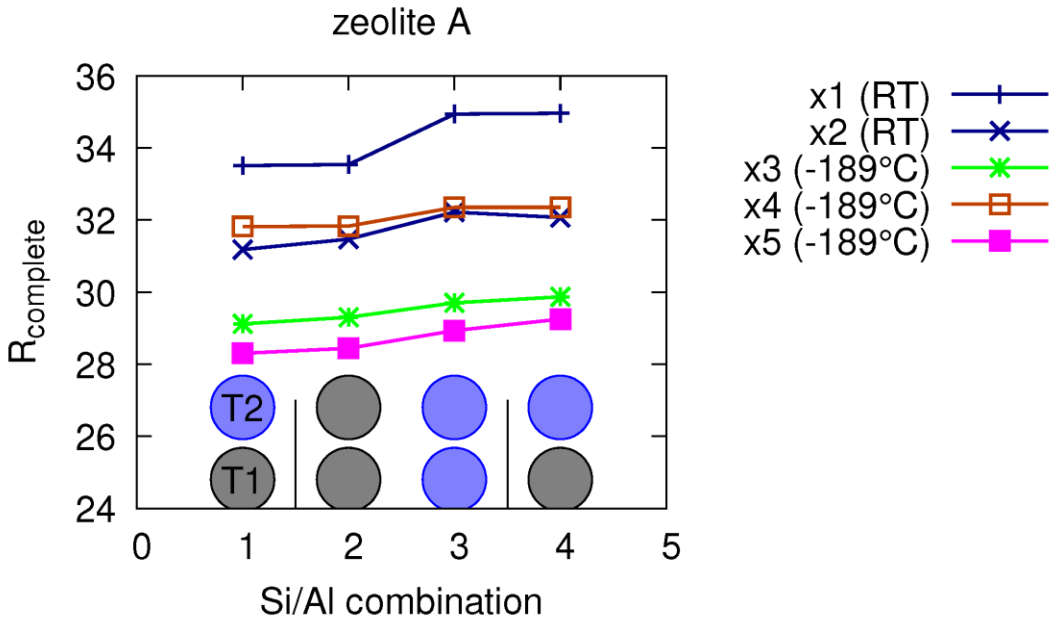

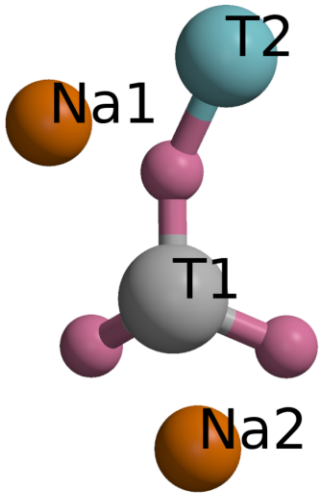

Electron diffraction demonstrates capability of energy discrimination to suppress noise and enables distinguishing between silicon and aluminum

Institute for Chemical and Bioengineering, ETH Zurich, Zurich, Switzerland
Laboratory for Catalysis and Sustainable Chemistry, Paul Scherrer Institute, Villigen, Switzerland

In situ TPR of CZA catalyst

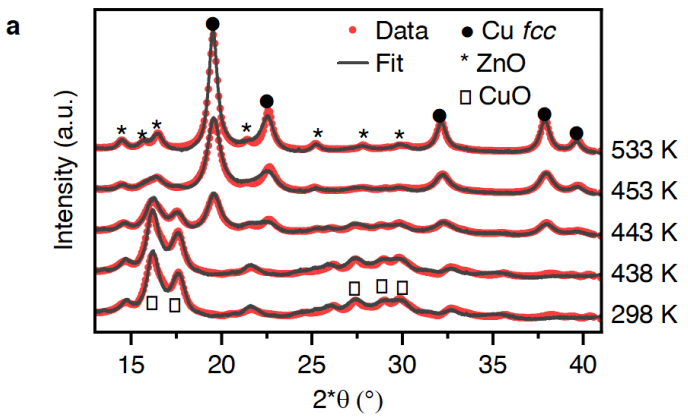

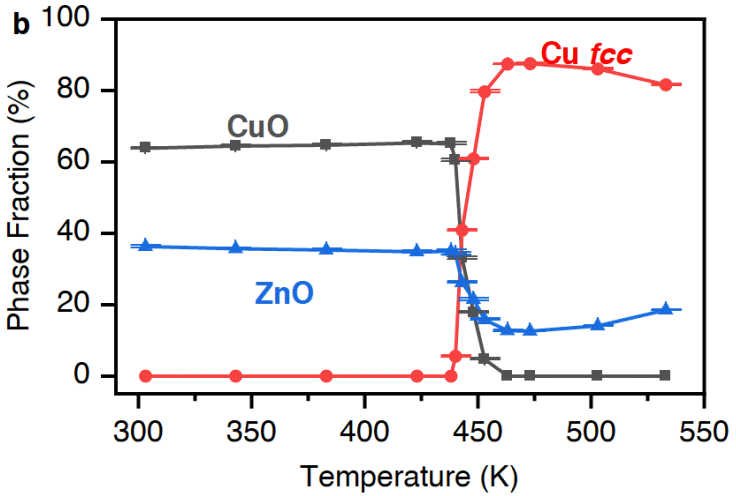

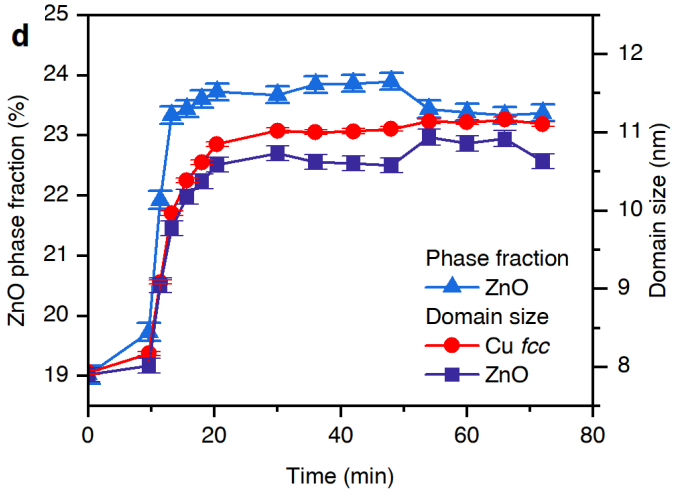

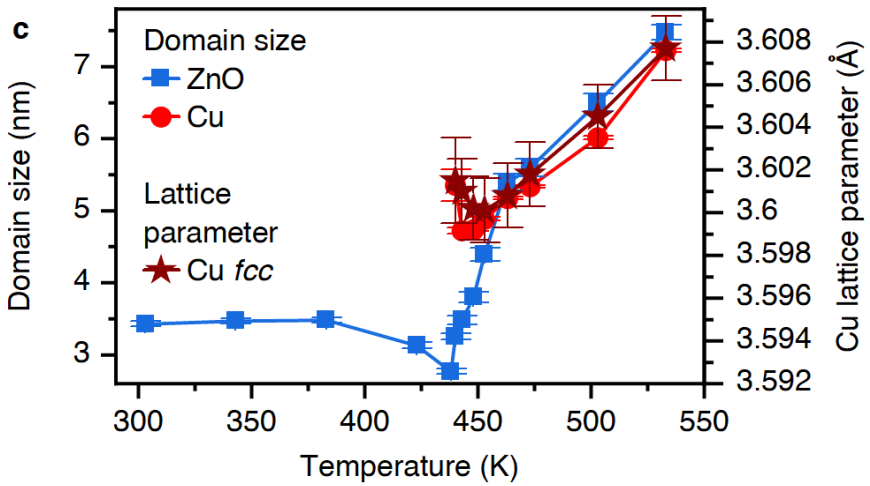

Institute for Chemical and Bioengineering, ETH Zurich, Zurich, Switzerland
Laboratory for Catalysis and Sustainable Chemistry, Paul Scherrer Institute, Villigen, Switzerland

In situ TPR of CZA catalyst

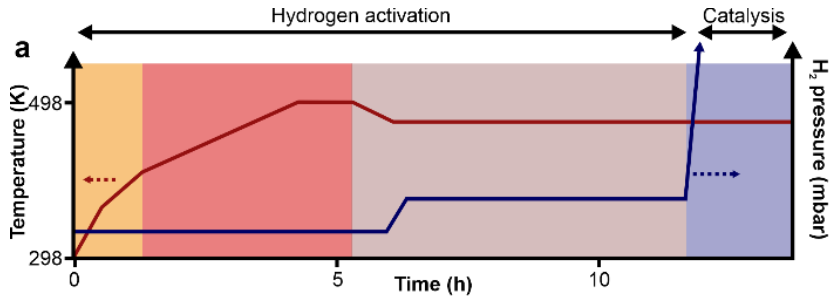

Genesis and transformation of the CZA precursor to the working catalyst upon typical reported industrial activation protocol.

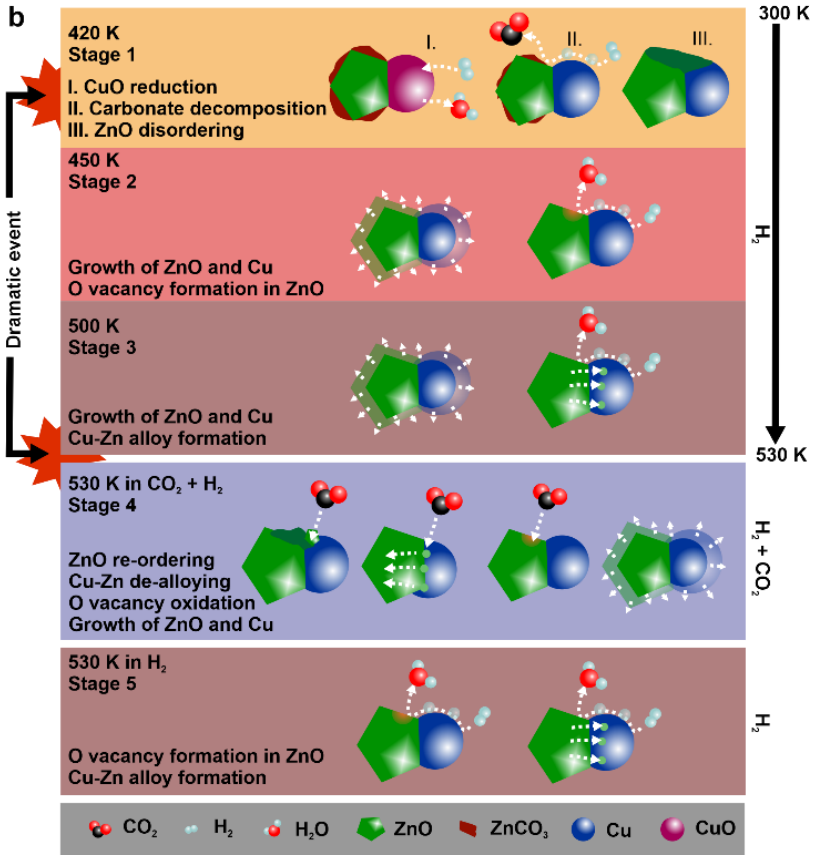

Institute for Chemical and Bioengineering, ETH Zurich, Zurich, Switzerland
Laboratory for Catalysis and Sustainable Chemistry, Paul Scherrer Institute, Villigen, Switzerland

Phase transition

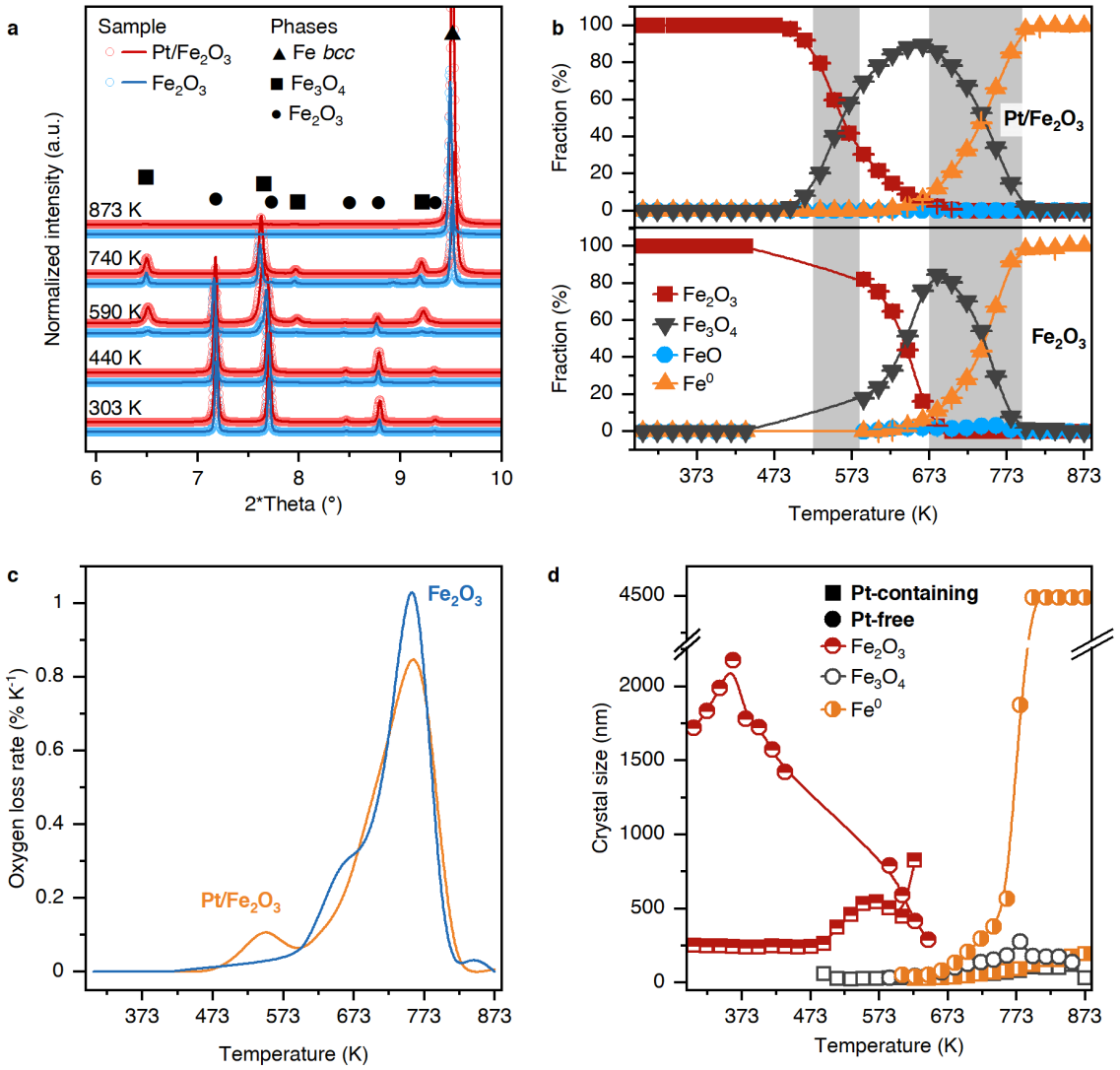

Iron oxides phase transition upon hydrogen in the presence and absence of platinum

Institute for Chemical and Bioengineering, ETH Zurich, Zurich, Switzerland
Laboratory for Catalysis and Sustainable Chemistry, Paul Scherrer Institute, Villigen, Switzerland

Przemyslaw Rzepka 25.10.2022

Spinel structure of γ-Al_2O_3

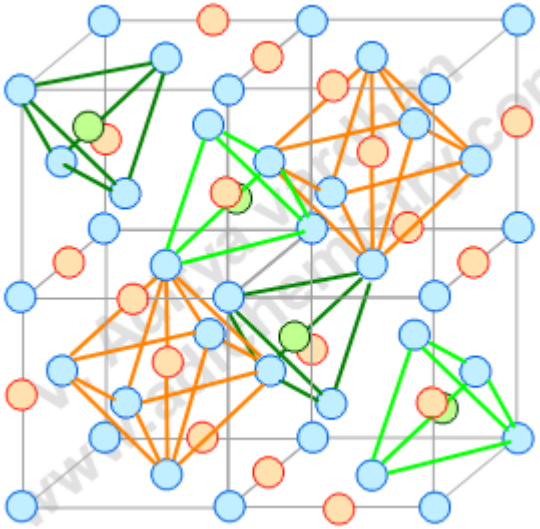

$(A^{II})^{tet}{}_8(B^{III})_{16}{}^{oct}O_{32}$

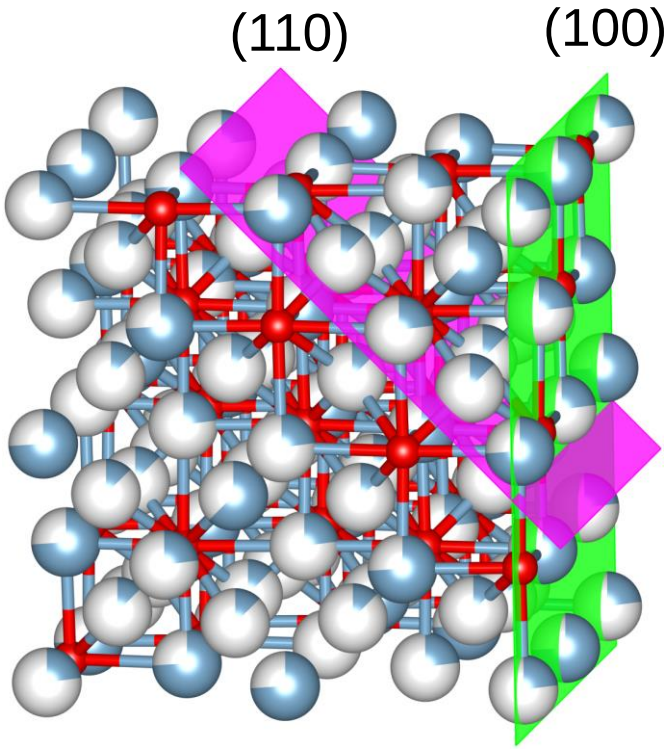

Al cations are distributed over the octahedral (*16d*) and tetrahedral (*8a*) site

{100} set of planes is specific for octahedral aluminum

Institute for Chemical and Bioengineering, ETH Zurich, Zurich, Switzerland
Laboratory for Catalysis and Sustainable Chemistry, Paul Scherrer Institute, Villigen, Switzerland

Structure of zeolite LTA

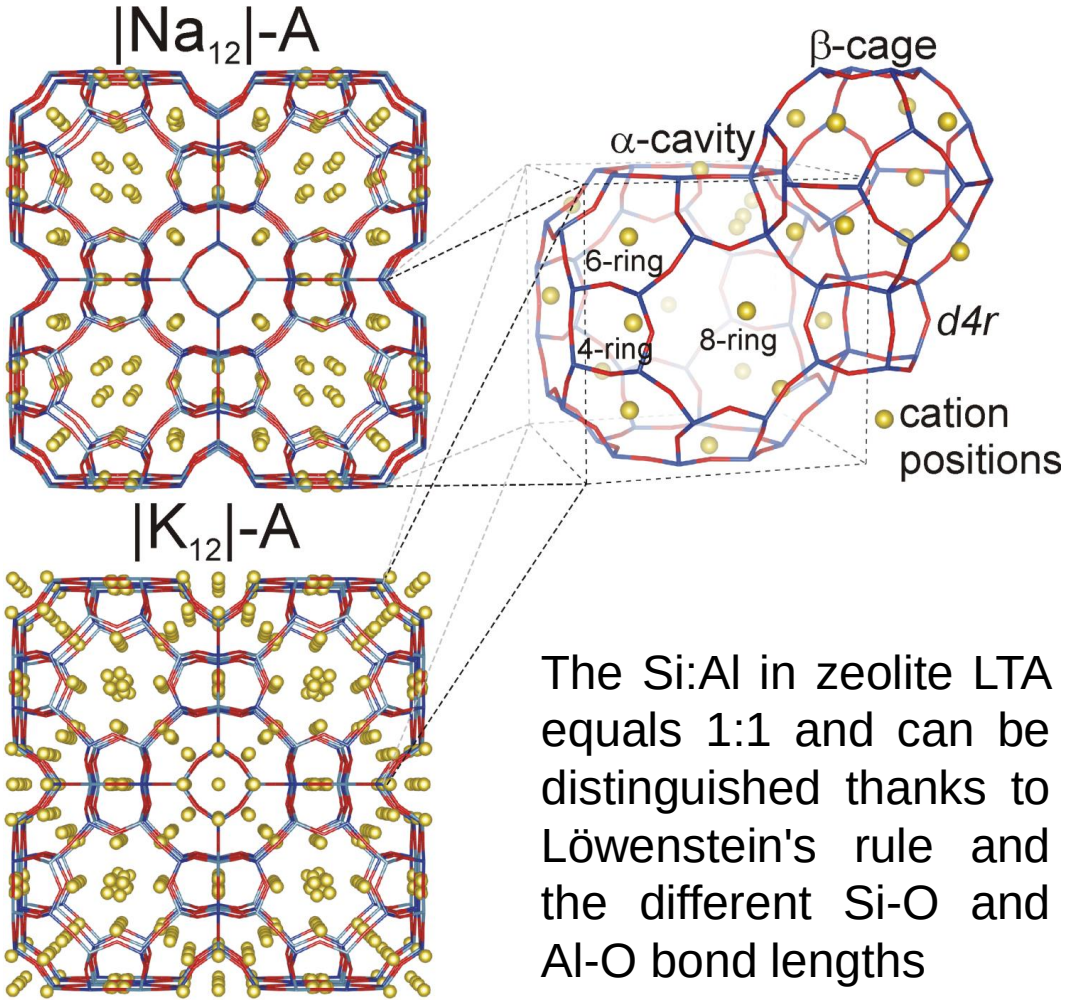

The Si:Al in zeolite LTA equals 1:1 and can be distinguished thanks to Löwenstein's rule and the different Si-O and Al-O bond lengths

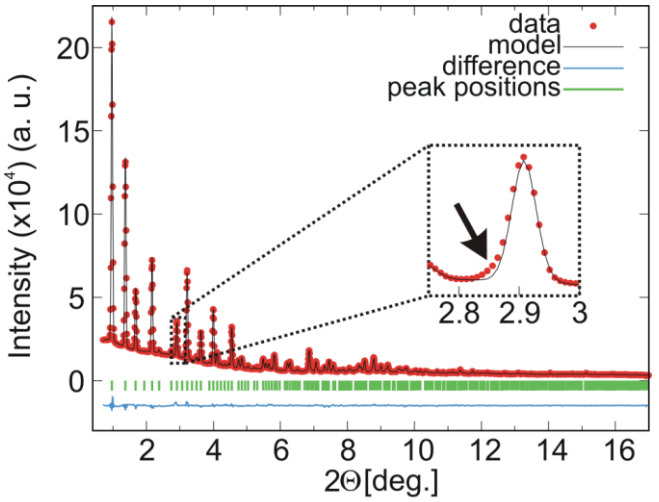

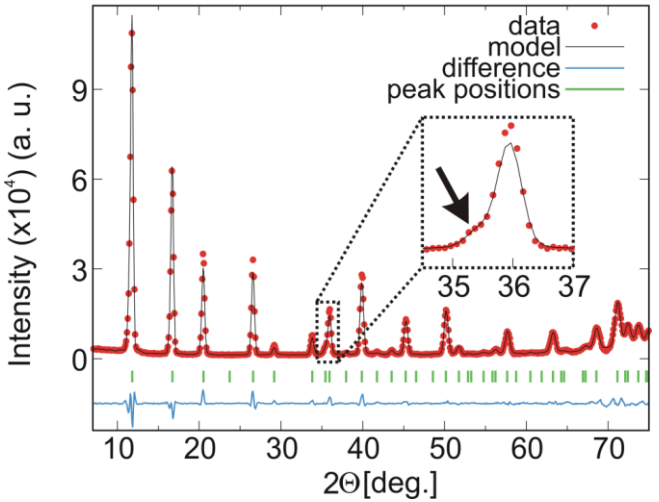

Institute for Chemical and Bioengineering, ETH Zurich, Zurich, Switzerland
Laboratory for Catalysis and Sustainable Chemistry, Paul Scherrer Institute, Villigen, Switzerland

X-ray Anomalous Form Factor

Silicon and aluminum have similar atomic numbers (Z=14 and 13) and are difficult to be distinguished

At X-ray absorption energy level, the f' and f'' contributions become significant and the scattering power of an element changes

$$f = f_0 + f' + i \cdot f''$$

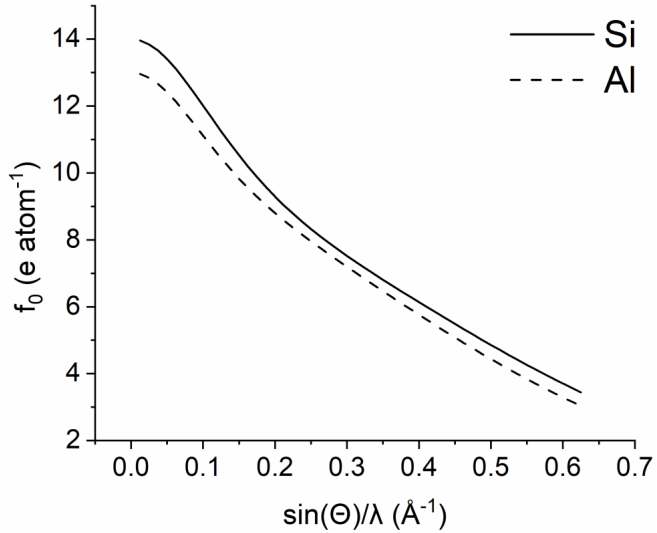

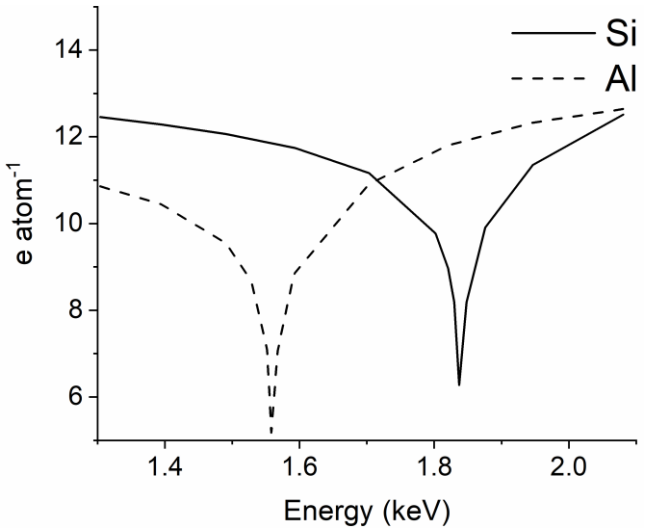

Institute for Chemical and Bioengineering, ETH Zurich, Zurich, Switzerland
Laboratory for Catalysis and Sustainable Chemistry, Paul Scherrer Institute, Villigen, Switzerland

Refinement of resonant data collected from LTA

The F_{hkl} values calculated for zeolite A across Al K-edge energies. The small but significant differences arise from near the Al K-edge. Each reflection is affected slightly differently by the changes in the aluminum scattering factor and these allow the aluminium distribution to be determined

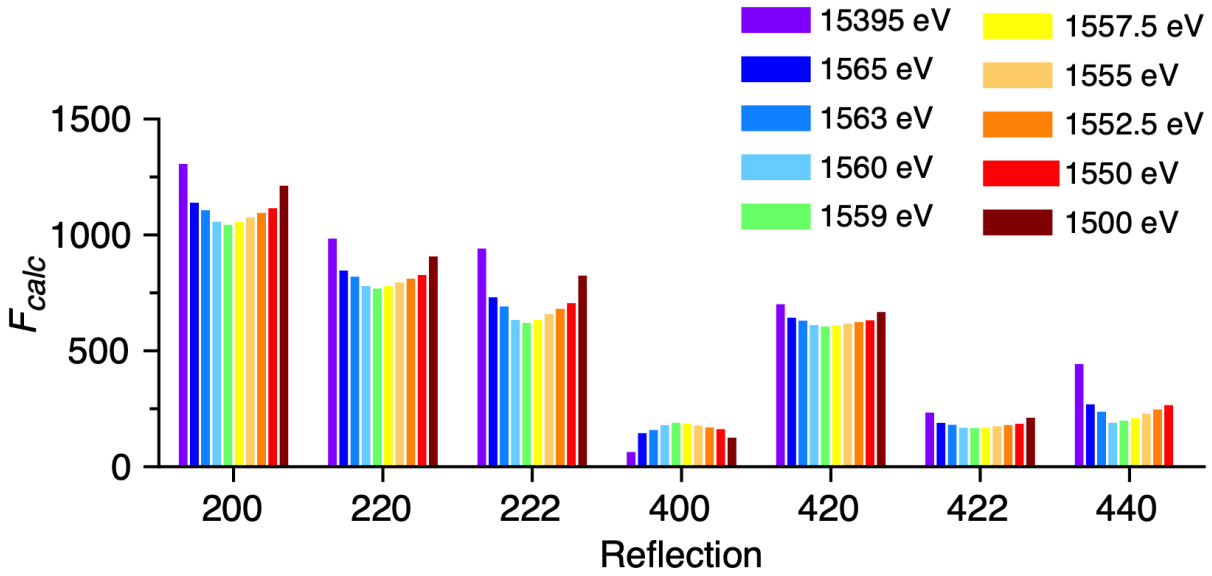

Institute for Chemical and Bioengineering, ETH Zurich, Zurich, Switzerland
Laboratory for Catalysis and Sustainable Chemistry, Paul Scherrer Institute, Villigen, Switzerland

Structure Refinement using conventional and Al K-edge data

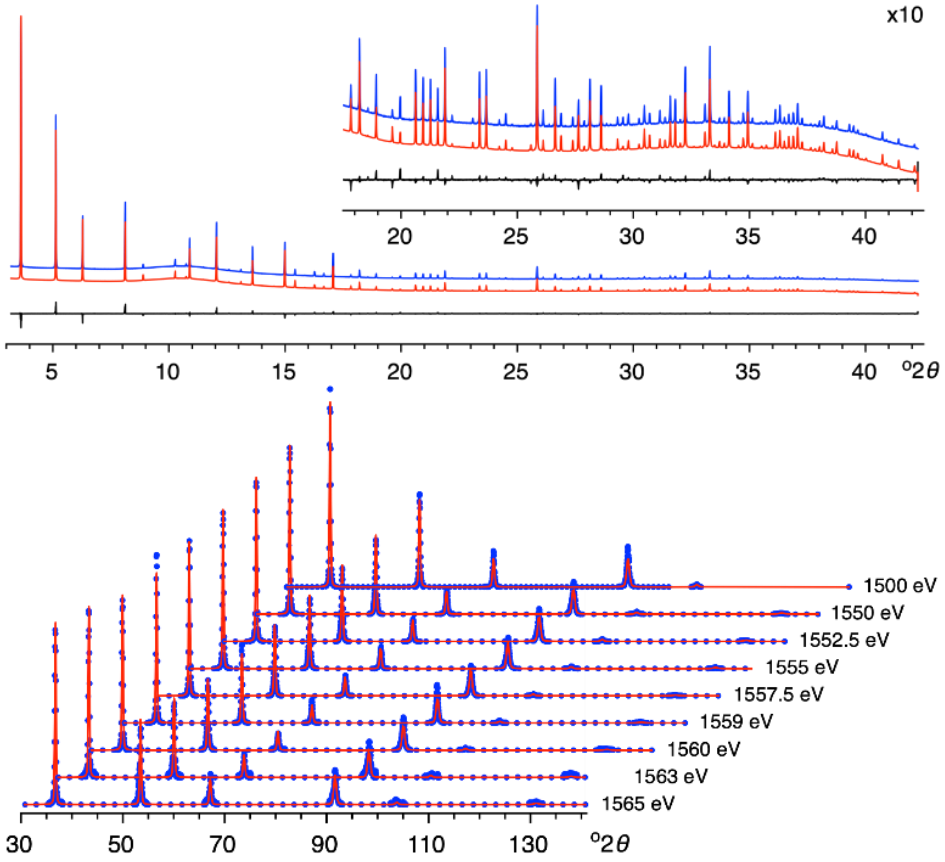

Structure refinement of Zeolite A

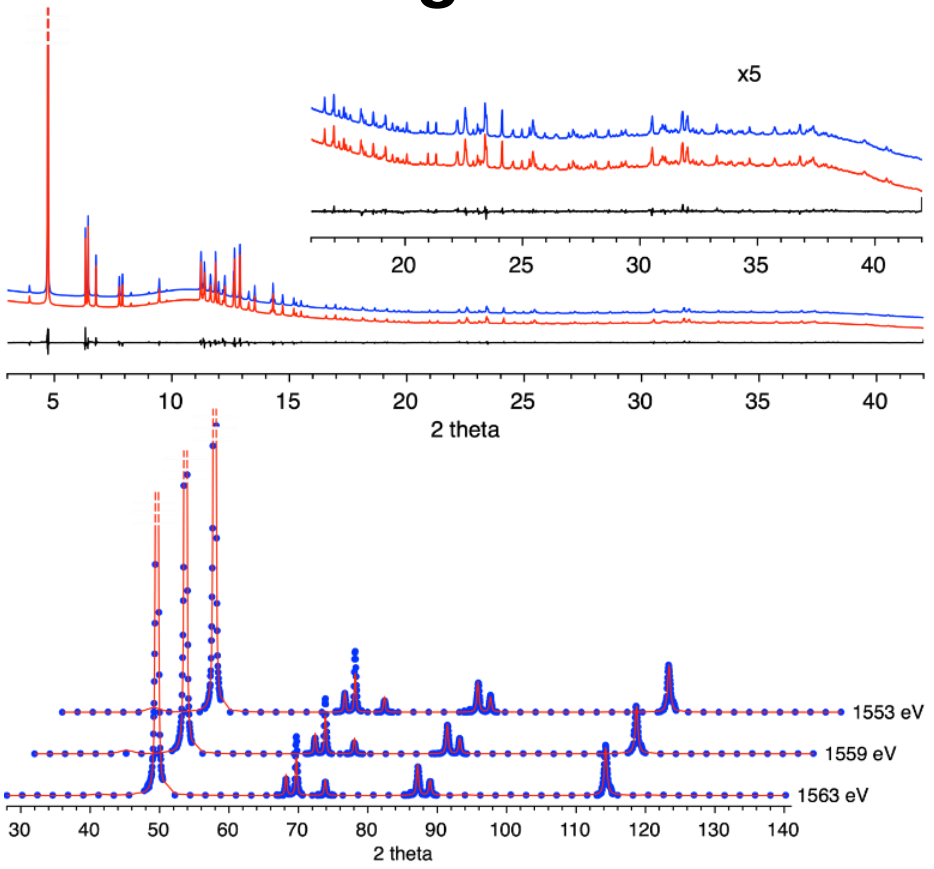

Structure refinement of zeolite FER

Institute for Chemical and Bioengineering, ETH Zurich, Zurich, Switzerland
Laboratory for Catalysis and Sustainable Chemistry, Paul Scherrer Institute, Villigen, Switzerland

Refinement of resonant data collected from FER

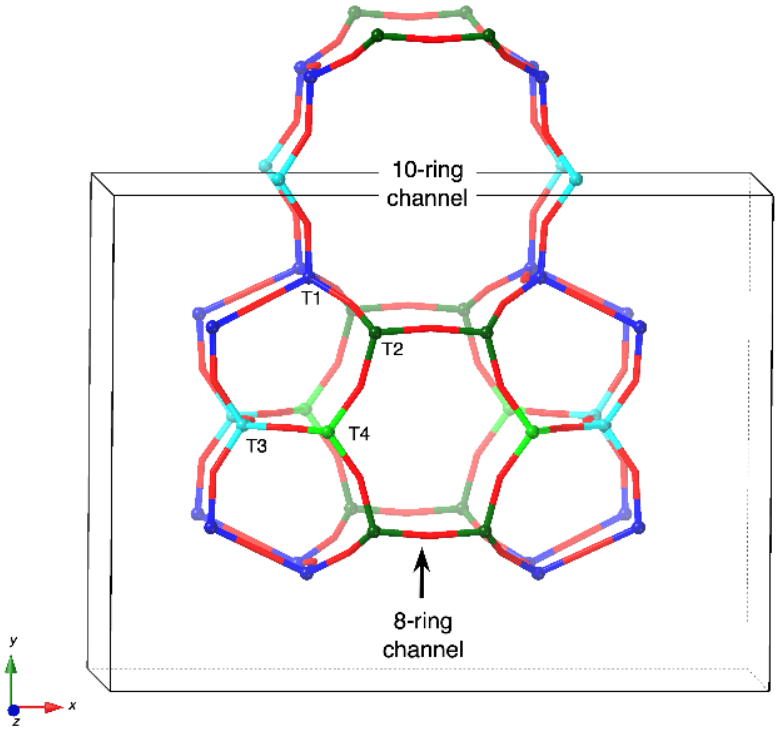

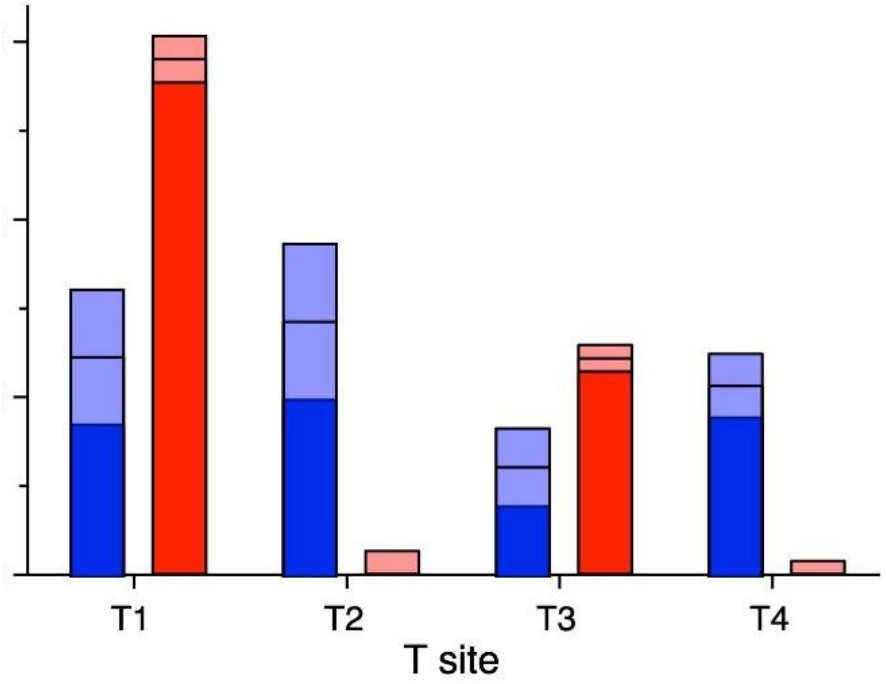

The ordering of the 2.2 aluminium atoms per unit cell over the four T-sites in FER1 (blue) and FER-PYRR (red)

Institute for Chemical and Bioengineering, ETH Zurich, Zurich, Switzerland
Laboratory for Catalysis and Sustainable Chemistry, Paul Scherrer Institute, Villigen, Switzerland

Anomalous diffraction across copper K-edge

The aim of this project is to exploit anomalous scattering at the Cu K-edge to elucidate the structure of the copper species present during the partial oxidation of methane to methanol (MtM)

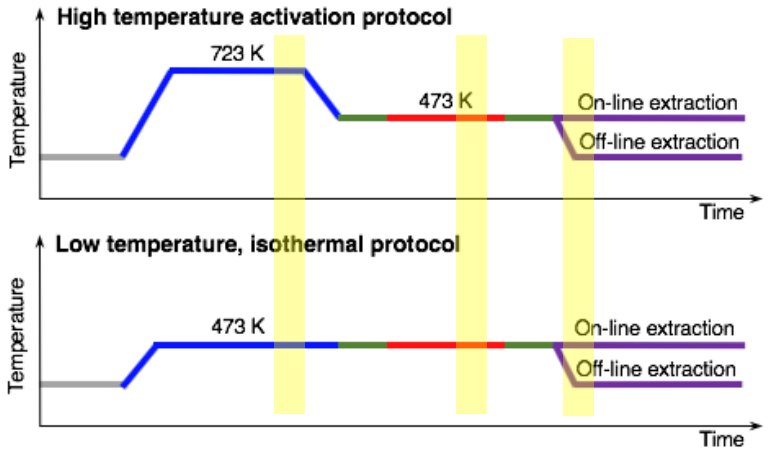

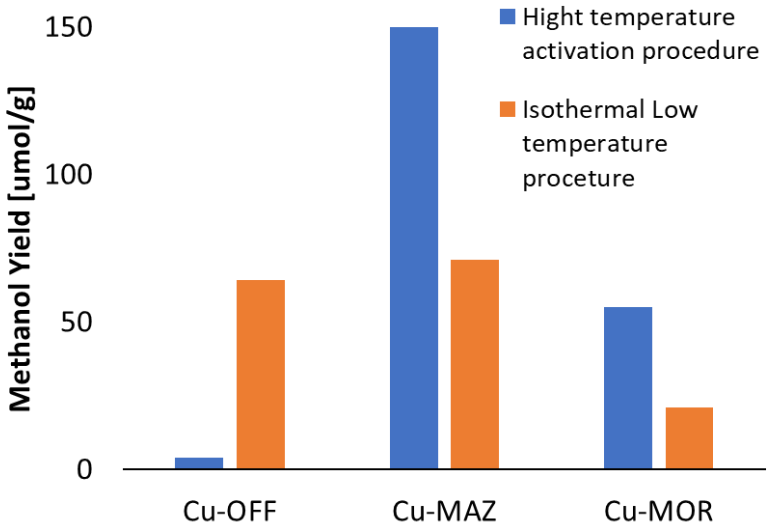

Copper offretite underwent isothermal and high-temperature procedures for methane-to-methanol conversion

Cu-offretite preforms better at lower temperature

Institute for Chemical and Bioengineering, ETH Zurich, Zurich, Switzerland
Laboratory for Catalysis and Sustainable Chemistry, Paul Scherrer Institute, Villigen, Switzerland

Anomalous diffraction across copper K-edge

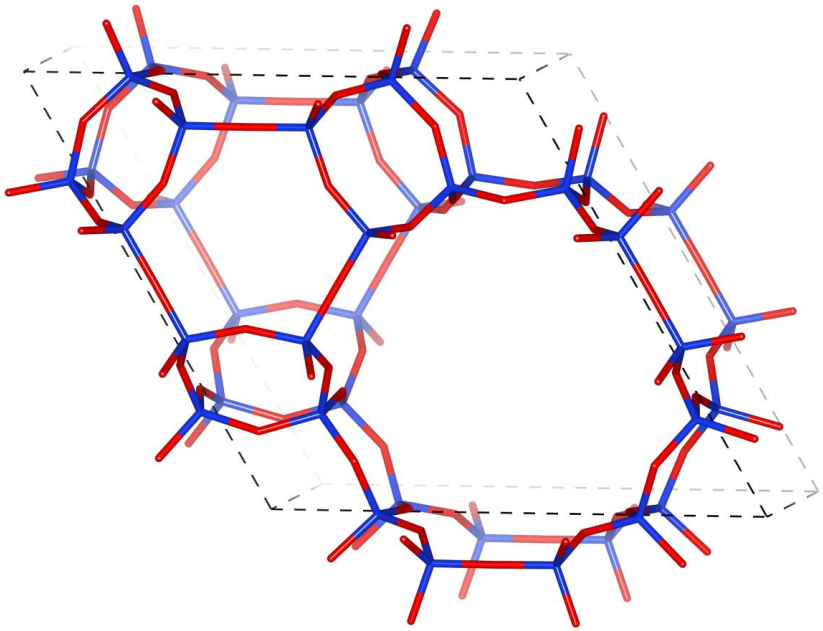

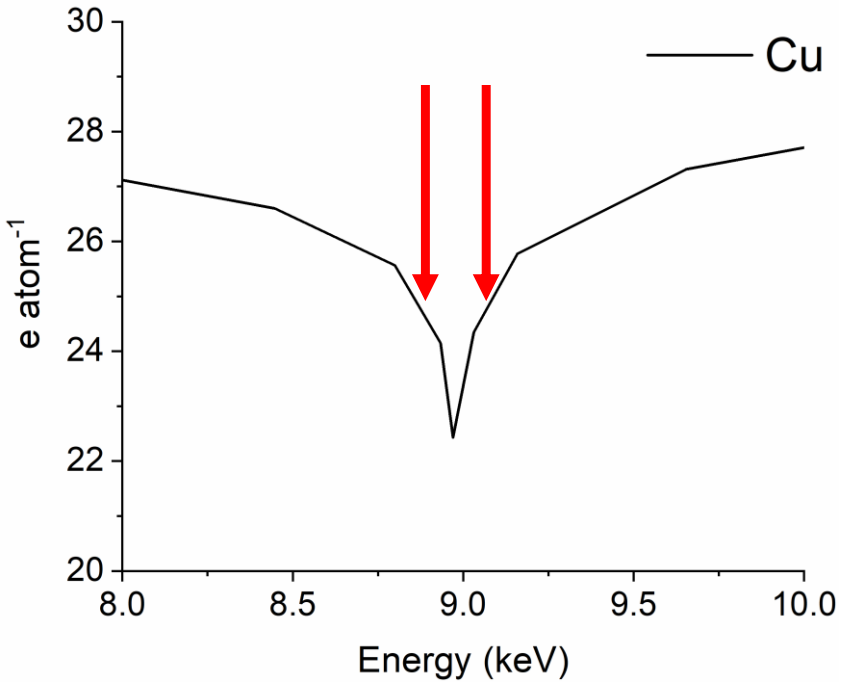

Offretite is hexagonal structure with 12-ring channels along z-axis. It is composed of gmelinite and cancrinite cages

Each sample was measured at off-resonance (17.5 keV) and on-resonance conditions (8.97 keV and 8.98 keV)

High resolution diffraction of offretite

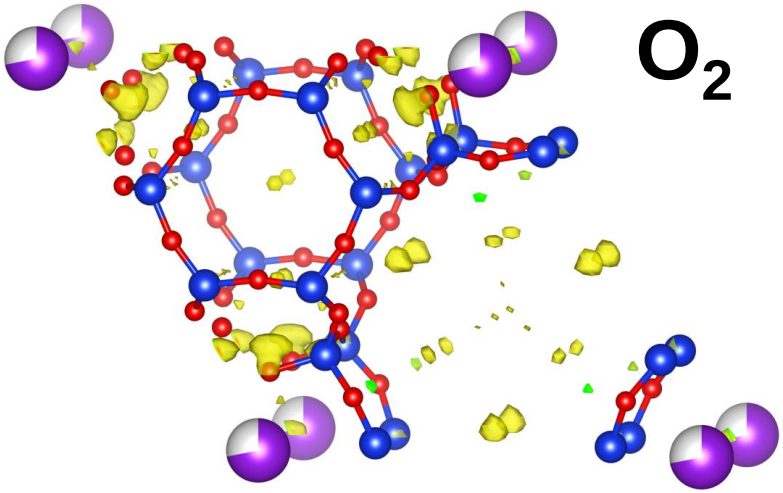

O_2

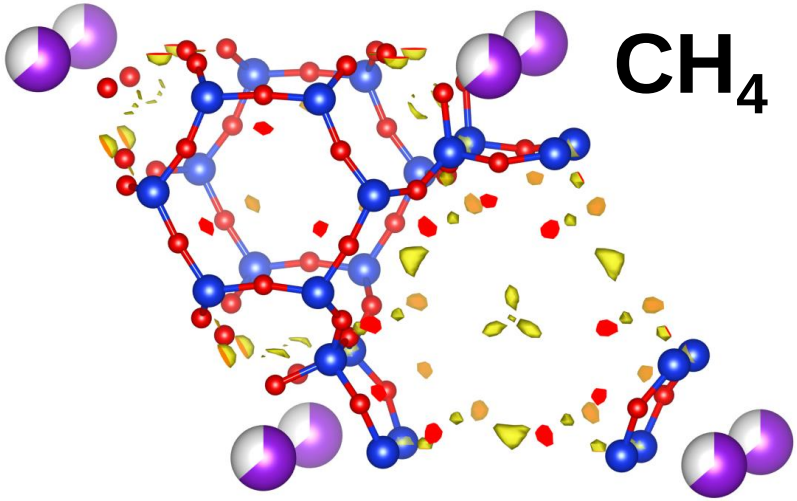

CH_4

OFF structure reveals the electron densities near 8-ring window of gmelinite cage upon MtM protocol. Similar observation was done on Cu-Omega

Anomalous diffraction is needed for ambiguous assignment of these densities to copper, oxygen or carbon

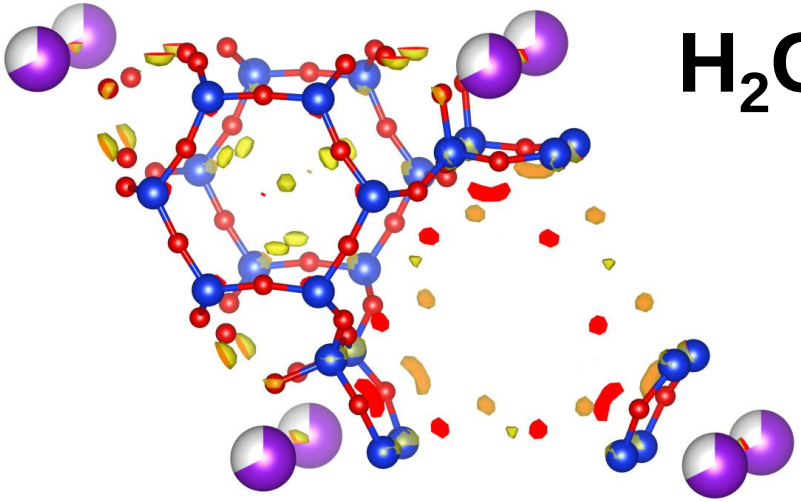

H_2O

Institute for Chemical and Bioengineering, ETH Zurich, Zurich, Switzerland
Laboratory for Catalysis and Sustainable Chemistry, Paul Scherrer Institute, Villigen, Switzerland

The population of Na^+ and K^+ in $|Na_{12-x}K_x|$-A

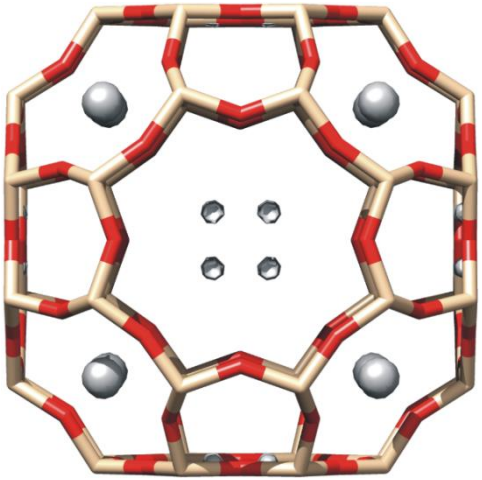

$|Na_{12}|$-A

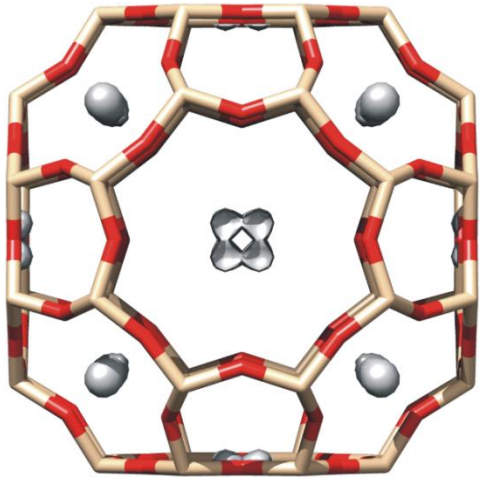

$|Na_9K_3|$-A

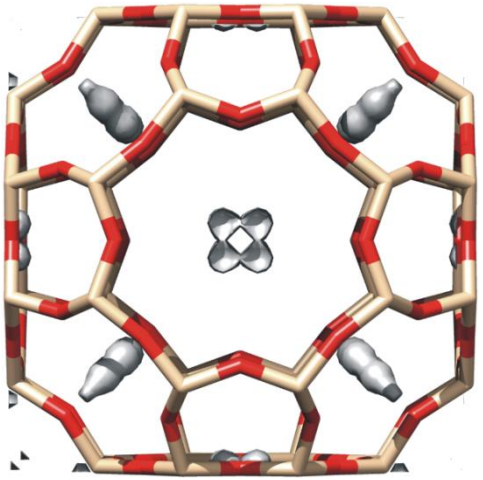

$|Na_{5.3}K_{6.7}|$-A

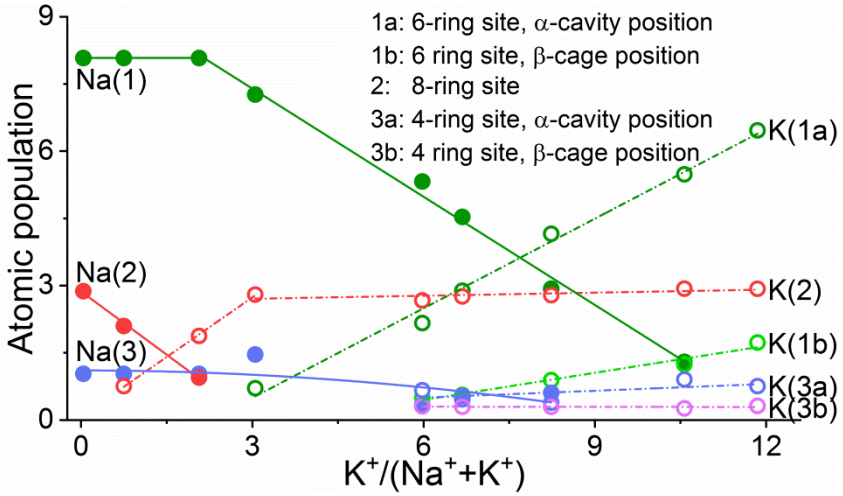

- K^+ and Na^+ populations are well resolved due to different positioning
- 8-ring is favored by cation replacement at low K^+-content
- K^+ gradually substitutes Na^+ in 6-ring

Institute for Chemical and Bioengineering, ETH Zurich, Zurich, Switzerland
Laboratory for Catalysis and Sustainable Chemistry, Paul Scherrer Institute, Villigen, Switzerland

The chemical nature of physisorbed CO_2

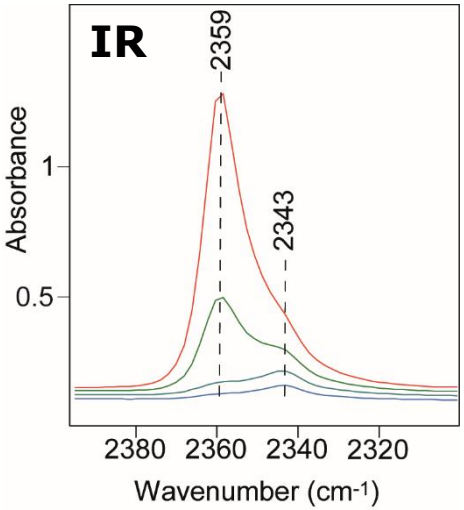

IR bands showed differentiation of physisorbed CO_2 at $|Na_{12}|$-A

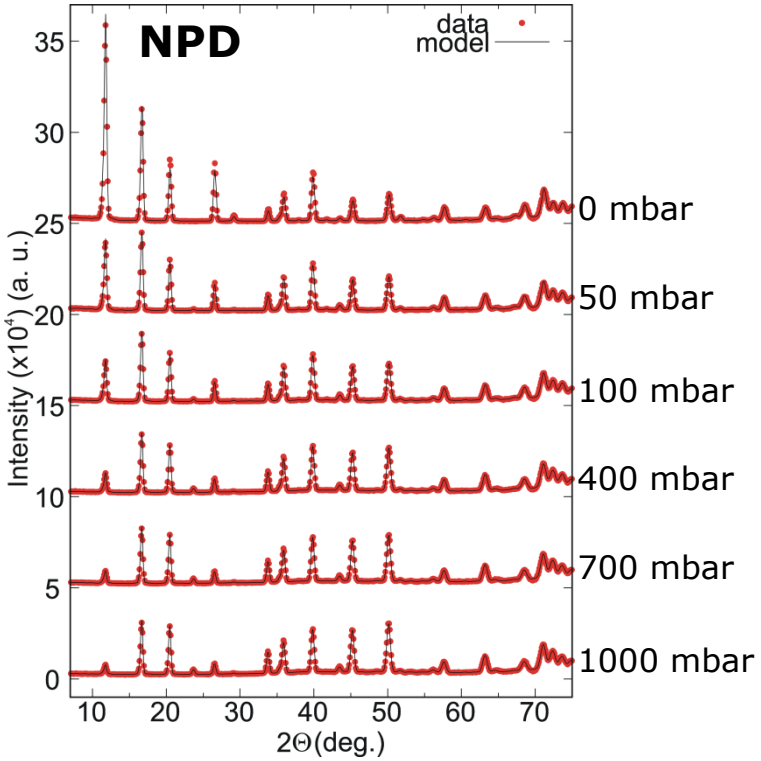

Rietveld analyses of the *in situ* neutron powder diffraction patterns of $|Na_9K_3|$-A

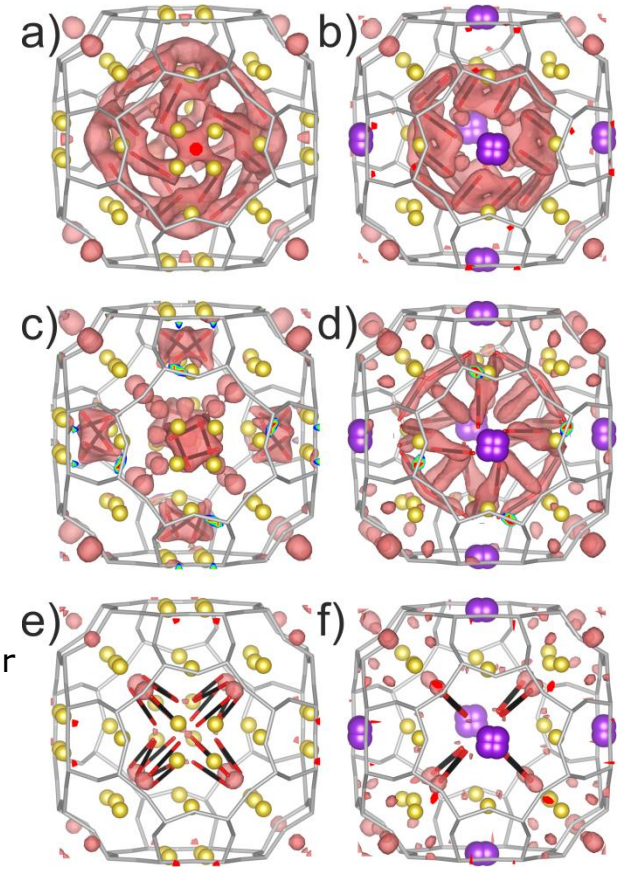

Difference Fourier maps of 3 sites of CO_2 for $|Na_{12}|$-A (left) and $|Na_9K_3|$-A (right)

Institute for Chemical and Bioengineering, ETH Zurich, Zurich, Switzerland
Laboratory for Catalysis and Sustainable Chemistry, Paul Scherrer Institute, Villigen, Switzerland

Site-specific physisorption of CO_2

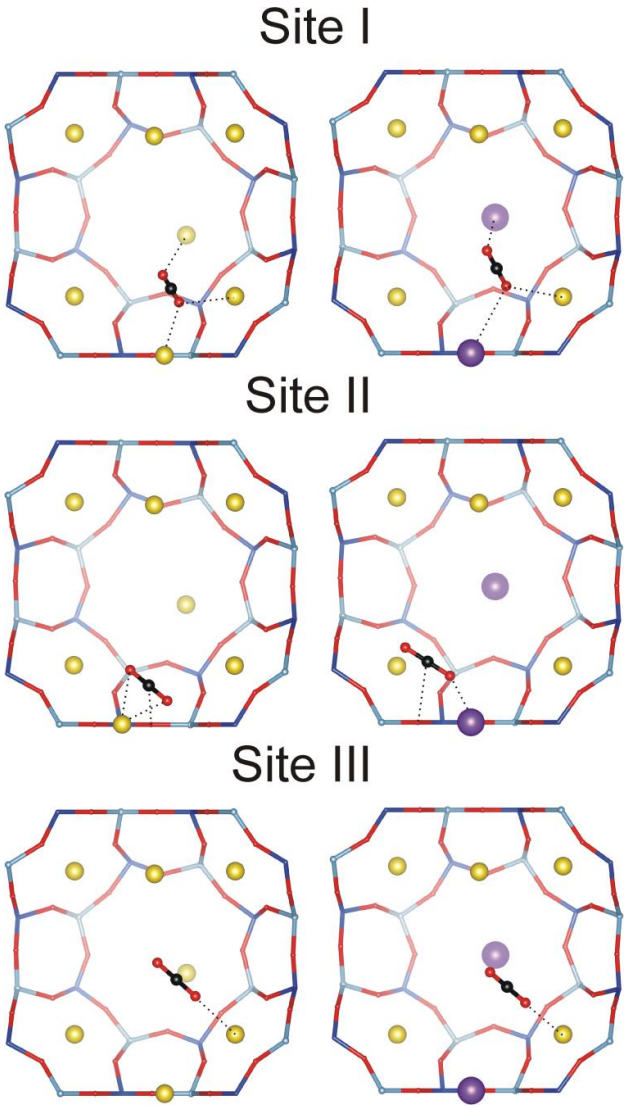

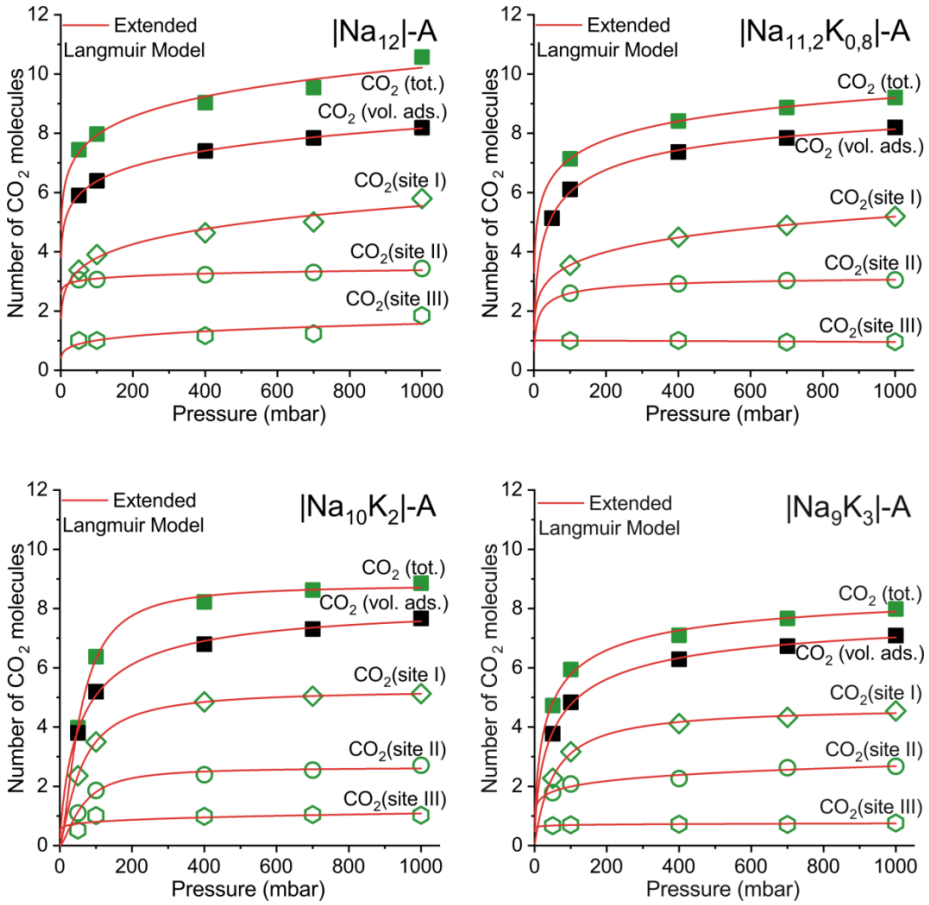

Atomic positions and site specific isotherms of adsorbed CO_2

Institute for Chemical and Bioengineering, ETH Zurich, Zurich, Switzerland
Laboratory for Catalysis and Sustainable Chemistry, Paul Scherrer Institute, Villigen, Switzerland

Adsorption of deuterated olefins

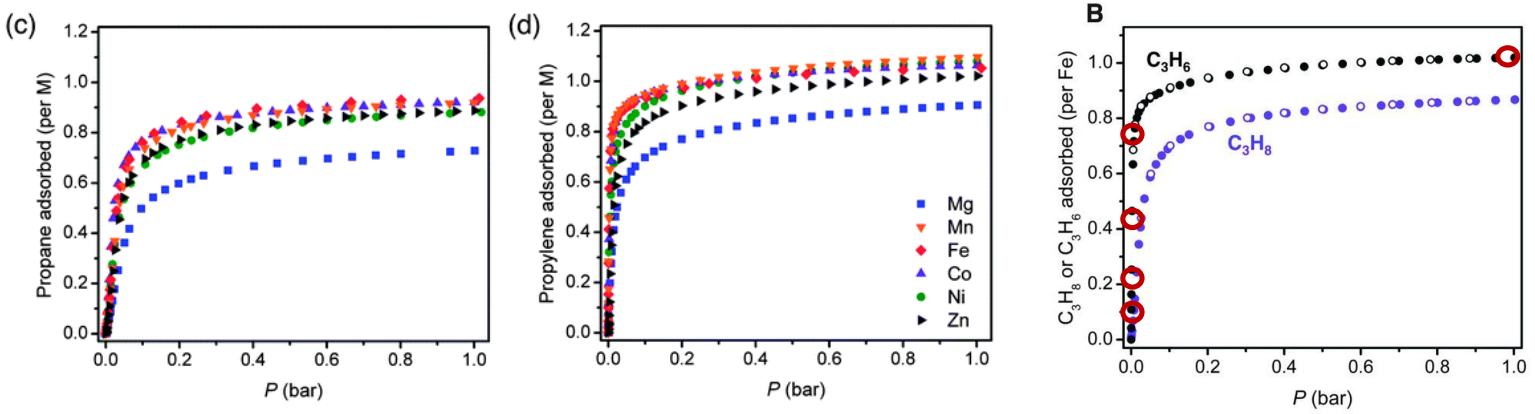

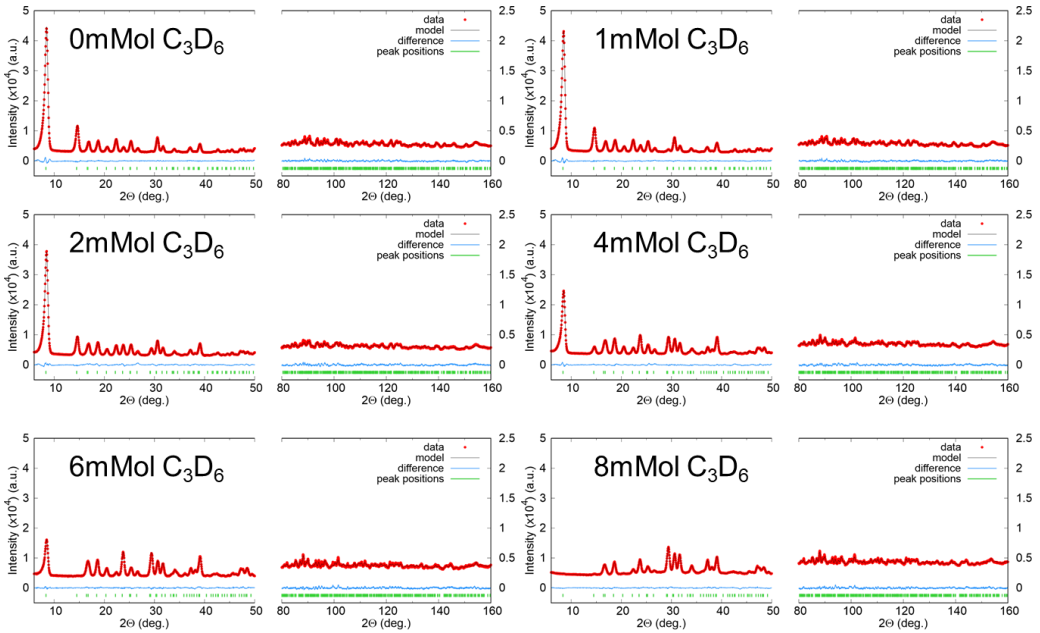

Rietveld refinement profile for Zn-MOF-74 as function of D_6H_{12} adsorption

Institute for Chemical and Bioengineering, ETH Zurich, Zurich, Switzerland
Laboratory for Catalysis and Sustainable Chemistry, Paul Scherrer Institute, Villigen, Switzerland

Adsorption of deuterated olefins

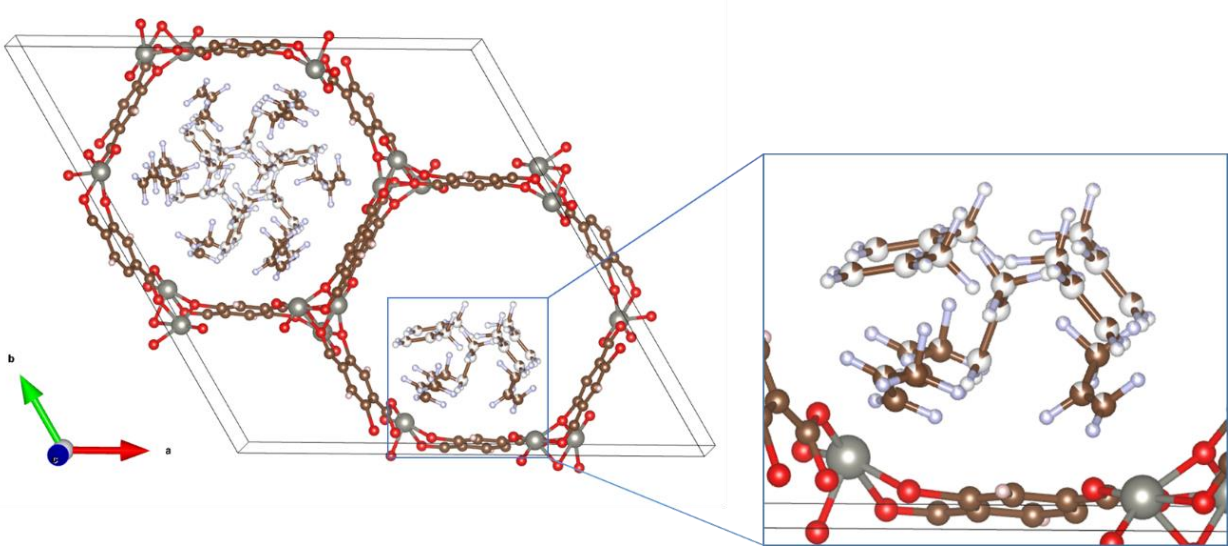

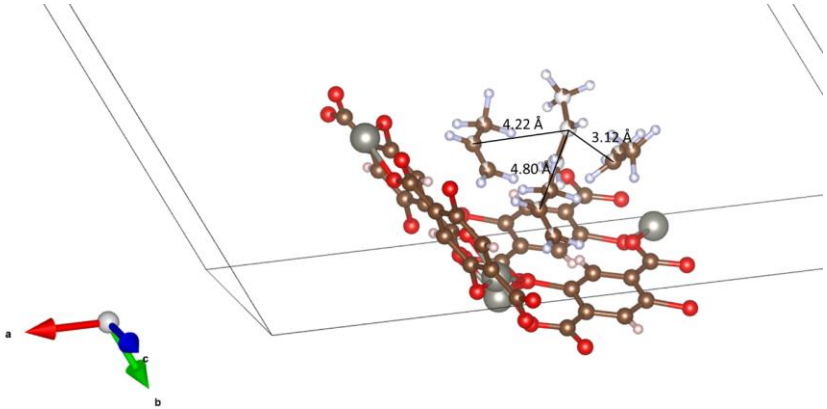

The refined propene-loaded Zn-MOF-74 structure with intermolecular distances

The propene density is increased inside the porous system upon formation of 2nd layer of adsorption

Institute for Chemical and Bioengineering, ETH Zurich, Zurich, Switzerland
Laboratory for Catalysis and Sustainable Chemistry, Paul Scherrer Institute, Villigen, Switzerland

References

1. http://pd.chem.ucl.ac.uk/pd/welcome.htm

2. http://prism.mit.edu/xray/education/downloads.html

3. http://www.crystal.mat.ethz.ch/people/staff/mlynne/

Thank you for your attention!